

1-8

**FINAL REPORT**  
**DESIGN FEASIBILITY STUDY FOR CONSTRUCTION**  
**OF A MICROBIAL ECOLOGY EVALUATION DEVICE (MEED)**

**September 1970**

Available to U.S. Government  
Agencies and NASA Contractors  
ONLY  
*(Candidates)*

**Prepared for**  
**NASA MANNED SPACECRAFT CENTER**  
**HOUSTON, TEXAS**

**on**  
**Contract NAS 9-10820**

STANDARD FACILITY FORM 602

<u>N70-42268</u> (ACCESSION NUMBER)	<u>1</u> (THRU)
<u>201</u> (PAGES)	<u>05</u> (CODE)
<u>CR-108661</u> (NASA CR OR TMX OR AD NUMBER)	<u>05</u> (CATEGORY)



**by**  
**AEROJET MEDICAL & BIOLOGICAL SYSTEMS**  
**9200 East Flair Drive**  
**El Monte, California**

Reproduced by  
**NATIONAL TECHNICAL**  
**INFORMATION SERVICE**  
Springfield, Va. 22151

CP-108661  
a.1

FINAL REPORT  
DESIGN FEASIBILITY STUDY FOR CONSTRUCTION  
OF A MICROBIAL ECOLOGY EVALUATION DEVICE  
(MEED)

September 1970

Prepared by  
A.M. Taylor


Prepared for  
NASA MANNED SPACECRAFT CENTER  
HOUSTON, TEXAS

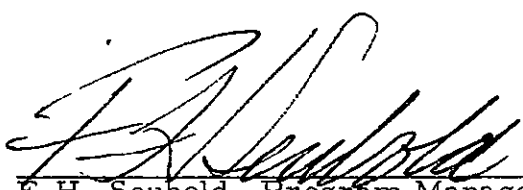
Contract NAS 9-10820

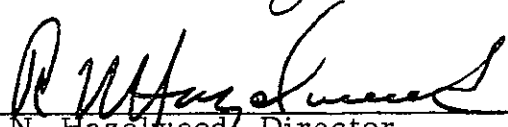
by

AEROJET MEDICAL & BIOLOGICAL SYSTEMS  
9200 East Flair Drive  
El Monte, California

  
A.M. Taylor, Project Engineer

  
W.H. Hartung, Manager, Engineering

  
F.H. Seubold, Program Manager

  
R.N. Hazelwood, Director  
Research & Development

# CONTENTS

	<u>Page</u>
SECTION 1 - INTRODUCTION .....	1-1
SECTION 2 - PROGRAM DEFINITION .....	2-1
2.1 Objectives .....	2-1
2.2 Technical Approach .....	2-1
2.3 Definition of Terms .....	2-2
2.3.1 MEED System .....	2-2
2.3.2 MEED Flight Assembly .....	2-2
2.3.3 CM Subassembly .....	2-2
2.3.4 Lunar Subassembly .....	2-2
2.3.5 MEED Unit .....	2-2
2.3.6 Cuvette .....	2-2
2.3.7 MEED Ground Assembly .....	2-3
2.3.8 Ancillary Equipment .....	2-3
SECTION 3 - SUMMARY AND CONCLUSIONS .....	3-1
3.1 Summary .....	3-1
3.1.1 MEED Flight Assembly .....	3-1
3.1.2 Mock-up - Flight Assembly .....	3-1
3.1.3 MEED .....	3-1
3.1.4 Tray .....	3-1
3.1.5 Cuvettes .....	3-2
3.1.6 Radiation Filters .....	3-2
3.1.7 Temperature Range Indicator .....	3-2
3.1.8 Radiation Level Indicator .....	3-2
3.1.9 Temperature Control .....	3-2
3.2 Conclusions .....	3-3
SECTION 4 - TECHNICAL DISCUSSION .....	4-1
4.1 General Requirements .....	4-1
4.1.1 Lunar Subassembly Capabilities .....	4-1
4.1.2 Temperature .....	4-1
4.1.3 Pressure .....	4-1
4.1.4 Microbial Filters .....	4-2
4.1.5 Ultraviolet Irradiation Requirements .....	4-2
4.1.6 Cuvettes .....	4-3
4.1.7 Size and Weight .....	4-3
4.1.8 Sterilization .....	4-3
4.1.9 Environmental Test Requirements .....	4-3
4.2 Concept Evaluation .....	4-3
4.2.1 Concepts .....	4-4
4.2.2 Baseline Design Concept .....	4-16

CONTENTS (Continued)

	<u>Page</u>
4.3 Feasibility Investigations . . . . .	4-19
4.3.1 MEED Flight Assembly . . . . .	4-19
4.3.2 MEED . . . . .	4-34
4.3.3 Tray . . . . .	4-34
4.3.4 Cuvette . . . . .	4-42
4.3.5 Radiation Filters . . . . .	4-68
4.3.6 Temperature Range Indicator . . . . .	4-80
4.3.7 Radiation Level Indicator (Actinometer) . . . . .	4-96
4.3.8 Temperature Control . . . . .	4-121
4.3.9 Weight Analysis . . . . .	4-139
4.3.10 Protocal Development . . . . .	4-139
SECTION 5 - EQUIPMENT LIST . . . . .	5-1
APPENDIX A - TEMPERATURE CONTROL - COMPUTER PROGRAM DESCRIPTION	
APPENDIX B - MISCELLANEOUS CALCULATIONS	
APPENDIX C - WEIGHT ANALYSIS	
APPENDIX D - PROTOCOLS	

## ILLUSTRATIONS

<u>Figure</u>		<u>Page</u>
4.2-1	MEED Assembly in Carrying Case . . . . .	4-5
4.2-2	MEED Flight Assembly Deployment . . . . .	4-6
4.2-3	MEED Assembly - Lunar Surface . . . . .	4-8
4.2-4	General Concepts . . . . .	4-9
4.2-5	Alternate Well Arrangements . . . . .	4-11
4.2-6	Circular Well Drilled in Section Block . . . . .	4-12
4.2-7	Circular Quartz Well . . . . .	4-13
4.2-8	Seal Detail . . . . .	4-14
4.2-9	Well Seal Detail . . . . .	4-15
4.2-10	Cuvette Types . . . . .	4-17
4.2-11	Sealed Tray - Square Wells (Baseline Design) . . . . .	4-18
4.3.1-1	MEED Flight Assembly . . . . .	4-22
4.3.1-2	Manipulation of Latches . . . . .	4-23
4.3.1-3	Mock-up Carrying Case . . . . .	4-24
4.3.1-4	Mock-up in Carrying Case . . . . .	4-25
4.3.1-5	Mock-up Flight Assembly on Soft Mounts . . . . .	4-26
4.3.1-6	Lunar Subassembly Mock-up . . . . .	4-27
4.3.1-7	Mock-up of Deployed MEEDs . . . . .	4-29
4.3.1-8	MEED Clamp Assembly . . . . .	4-30
4.3.1-9	MEED Modified Strut Clamp Assembly . . . . .	4-31
4.3.1-10	Modified Mock-up Clamp Assembly . . . . .	4-32
4.3.2-1	MEED Design Features . . . . .	4-35
4.3.3-1	MEED Tray Components . . . . .	4-36
4.3.3-2	MEED Tray Assembly . . . . .	4-38
4.3.3-3	MEED Tray Drill Jig . . . . .	4-40
4.3.3-4	"O" Ring Groove Tooling . . . . .	4-41

## ILLUSTRATIONS (Continued)

<u>Figure</u>	<u>Page</u>
4.3.4-1 Spectrophotometer Holder . . . . .	4-46
4.3.4-2 MEED Quartz Cuvette Assembly . . . . .	4-48
4.3.4-3 Quartz Cuvettes . . . . .	4-49
4.3.4-4 Air Bubble in Cuvette Fluid . . . . .	4-50
4.3.4-5 Desiccation Apparatus . . . . .	4-51
4.3.4-6 KEL-F Plastic Cuvette Design . . . . .	4-54
4.3.4-7 KEL-F Cuvette Components . . . . .	4-56
4.3.4-8 Plexiglas Cuvette with Quartz Window . . . . .	4-57
4.3.4-9 Plexiglas Cuvette with Wax Seal . . . . .	4-58
4.3.4-10 Body of Plexiglas Cuvette . . . . .	4-60
4.3.4-11 Alternate Design, Plexiglas Cuvette . . . . .	4-61
4.3.4-12 Sealed, Dry Sample Cuvette . . . . .	4-62
4.3.4-13 Exploded View, Simulated Dry Sample Cuvette . . . . .	4-64
4.3.4-14 Assembled Dry Sample Cuvette . . . . .	4-65
4.3.4-15 Vented, Dry Sample Cuvette . . . . .	4-66
4.3.4-16 Dry Sample, Vented Cuvette . . . . .	4-67
4.3.5-1 Approximate Irradiation on Sample for Various Filter Half-Peak Bandwidths: Exposure Time = 10 Minutes	4-69
4.3.5-2 UV Exposure Required to Kill Various Kinds of Organisms (from Ultraviolet Radiation by Lewis Koller, John Wiley & Son, 1965, Sec. Edition, p. 243)	4-70
4.3.5-3 Solar Spectral Irradiance (Composite Data) . . . . .	4-72
4.3.5-4 Solar Spectral Irradiation Passing through Interference Filter with Half-Peak Bandwidth = 25 nm . . . . .	4-73
4.3.5-5 Solar Spectral Irradiation Passing through Interference Filter with Half-Peak Bandwidth = 10 nm . . . . .	4-74
4.3.5-6 Measured Transmission Characteristics of Interference Filters and Quartz Glass . . . . .	4-77

ILLUSTRATIONS (Continued)

<u>Figure</u>		<u>Page</u>
4.3.5-7	Measured Transmission Characteristics of Interference Filters and KEL-F . . . . .	4-78
4.3.5-8	Radiation Filter Model . . . . .	4-79
4.3.6-1	Melting Point Indicator . . . . .	4-84
4.3.6-2	Tetradecanol . . . . .	4-86
4.3.6-3	Liquid Crystal Molecular Order . . . . .	4-88
4.3.6-4	Liquid Crystal Systems . . . . .	4-89
4.3.6-5	Bimetallic Temperature Indicator Element . . . . .	4-92
4.3.6-6	Bimetallic Indicator with Cover Open . . . . .	4-93
4.3.6-7	Bimetallic Indicator Trace Due to Temperature Change . . . . .	4-94
4.3.7-1	Actinometer Solution Absorption . . . . .	4-98
4.3.7-2	Calibration Curve . . . . .	4-101
4.3.7-3	Emission Curves, High-Pressure Arc . . . . .	4-105
4.3.7-4	Transmission Curves, Longwave and Shortwave Ultraviolet Filters . . . . .	4-107
4.3.7-5	Transmission Spectra, Beckman Standard Cuvette . . . . .	4-108
4.3.7-6	Emission Curves, Shortwave Ultraviolet Lamps . . . . .	4-112
4.3.7-7	Spectral Sensitivity . . . . .	4-118
4.3.7-8	Summary of Spectral Sensitizings . . . . .	4-120
4.3.8-1	Thermal Balance . . . . .	4-127
4.3.8-2	Transient Thermal Model . . . . .	4-128
4.3.8-3	Reflectance of Baird - Atomic Interference Filter 10-33-3 Normal Incidence . . . . .	4-129
4.3.8-4	Response of the Enclosed MEEDs for Duration of Lunar Mission Following UV Exposure Period . . . . .	4-137

## TABLES

	<u>Page</u>
4.3.1-1 Preliminary Vibration Requirements . . . . .	4-20
4.3.1-2 Preliminary Acceleration Requirements . . . . .	4-20
4.3.4-1 Percent Transmission of Candidate Plastics . . . . .	4-45
4.3.6-1 Melting Points of Organic Compounds . . . . .	4-82
4.3.7-1 Actinometer Calibration Table . . . . .	4-100
4.3.7-2 Preliminary Actinometry . . . . .	4-104
4.3.7-3 B-100 Blak-Ray with Roundel Filter - 5 Minute Exposure	4-109
4.3.7-4 B-100 Blak-Ray without Filter - 2.5-Minute Exposure	4-110
4.3.7-5 Mineralight UV S-12 without Filter - 10-Minute Exposure	4-113
4.3.7-6 250 nm Bandpass Filter - One-Hour Exposure . . . . .	4-115
4.3.7-7 MEED Quartz Cuvette . . . . .	4-117
4.3.8-1 Results of Transient Model after 10-Minute Exposure	4-131



## ACKNOWLEDGEMENTS

The following were major participants in the performance of the design feasibility study and the preparation of this report:

John Misselhorn  
Fletcher Mulligan  
John J. O'Connor  
Stanley Turner

## Section 1

### INTRODUCTION

This document is the Final Report for the Design Feasibility Study for Construction of a Microbial Ecology Evaluation Device (MEED). The work was performed under Contract NAS 9-10820 for the NASA Manned Spacecraft Center, Houston, Texas by the Aerojet Medical and Biological Systems Division of Aerojet-General Corporation. The report includes a discussion of the results of the feasibility investigations and the conclusions reached, data on alternate designs, a recommended design approach, and the major protocols that define the procedures required for use of the hardware.

Long-duration space missions may result in microbial mutants that are more virulent than the initial microbial forms. The conditions that may lead to the mutations are 1) lowered gravity states, 2) ultra-violet irradiation, 3) variations of the oxygen content in the environment and 4) exposure to the hard vacuum of space. The equipment (MEED) for which design feasibility was established in this study can be developed and used in space experiments to determine the effects of these environmental factors on selected microbial systems.

The general plan for the proposed flight experiments is to carry three packages (MEEDs) of microbial samples to the lunar surface, where two will be exposed to the solar radiation of space. The third MEED will serve as an unexposed control unit on the lunar surface. A fourth MEED will be an unexposed control unit in orbit around the moon in the Command Module. A fifth MEED will be kept as a control unit under carefully controlled conditions at the Manned Spacecraft Center, Houston.

This study had the objective of establishing the feasibility of designing and fabricating hardware for the proposed flight experiments. In the study, requirements were defined, concepts were evaluated, selected hardware was fabricated, analyses and feasibility tests were performed and a mock-up of the flight assembly was completed.

Further definition of experiment requirements may alter the design features of the concepts; however, the design features selected were all found to be feasible. No problems were encountered that would prevent the development and use of practicable hardware, capable of performing the proposed experiments.

## Section 2

### PROGRAM DEFINITION

#### 2.1 OBJECTIVES

The objective of the study program was to establish the feasibility of designing and constructing a Microbial Ecology Evaluation Device (MEED) that can be transported to the lunar surface, deployed for ultraviolet exposure of biological samples, exposed to the lunar environment and returned to earth.

The basic objective of the experiment for which the MEED is to be designed is to determine the type and degree of alteration produced in selected biological systems by parameters of the spacecraft and lunar environment. These parameters are: 1) alterations in oxygen partial pressure, 2) changes in total pressure from one atmosphere to a hard vacuum, 3) alterations in gravity with "zero gravity" state for an extended time, and 4) controlled irradiation with ultraviolet light.

#### 2.2 TECHNICAL APPROACH

The evaluation of the feasibility of designing and constructing MEED hardware capable of performing the desired experiments was performed as follows:

1. The requirements and major problem areas were defined.
2. Conceptual designs that generally met the requirements were established and compared with each other.
3. A baseline design concept was selected.
4. Alternate design concepts were selected as backups in selected areas.
5. Selected experimental models and components were designed, fabricated and tested.
6. Preliminary protocols, consistent with the experiment and hardware design concepts, were developed.
7. Mock-up evaluation devices were delivered to permit customer evaluation of the proposed systems.

## 2.3 DEFINITION OF TERMS

### 2.3.1 MEED SYSTEM

All of the flight hardware, protocols and ancillary equipment required for the operation of the experiment.

### 2.3.2 MEED FLIGHT ASSEMBLY

The flight unit - this assembly is comprised of two sub-assemblies: the Command Module (CM) Subassembly and the Lunar Subassembly.

### 2.3.3 CM SUBASSEMBLY

The portion of the Flight Assembly that remains in the Command Module at all times. This unit contains one MEED unit with a carrying case.

### 2.3.4 LUNAR SUBASSEMBLY

This portion of the Flight Assembly is transported between the CM and LM and the lunar surface. The unit contains three MEEDs, a carrying case (insulated), and ancillary equipment for attachment and deployment.

### 2.3.5 MEED UNIT

A container with approximate dimensions of 7" x 3" x 1-1/2", containing approximately 384 exposure chambers (cuvettes). These units are of two general types:

1. MEED Unit Type A

This unit contains ultraviolet filters and is covered by a quartz plate to allow for differential irradiation with UV light.

2. MEED Unit Type B

This unit is not exposed to ultraviolet irradiation and therefore requires no UV filters or quartz cover.

### 2.3.6 CUVETTE

Individual exposure chambers, approximately 5 mm cubed, with one side of quartz for UV penetration. These are of three types:

1. Cuvette Type A

Unvented for liquid culture retention.

2. Cuvette Type B

Unvented for dry culture retention.

3. Cuvette Type C

Vented through a microbiological filter for dry culture retention under lunar surface conditions.

### 2.3.7 MEED GROUND ASSEMBLY

That MEED unit which remains on the ground as an ambient control. This is a non-flight qualified unit consisting of one Type B MEED Unit.

### 2.3.8 ANCILLARY EQUIPMENT

This group includes devices necessary for loading, unloading, organizing, and cataloguing the MEED devices within the biological cabinetry at MSC.

## Section 3

### SUMMARY AND CONCLUSIONS

#### 3.1 SUMMARY

The technical accomplishments of MEED feasibility study and the conclusions reached during the study are summarized in this section.

The phases of the program were 1) the establishment of the physical and performance requirements for the assemblies and components, 2) the generation of concepts for the MEED Flight Assembly, 3) the selection of concepts for subsystems and components, and 4) the investigation of the feasibility of selected assemblies, subassemblies and components. Specific investigations are as follows.

##### 3.1.1 MEED FLIGHT ASSEMBLY

A design of the MEED Flight Assembly was completed. The assembly includes a Command Module control MEED (CM Subassembly), and a Lunar Subassembly for the deployment of microbial samples on the lunar surface.

##### 3.1.2 MOCK-UP - FLIGHT ASSEMBLY

A mock-up of the MEED Flight Assembly was completed to assist in visualizing problems of mounting and deployment.

##### 3.1.3 MEED

The baseline MEED concept of a pressurized tray, with transparent quartz window, containing 384 cuvettes was designed in greater detail to serve as a basis for analysis and test. The requirements were expanded to include a vented section with self-venting cuvettes.

##### 3.1.4 TRAY

Three MEED trays were fabricated. The following feasibility investigations were performed on the MEED Tray and its components:

Burst tests were performed on the tray. The factor of safety was over 10:1 for deployment on the lunar surface with an internal pressure of 14.7 psig.

Leak tests were performed on a tray with a preliminary "O" ring design. Leakage was within limits. The final seal design was established.

### 3.1.5 CUVETTES

Cuvettes were fabricated from quartz, KEL-F plastic, and a combination of quartz and plexiglas (Lucite). The feasibility investigations performed are as follows:

The design requirements for the three types of cuvettes were established, and seventeen cuvette window materials were investigated for ultraviolet transmission.

The selected designs of Types A, B and C cuvettes all contain quartz windows and plastic bodies, and wax seals where appropriate.

Bubble elimination investigations were performed.

Dry sample sealed cuvettes (Type B) and dry sample vented cuvettes (Type C) were fabricated, and assembly and sealing tests were performed.

### 3.1.6 RADIATION FILTERS

Radiation filters were evaluated for the wavelength range between 250 and 300 nm. The selected filter system includes interference filters to narrow the wavelength band of the ultraviolet radiation, and neutral density filters to attenuate the radiation intensity to the desired levels.

### 3.1.7 TEMPERATURE RANGE INDICATOR

Experimental versions of three types of temperature range indicators were investigated: 1) the "liquid crystal" indicator, 2) the organic solvent melting point indicator, and 3) a bimetallic indicator. Of these, only the bimetallic will measure the minimum as well as the maximum temperatures. The bimetallic unit was selected as the most promising type, but further development will be required.

### 3.1.8 RADIATION LEVEL INDICATOR

The potassium ferrioxalate actinometer was tested at the test tube level. The method appears fully feasible.

### 3.1.9 TEMPERATURE CONTROL

The MEED Lunar Subassembly was analyzed using established transient and steady-state computer programs. Temperature can be controlled by design to remain within limits during the exposure to ultraviolet radiation. Passive temperature control by use of super-insulation during the 72-hour stay on the lunar surface appears feasible, but may be marginal.



### 3.2 CONCLUSIONS

The selected design for the MEED Flight Assembly will meet the requirement imposed by the Apollo mission and the planned experiments.

The major development efforts that must be performed during the early phases of a hardware program are 1) the miniaturization design of the bimetallic temperature indicator, 2) testing the selected cuvettes with experiment microorganisms, and 3) thermal and radiation testing of the Flight Assembly in a vacuum chamber while undergoing simulated solar radiation.

The radiation filter system and the vented cuvette/tray systems are feasible and present no potentially serious development problems

The microbial sample temperature should be measured in one location in each MEED, and then related to temperatures in other locations in the MEED by prior calibration tests.

The potassium ferrioxalate actinometer is fully feasible for the measurement of radiation.

Bubble formation will not be a problem in the cuvette unless the microbes produce an excessive amount of gas.

## Section 4

### TECHNICAL DISCUSSION

#### 4.1 GENERAL REQUIREMENTS

The general design requirements on which the concept studies and the feasibility investigations were based are as follows.

##### 4.1.1 LUNAR SUBASSEMBLY CAPABILITIES

The Lunar Subassembly must be designed to meet the following functions:

- Transport from CM to LM.
- Attachment, with suitable shock mounts, to LM component inside crew compartment.
- Transport from LM to lunar surface.
- Attachment to LM external component as required.
- Accurate and stable alignment relative to incoming irradiation.
- Exposure to ultraviolet irradiation for a ten-minute period.
- Replacement into light-tight configuration.
  
- Attachment, with suitable shock mounts, to LM component inside crew compartment.
  
- Transport from LM to CM.
- Attachment, with suitable shock mounts, to CM component inside crew compartment. Re-uniting with CM Subassembly.

##### 4.1.2 TEMPERATURE

The temperature of the test samples will be maintained within  $20 \pm 5^{\circ}\text{C}$ . The maximum and minimum values of the temperature range will be measured or calculated from calibrated relationships.

##### 4.1.3 PRESSURE

Approximately 75 percent of the MEED (384 cuvettes) will be sealed and capable of withstanding a differential pressure of one atmosphere (outward). Approximately 25 percent of the MEED will be vented and open to ambient atmospheric conditions across suitable microbial filters.

#### 4.1.4 MICROBIAL FILTERS

All microbial filters used will be impermeable to test microorganisms. Test organisms will be restricted to bacteria and fungi which have their smallest dimension no less than 0.5 microns.

Microbial filters will not be damaged by pressure changes within the MEED during the flight. Pressures ranging from one atmosphere to a "hard vacuum" are expected.

Two microbial filtering systems will be provided:

a. Each Type C cuvette will be provided with a microbial filtering system which will allow passage of gases but prevent passage of the microbial test systems.

b. That section of the MEED which contains the Type C cuvettes will be vented to the atmosphere through a differentially permeable membrane, allowing passage of gases but not the microbial test systems.

#### 4.1.5 ULTRAVIOLET IRRADIATION REQUIREMENTS

Wavelengths - Test chambers (cuvettes) will have a suitable bandpass and/or interference filters to select irradiation with peaks at 254, 260, 280, and 300 nm wavelengths. The half-peak bandwidth and transmissivity of each will be established.

Intensity - Selected total energy levels from  $10$  to  $10^5$  ergs per chamber (about  $0.25 \text{ cm}^2$  surface area) will be available for the ten-minute exposure period. Methods of selecting desired energy levels over this range will be defined.

Half-Peak Bandwidth - The half-peak bandwidth will be as narrow as is consistent with the intensity required and the availability of filters.

Energy Measurements - A suitable method (or methods) for recording the energy flux within the test systems will be provided.

Type A MEED units must be protected from all incoming visible and ultraviolet irradiation except during the ten-minute exposure period.

A method must be developed to assure that the incoming UV irradiation is perpendicular to the exposed surface of the cuvettes.

#### 4.1.6 CUVETTES

Cuvettes must have one side permeable to ultraviolet irradiation and all other sides opaque to UV.

Types A and B will contain calibrated volumes between 25 and 50 microliters (  $\lambda$  ).

Each cuvette will be self-contained.

A cuvette identification system is required. Any identifying marks must be visible under red light inside Class III biological cabinetry.

#### 4.1.7 SIZE AND WEIGHT

The weight of this loaded MEED will not exceed 2 pounds and its dimensions will not exceed 3 in x 7 in x 1.5 in.

The weight of the Flight Assembly will not exceed 10 pounds and its dimensions will not exceed 8 in x 6 in x 4.5 in.

Soft mounts are required for the Flight Assembly in the Command Module.

#### 4.1.8 STERILIZATION

All parts of the MEEDs and the associated ground support equipment will be capable of being sterilized. The sterilization must render them free of viable microorganisms, but not inhibit the test samples which come in contact with them.

#### 4.1.9 ENVIRONMENTAL TEST REQUIREMENTS

The Flight Assembly and its subassemblies and components must be capable of meeting the Apollo mission requirements for vibration, shock, acceleration, and acoustic noise.

#### 4.2 CONCEPT EVALUATION

The concept evaluation was centered around 1) the design of the MEED Lunar Subassembly, 2) the mounting of the MEEDs in the Apollo Command Module and Lunar Module, and deployment of the MEEDs on the lunar surface, 3) the design of the MEED, and 4) the design of the biological sample container (well or cuvette) within the MEED. The approach comprised evaluation of one or more design concepts in each of the above areas.

A preliminary screening of the concepts was completed, followed by the definition of a baseline design concept. Alternate designs were established where the design problems involved were considered to be difficult, or where requirements were not fully established.

#### 4.2.1 CONCEPTS

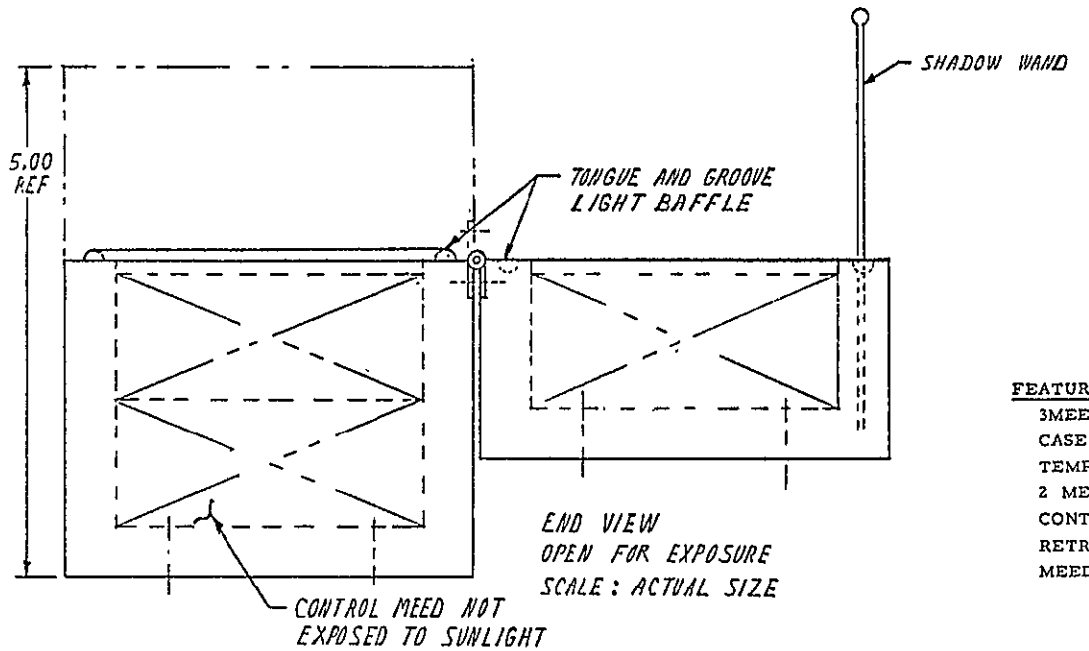
##### 4.2.1.1 MEED LUNAR SUBASSEMBLY DESIGN

The design features of the Lunar Subassembly concept are shown in Figure 4.2-1. The design includes a control MEED, two MEEDs that will be exposed to solar radiation, an insulated carrying case, a light baffle, and a retractable shadow wand to provide for the alignment of the MEEDs perpendicular to the sun's rays. The carrying case is doubled-walled, and the space between the walls is filled with "super-insulation". A tongue-in-groove light baffle is shown, but a preferred design consists of sliding opaque sheets similar to those used on large camera film packs.

##### 4.2.1.2 MOUNTING AND DEPLOYMENT

The concept of the general arrangement of the MEED Flight Assembly, its separation into the Lunar Subassembly, and the CM Subassembly (Command Module Subassembly) are shown in Figure 4.2-2. Sketch 1a shows a method of attaching the MEED flight assembly on its soft mounts in the Command Module. The lowest section of the Flight Assembly represents the Command Module Subassembly. The second section represents one of the MEEDs to be exposed; the third section includes the other MEED to be exposed, and the control MEED; and the top section represents the cover which encloses a clamping device. Sketch 1b represents the MEED Flight Assembly in place. Sketches 1c and 1d show the Lunar Subassembly separated for transfer to the LM and the CM Subassembly left on the soft mounts. Sketch 1e represents an LM mounting base with soft mounts and sketch 1f shows the Lunar Subassembly mounted on the base for the descent to the lunar surface. Sketch 1g shows the Lunar Subassembly in position on the lunar surface and 1h depicts one method for deployment of a clamp to attach the unit to an existing brace on the leg of the LM. Sketch 1i shows the Lunar Subassembly opened to expose the two MEEDs to the solar ultraviolet radiation.

Three concepts were evaluated for positioning the Lunar Subassembly on the lunar surface. The concepts and their features are as follows:



CONCEPT SKETCH NO. 9

FEATURES

- 3MEEDS ENCLOSED IN CARRYING CASE
- CASE ENCLOSED IN SUPER INSULATION FOR TEMPERATURE CONTROL DURING EVA
- 2 MEEDS EXPOSED --10 MIN. MAX
- CONTROL MEED NOT EXPOSED TO SUNLIGHT
- RETRACTABLE SHADOW WAND FOR ALIGNMENT OF MEED WITH SUNS RAYS

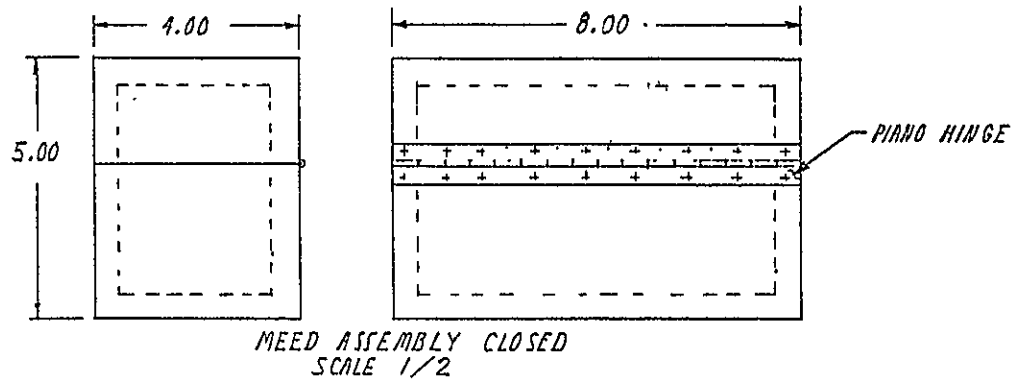


Figure 4.2-1. MEED Assembly in Carrying Case

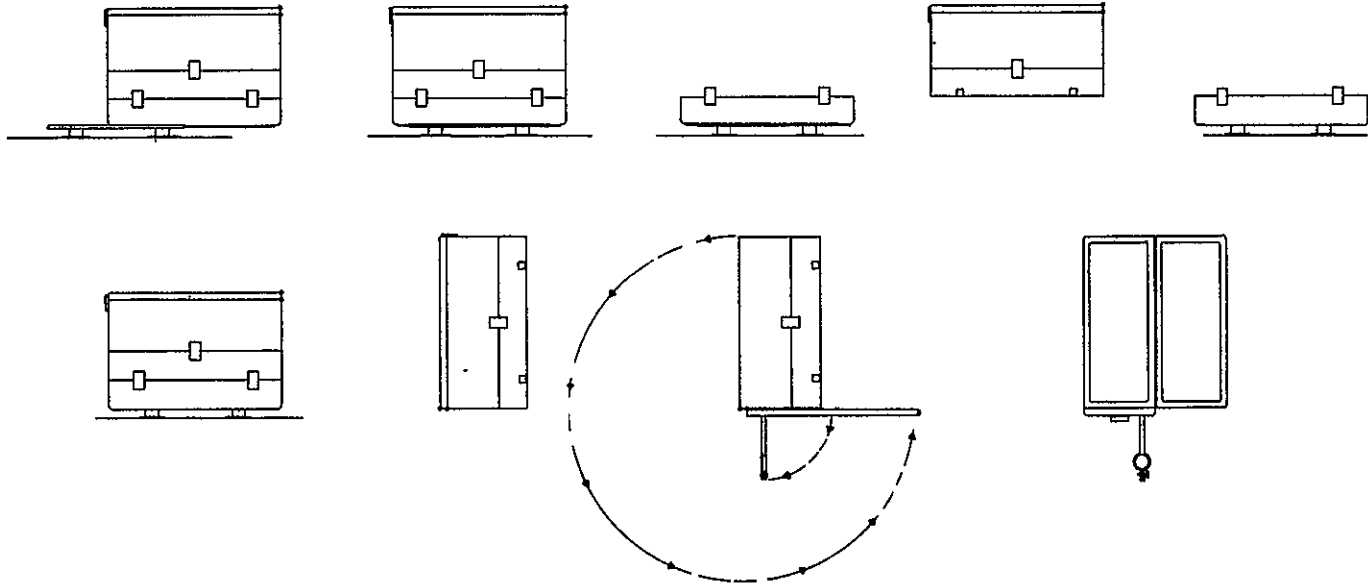


Figure 4.2-2. MEED Flight Assembly Deployment

- a. Attachment of the Lunar Subassembly to Existing Braces on the Legs of the LM (Figure 4.2-3)

At least one of the braces will always be facing the sun regardless of the landing position of the LM. The leg braces are at a reasonable height for astronaut access, and a firm base is provided from which the MEED can be directed toward the solar rays.

- b. Lunar Subassembly Sitting Directly on the Lunar Surface (Figure 4.2-3)

This approach requires a relatively flat lunar surface and ancillary equipment such as an isolation sheet to limit transfer.

- c. Lunar Subassembly Supported on a Spike Driven into the Lunar Surface (not shown)

This method eliminates heat transfer by conduction from the lunar surface, but requires stowage and deployment of a rigid spike. If the lunar surface is excessively hard or rocky, the successful use of the spike is questionable.

#### 4.2.1.3 MEED DESIGN CONCEPTS

Three concepts of the design of the MEED were investigated. These designs are shown in Figure 4.2-4.

- a. Sealed Tray - In this concept, the tray is a pressure vessel with a transparent quartz plate window through which the solar radiation is received. The biological samples are held either in individual wells inside the tray or in wells drilled in section plates. Atmospheric pressure is retained in the tray in the hard vacuum of space by elastomeric seals, and the biological samples are retained in the wells (or cuvettes) by a secondary seal. Preliminary calculations indicated that a quartz thickness of 0.25 inches (6.2 mm) would provide a safety factor of greater than 10:1.

- b. Sealed Sections - The tray holds 16 sections in this concept. Each section is sealed to retain atmospheric pressure, and contains 24 individual cuvettes or wells. The biological samples are retained by a secondary seal in the cuvettes. The features of this system are as follows:

- The quartz section covers can be relatively thin due to the reduced area.
- Accidental loss of pressure in one section does not affect other sections.



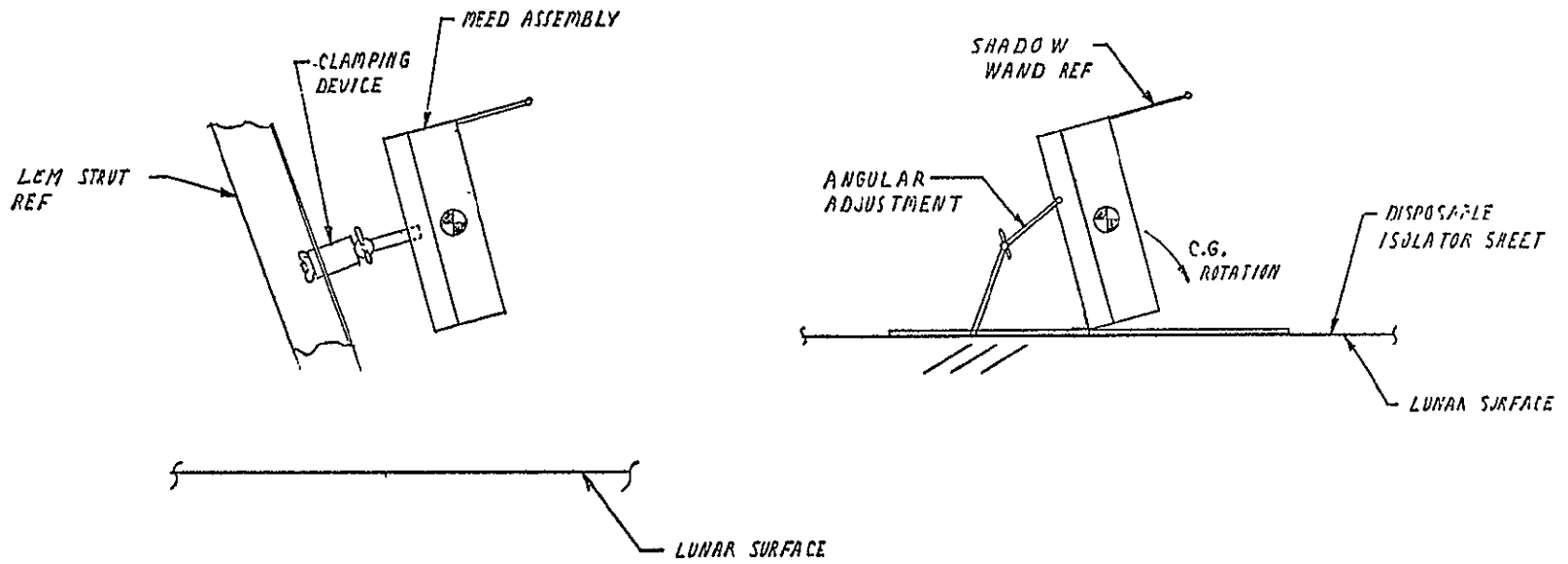
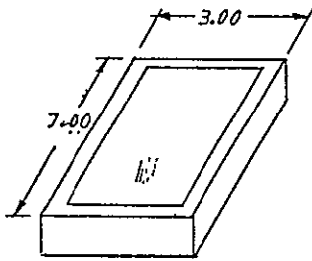
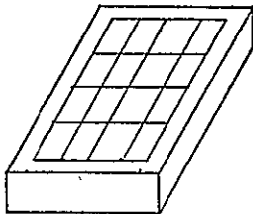


Figure 4.2-3. MEED Assembly - Lunar Surface



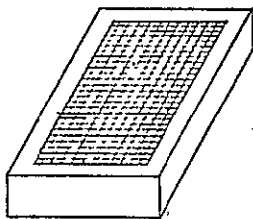
SEALED TRAY

1. TRAY IS PRESSURE VESSEL - QUARTZ COVER .
2. SECTIONS OR INDIVIDUAL WELLS INSIDE TRAY .



SEALED SECTIONS

1. SEALED SECTION IS PRESSURE VESSEL - QUARTZ COVER .
2. DRILLED WELLS OR INDIVIDUAL WELLS INSIDE SECTION .



SEALED WELLS :

1. TRAY AND SECTIONS NOT SEALED
2. WELLS ARE PRESSURE VESSELS .

Figure 4.2-4. General Concepts

- The seal required for the section will require a considerable fraction of the surface area.

c. Sealed Wells - The wells are sealed to hold atmospheric pressure in this concept, and the tray acts as a mechanical holder but is not sealed. The features of this concept are as follows:

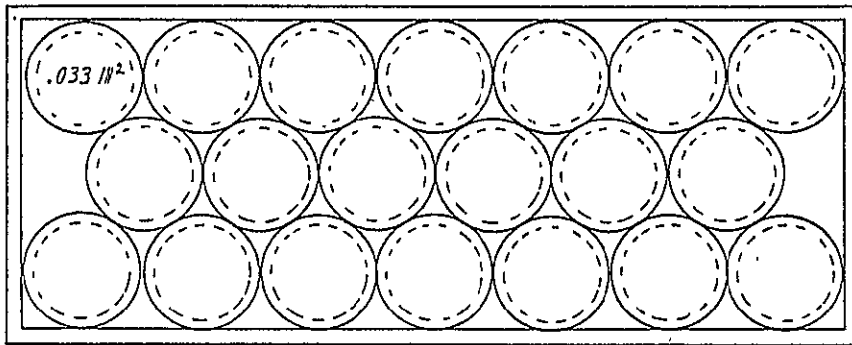
- The tray design is simplified.
- The design of the individual sealed well is complicated by the requirement to provide a positive seal in a space that is approximately 0.25 square centimeters in area.
- The wells are not physically held in place by a transparent cover.

#### 4.2.1.4 CUVETTE AND WELL DESIGN CONCEPTS

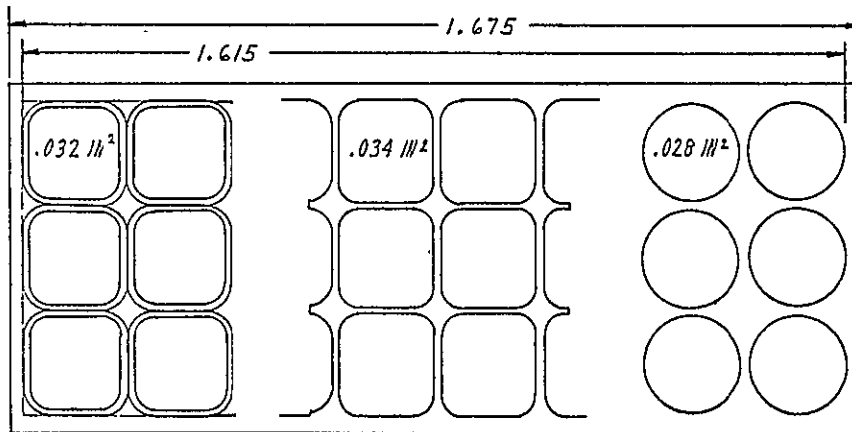
The arrangement and spacing of the individual wells for containing the biological samples depends upon whether they are separate containers or are wells machined in a plate. Variations of possible shapes and spacings are shown in Figure 4.2-5. A concept employing 16 sections of 24 wells each is shown. Wells drilled into a section plate provide a larger cross-sectional area because the double-walled feature of individual wells is eliminated. Circular wells are easier to manufacture, but do not use the available space effectively. The spacing of the wells in a rectangular grid is more effective than equilateral triangular spacing because it eliminates areas of wasted space at the end of each section.

The individual well with a square cross-section in a rectangular grid pattern was selected as the baseline design. The concept of square wells machined in a section plate was selected as an alternate design.

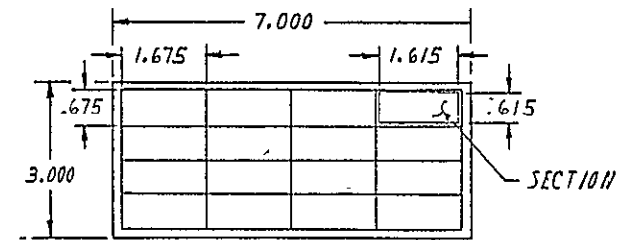
Details of possible individual wells, each with positive seals to retain atmospheric pressure, are shown in Figures 4.2-6 through 4.2-9. Each has a redundant pressure seal comprised of an "O" ring or some other form of elastic seal backed up by one or more secondary seals of potting compound or cement. All of the well designs include a small thin-walled quartz cuvette to hold the biological sample; a pressure control volume, to minimize pressure variation within the cuvette; and an individual filter pack for radiation wavelength and intensity control. These well design concepts do not require a pressurized external environment as provided by the pressurized tray with the single quartz window. The designs, while mechanically



20 WELL SECTION  
SCALE 10/1

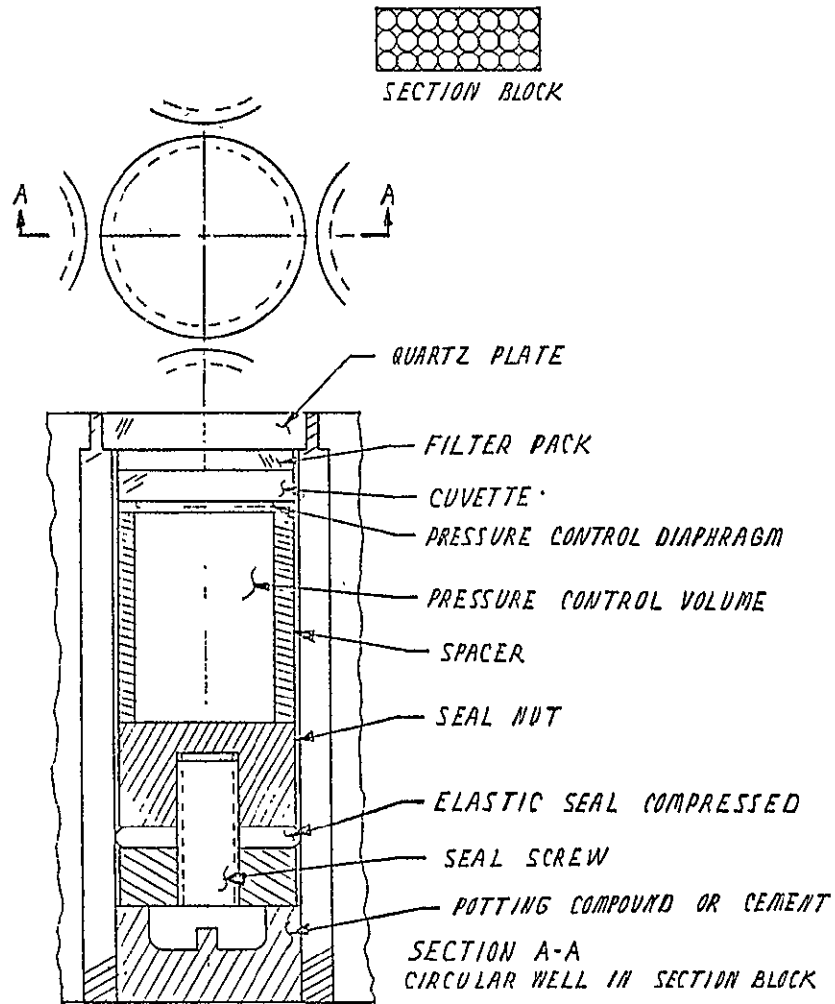


24 WELL SECTION  
OPTIONAL WELL SHADES  
SCALE 10/1



SECTIONS ARRANGEMENT IN TRAY  
SCALE 1/2

Figure 4.2-5. Alternate Well Arrangements



CONCEPT SKETCH NO. 4

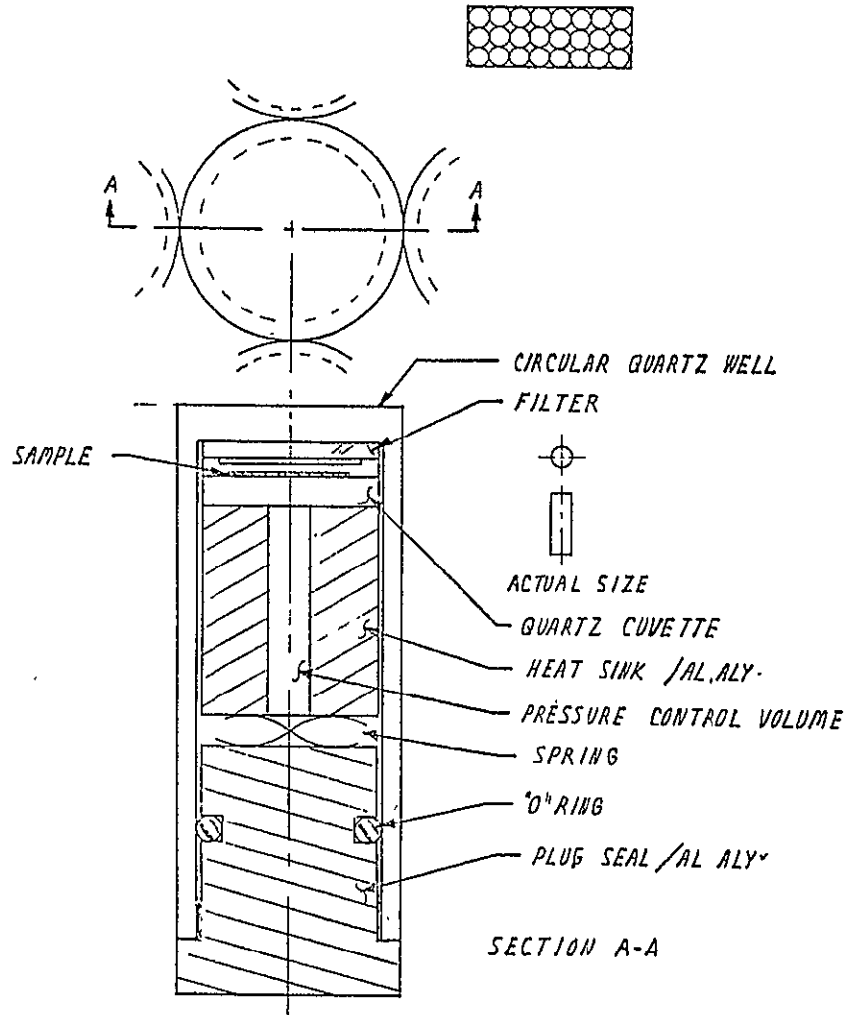
FEATURES

- CIRCULAR WELL DRILLED IN ONE-PIECE SECTIONS
- BONDED QUARTZ TOP
- SEPARATE QUARTZ BIOLOGICAL SAMPLE HOLDER ( CUVETTE)
- PRESSURE CONTROL VOLUME AND DIAPHRAGM
- TRIPLE SEAL- SAMPLE TO VACUUM

PROBLEMS

- SMALL PARTS TO ASSEMBLE IN GLOVE BOX
- BONDED TOP --POSSIBLE LEAK PATH
- PRESSURE HELD BY BONDING, FRICTION
- CIRCULAR SHAPE REDUCES SAMPLE AREA
- ( ALTERNATE DESIGN--SQUARE WELL CROSS SECTION )

Figure 4.2-6. Circular Well Drilled in Section Block



CONCEPT SKETCH NO. 5

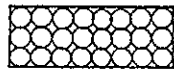
FEATURES

- SEPARATE CUVETTE (SAMPLE HOLDER)
- PRESSURE CONTROL VOLUME AND DIAPHRAGM
- SEAL-- "O" RING PLUS ADHESIVE

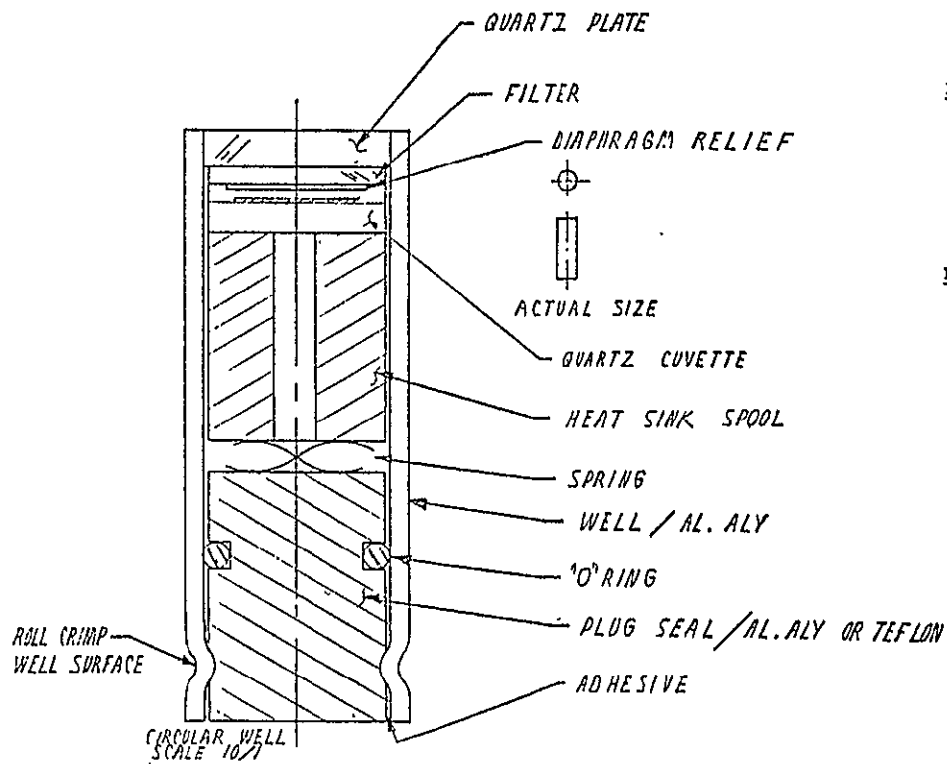
PROBLEMS

- PRESSURE HELD BY ADHESIVE BOND
- ADHESIVE APPLIED AFTER LOADING
- SAMPLE IN GLOVE BOX
- CIRCULAR SHAPE REDUCES SAMPLE AREA

Figure 4.2-7. Circular Quartz Well



SECTION ACTUAL SIZE



CONCEPT SKETCH NO. 6

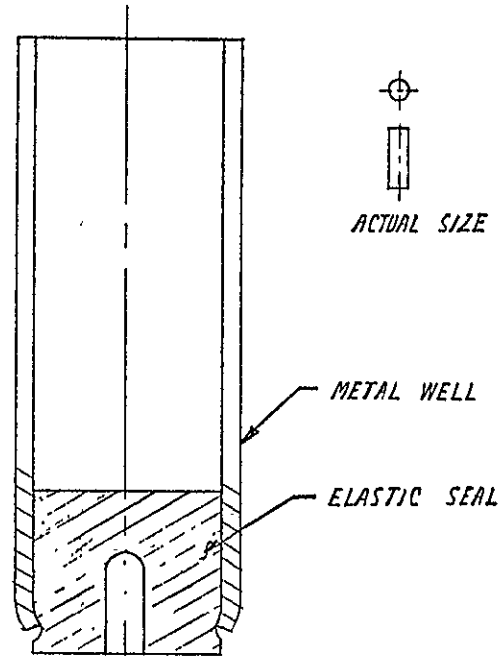
FEATURES

- ONE-PIECE CIRCULAR QUARTZ WELL
- SEPARATE CUVETTE (SAMPLE HOLDER)
- PRESSURE CONTROL VOLUME AND DIAPHRAGM
- MULTIPLE SEAL--CUVETTE, "O" RING, ROLL CRIMP, ADHESIVE

PROBLEMS

- CRIMPING OF WELL MUST BE DONE IN GLOVE BOX
- CIRCULAR WELL CROSS-SECTION REDUCES SAMPLE AREA

Figure 4.2-8. Seal Detail



CONCEPT SKETCH NO. 7

FEATURES

- ELASTIC SEAL STRETCHED INTO PLACE AND RELEASED
- CRIMPED METAL WELL END

PROBLEMS

- LEAKAGE OF GAS THROUGH SINGLE SEAL

Figure 4.2-9. Well Seal Detail



feasible, are excessively complex and intricate considering the large number of biological samples required.

Quartz cuvettes that would fit inside of pressurized wells are shown in Figure 4.2-10. The concepts provide for samples that are from a few microns to 3 or 4 millimeters thick. The cuvettes can be sealed by injecting a sealing compound (such as agar or paraffin) after loading the biological samples, or by crimping metal tubes bonded into the cuvette. All of the designs shown can be fabricated in circular or square cross-sections.

#### 4.2.2 BASELINE DESIGN CONCEPT

The baseline design concept comprises design features selected from the concepts reviewed in the concept evaluation.

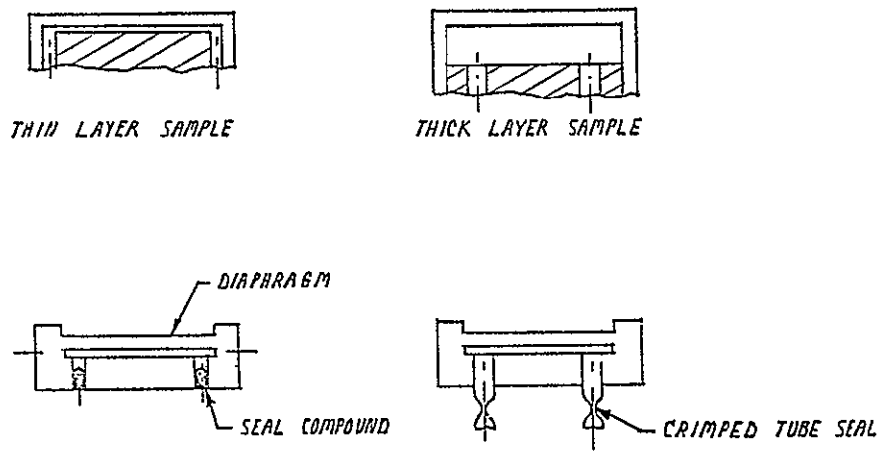
The baseline design of the MEED Flight Assembly is essentially that shown in Figure 4.2-1 (Lunar Subassembly), with an additional insulated MEED (CM Subassembly) attached as shown in Figure 4.2-2.

The concept selected as a baseline design for the MEED is based on features of the design shown in Figure 4.2-11.

These design features are as follows:

- The tray is a pressure vessel designed for earth atmospheric pressure inside and the hard vacuum of space on the outside.
- Radiation enters through a quartz plate window approximately 6 mm (0.25 in) thick. The selected method of sealing is an elastomeric "O" ring in a bolted flange.
- The quartz window will be either bonded to the tray or sealed by an "O" ring.
- The base of the tray will serve as a heat sink if that is required to maintain the biological sample temperature.
- The function of the well and the cuvette have been combined, thus eliminating the well, and the cuvettes are made of quartz and are crushable for easy extraction of the sample.
- The radiation filter packs are either individually sized for the cuvettes or cover a section of 24 cuvettes.

Anticipated problems include 1) the bonding of the quartz top to the aluminum tray, 2) the effect of the relatively thick quartz plate window on the incoming radiation and on temperature control, and 3) the reduction of leakage through the elastomeric seals to the required level.



*NOTES :*

1. ALL CUVETTES BONDED QUARTZ .
2. SEAL COMPOUND - AGAR OR BIO-STATIC ADHESIVE .
3. SQUARE OR ROUND CROSS SECTIONS .

Figure 4.2-10. Cuvette Types

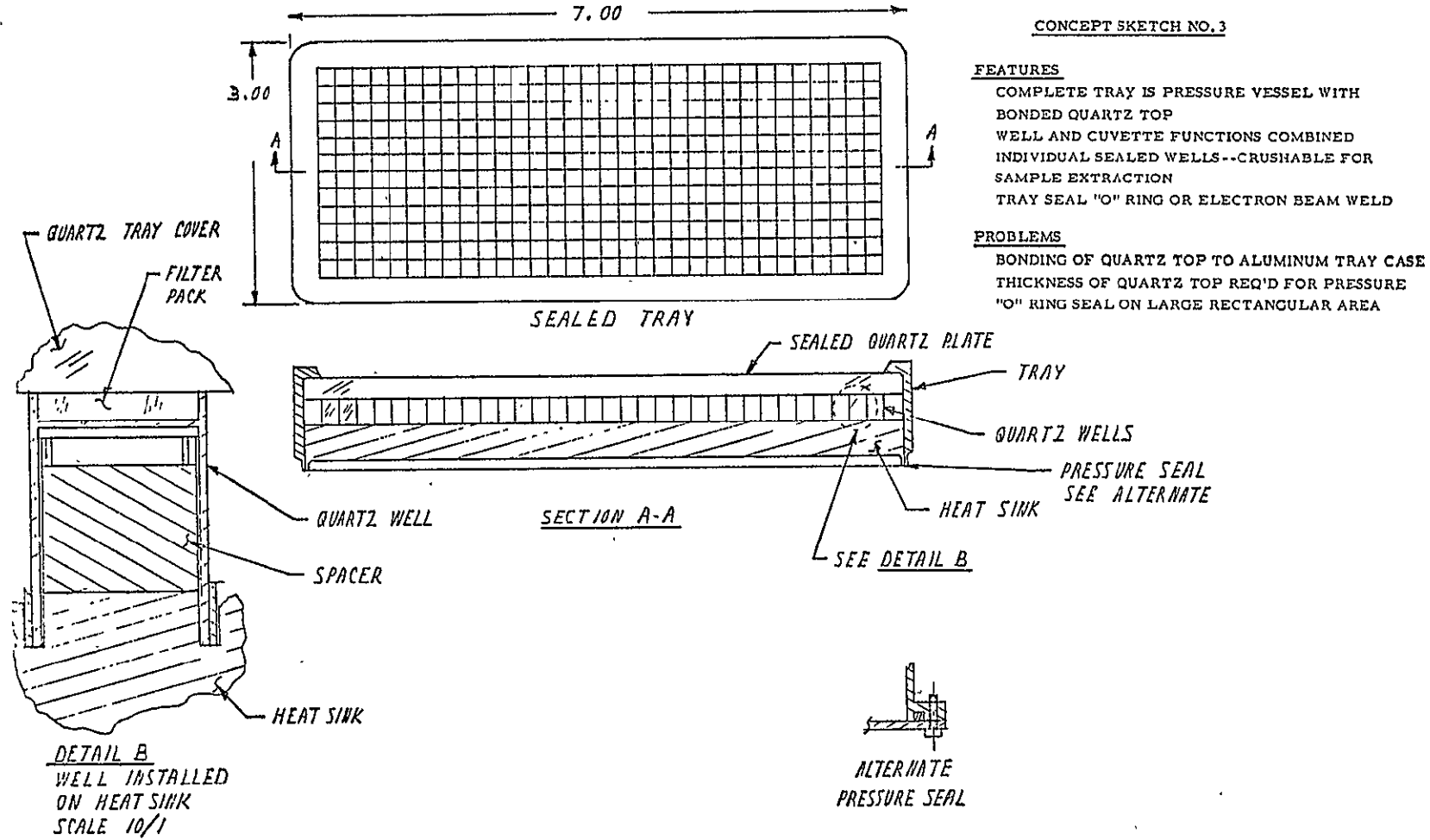


Figure 4.2-11. Sealed Tray - Square Wells (Baseline Design)

### 4.3 FEASIBILITY INVESTIGATIONS

The feasibility investigations were based on the problems and design uncertainties inherent in the baseline and alternate design concepts. The investigations comprise design studies, analyses, and experimentation (as appropriate) to establish the feasibility of the selected baseline concepts and to develop additional design details where required.

#### 4.3.1 MEED FLIGHT ASSEMBLY

##### 4.3.1.1 REQUIREMENTS

The MEED Flight Assembly will ultimately have to be capable of meeting the vibration, shock, acceleration, acoustic noise, and environment requirements imposed by the Apollo program.

A summary of the vibration requirements is included in Table 4.3.1-1. Acoustic noise is not considered to be a problem requiring investigation. The shock requirements of 78 "g's" for 25 ms (safety) and 45 "g's" for 25 ms (operation) require considerable design attention. The external pressure conditions will vary from earth atmospheric pressure prior to takeoff and after landing, approximately 7 psia of oxygen during the flight, and the hard vacuum of space while on the lunar surface. The acceleration requirements are included in Table 4.3.1-2. The other environmental requirements of sand and dust, salt spray, and fungus growth do not represent major constraints that require feasibility analysis, primarily because of the lack of electric equipment in the Flight Assembly.

The preliminary requirement for 384 sealed cuvettes for each MEED was modified at the completion of the concept selection study. The new requirement is for approximately 288 sealed cuvettes to be housed in a sealed position of the MEED with one atmosphere of air pressure inside, and 96 vented cuvettes to be housed in a vented section of the MEED. Suitable filters to retain microbes of 1/2 micron size are to be installed in both the vented cuvettes and the vented portion of the MEED.

##### 4.3.1.2 DESIGN

The feasibility study of this assembly was comprised of the development of detailed design concepts of the mechanical aspects of the carrying case and ancillary equipment, the construction of a flight assembly mock-up, the modification of the clamp and its deployment mechanism, the preliminary selection of shock

Table 4.3.1-1

PRELIMINARY VIBRATION REQUIREMENTS

Sinusoidal

Sweep 20 - 2000 Hz at 3 g peak

Random

Command Module Launch Mode (90 sec - 3 planes)

20 - 100 Hz	60 dB/octave increase
100 - 400 Hz	0.08 g <sup>2</sup> /Hz
400 - 2000 Hz	6 dB/octave decrease

Command Module High Q Above Mode (10 sec - 3 planes)

20 - 100 Hz	60 dB/octave increase
100 - 2000 Hz	0.08 g <sup>2</sup> /Hz

Lunar Module Launch Mode (12 min - 3 planes)

20 - 100 Hz	0.01 g <sup>2</sup> /Hz
100 - 120 Hz	12 dB/octave decrease
120 - 2000	0.005 g <sup>2</sup> /Hz

Table 4.3.1-2

PRELIMINARY ACCELERATION REQUIREMENTS

Longitudinal Axis	7.0 g*
Lateral Axis	4.0 g

Note: Axes are in respect to launch vehicle.

absorbers, and a weight analysis.

The design concept of the MEED Flight Assembly is derived from the baseline concepts of Figures 4.2-1, 4.2-2, and 4.2-4. Additional design details of the carrying case and ancillary equipment are shown in Figure 4.3.1-1. The side view of the flight assembly shows the double-walled carrying case construction. The Lunar Subassembly is completely enclosed in "super insulation" comprised of multiple layers of aluminized Mylar (not shown). The separation between the inner and outer walls is effected by insulating standoffs. The Lunar Subassembly contains two Type A MEEDs and one Type B MEED (control). The CM Subassembly contains one Type B MEED supported in a double-walled case that matches and clamps to the Lunar Subassembly case.

The latches shown are satisfactory for the deployment on the lunar surface, when modified with straps that can be grasped by the astronaut. The opening and closing of the strapped latches by heavily-gloved hands is shown in Figure 4.3.1-2. The latches shown will be supplemented by a steel strap with steel latches (not shown) that will insure the integrity of the Flight Assembly and the Lunar Subassembly during the launch and landing sequences on both the earth and the moon.

A mock-up of the MEED Flight Assembly was fabricated to provide a display of the design concepts and to serve as a working tool for design improvement. Figure 4.3.1-3 is a view of the mock-up in its carrying case. Figure 4.3.1-4 is a view of the open carrying case with the MEED Flight Assembly and the simulated LM brace. The MEED Flight Assembly is shown attached to the simulated Command Module soft mount in Figure 4.3.1-5. In Figure 4.3.1-6, the Lunar Subassembly has been detached to simulate transport to the LM. In this view, the CM Subassembly remains on the Command Module soft mount. This unit serves as a control unit, and remains in lunar orbit while the Lunar Subassembly is on the lunar surface. The mock-up of the CM Subassembly shows a simulated Type A MEED. A Type B MEED will be used in this assembly during the experiment since the CM control unit is not exposed to radiation and does not require a quartz cover and radiation filters.

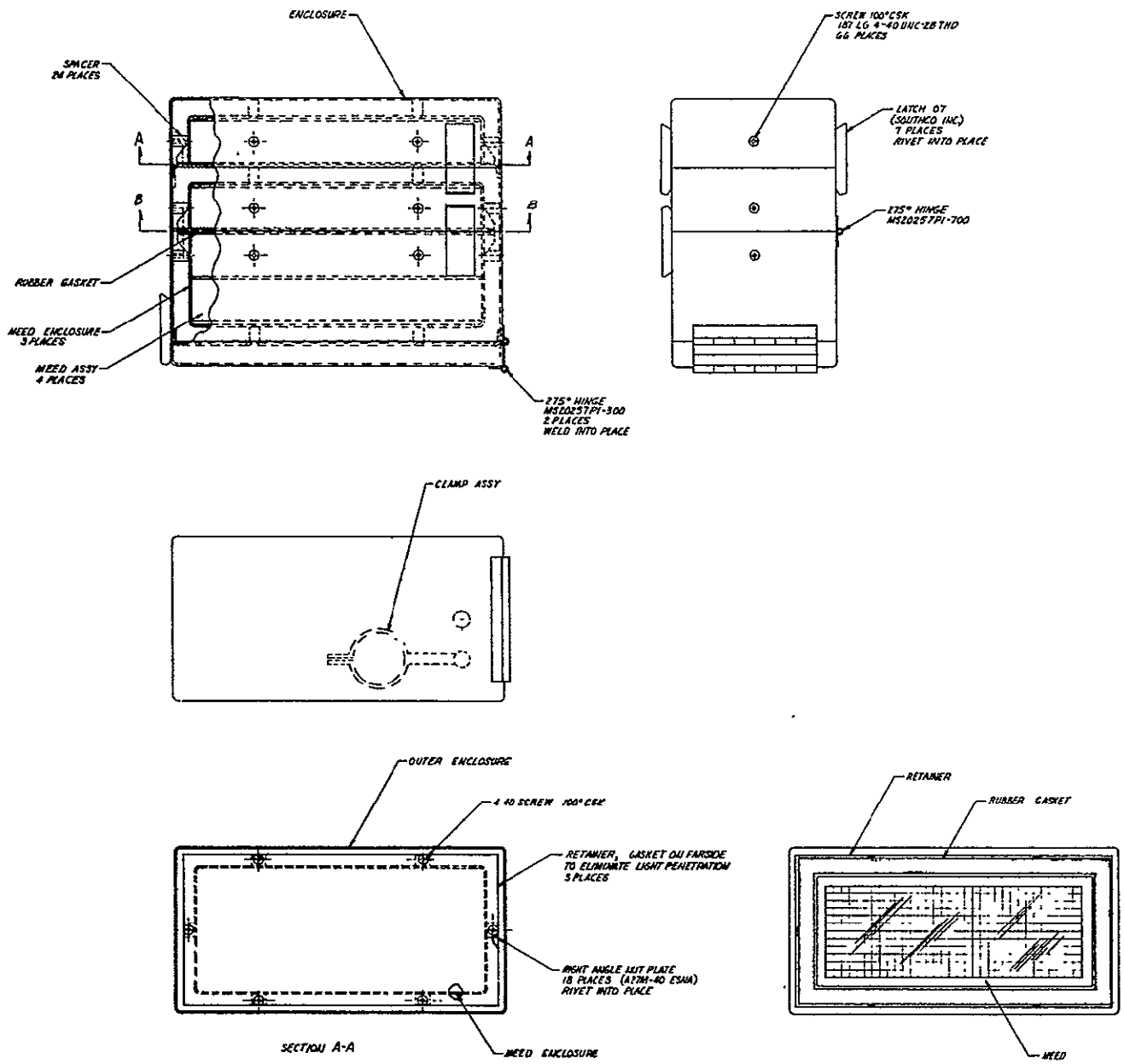


Figure 4.3.1-1. MEED Flight Assembly

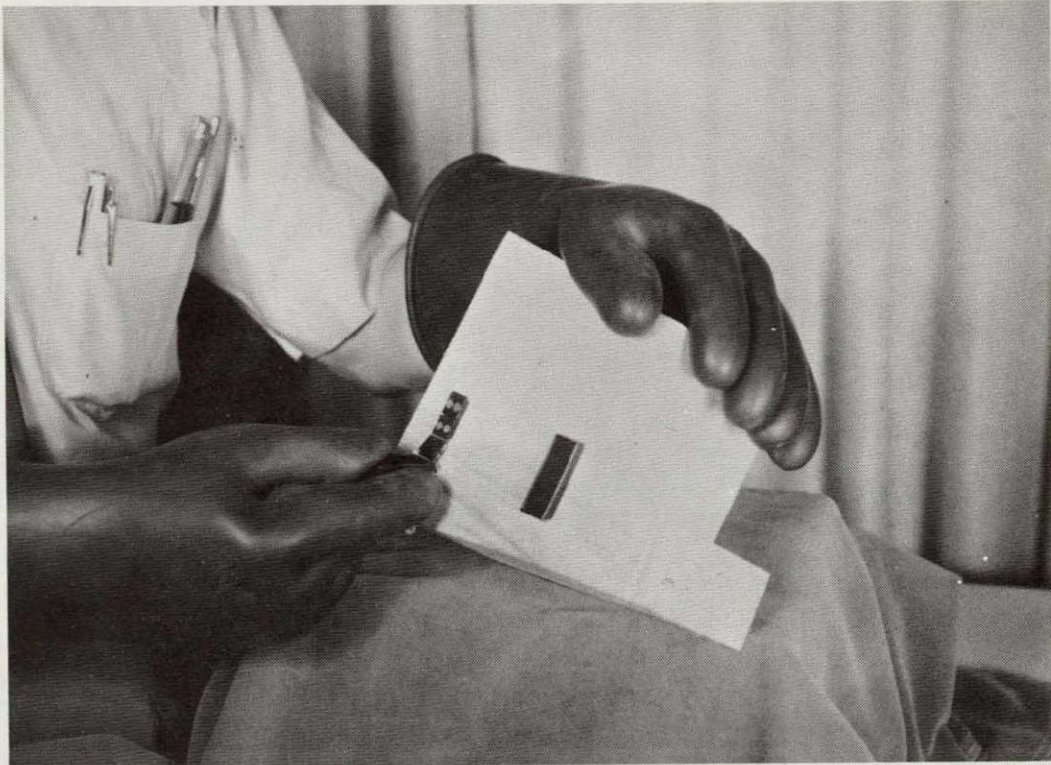


Figure 4.3.1-2. Manipulation of Latches





Figure 4.3.1-3. Mock-up Carrying Case

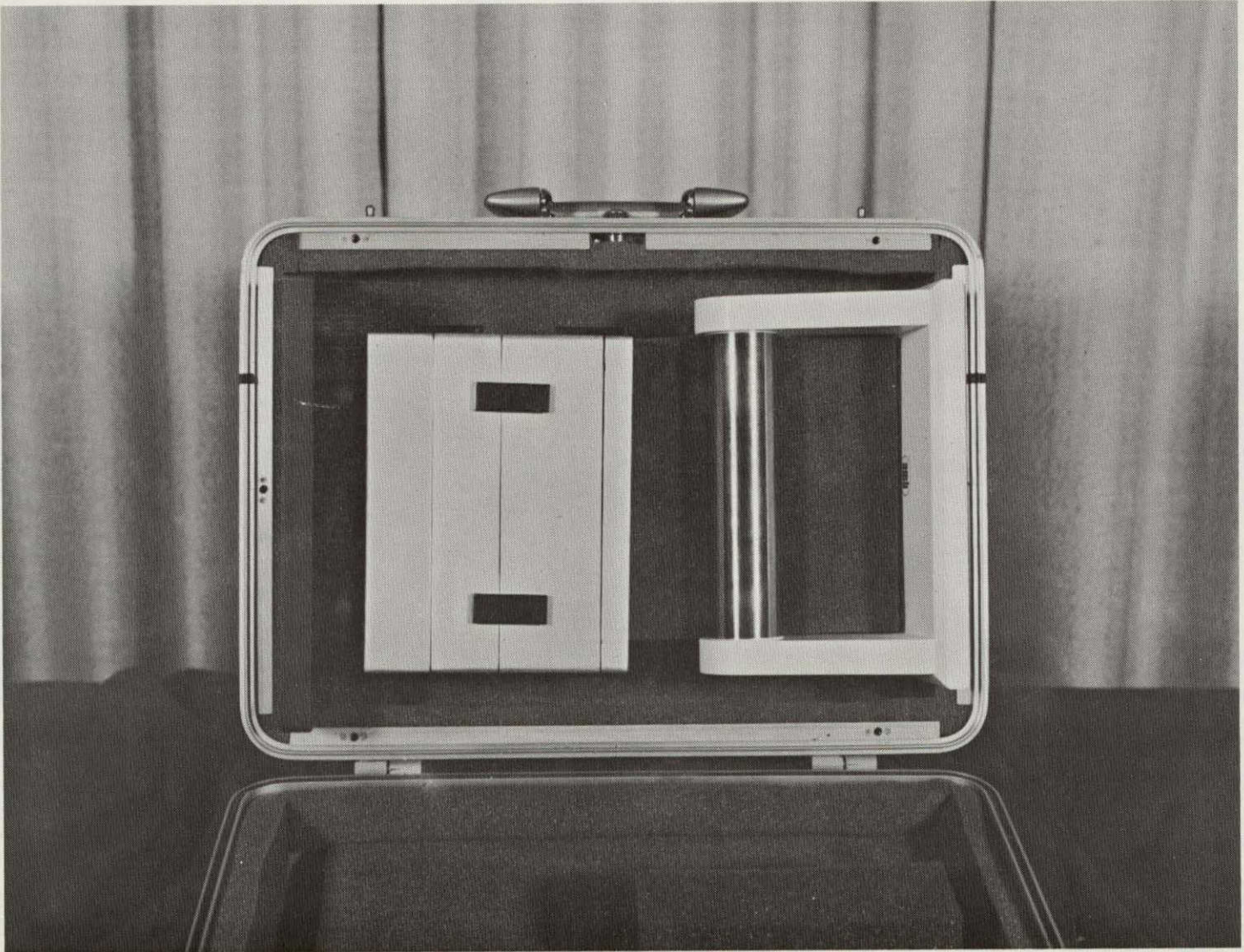


Figure 4.3.1-4. Mock-up in Carrying Case

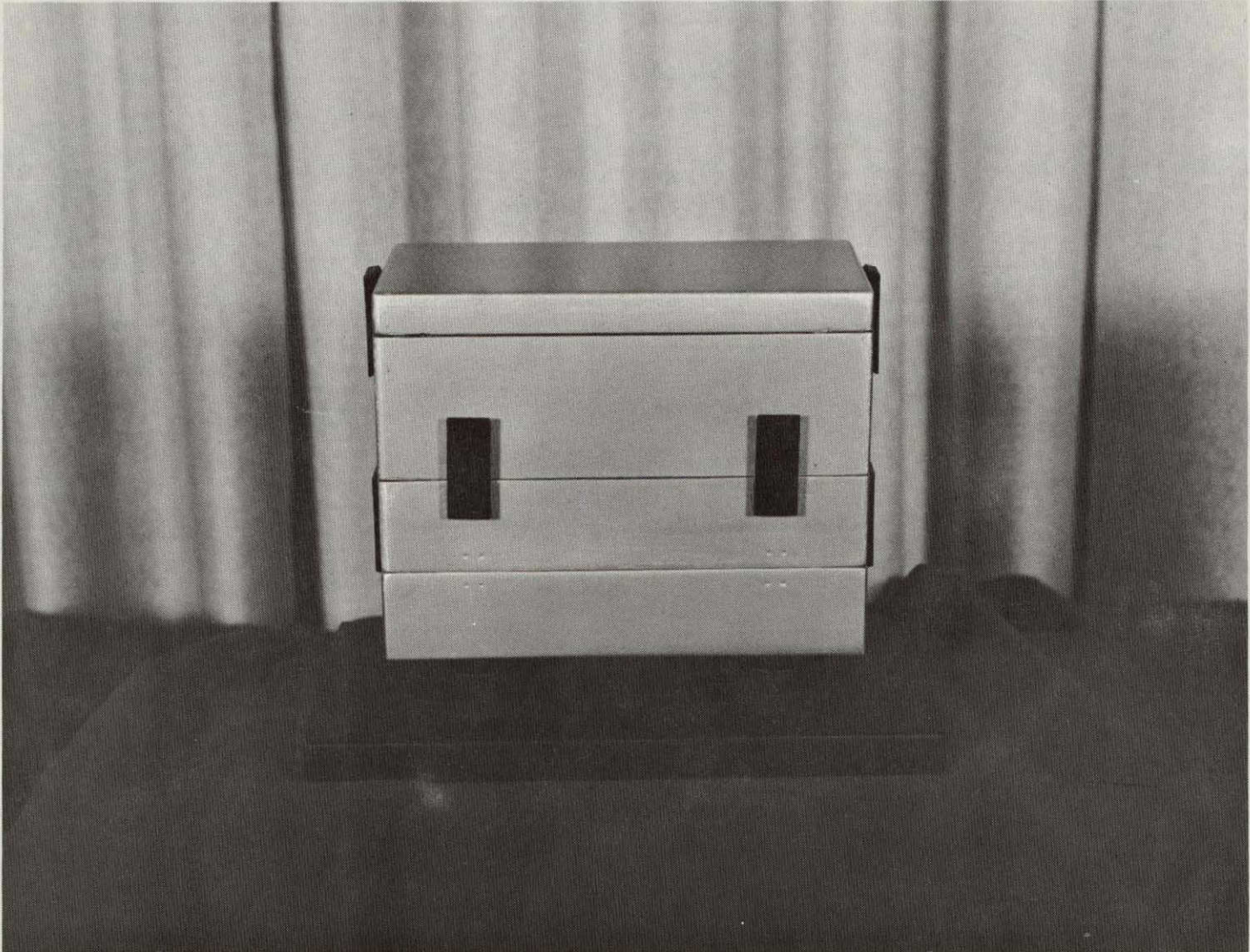


Figure 4.3.1-5. Mock-up Flight Assembly on Soft Mounts

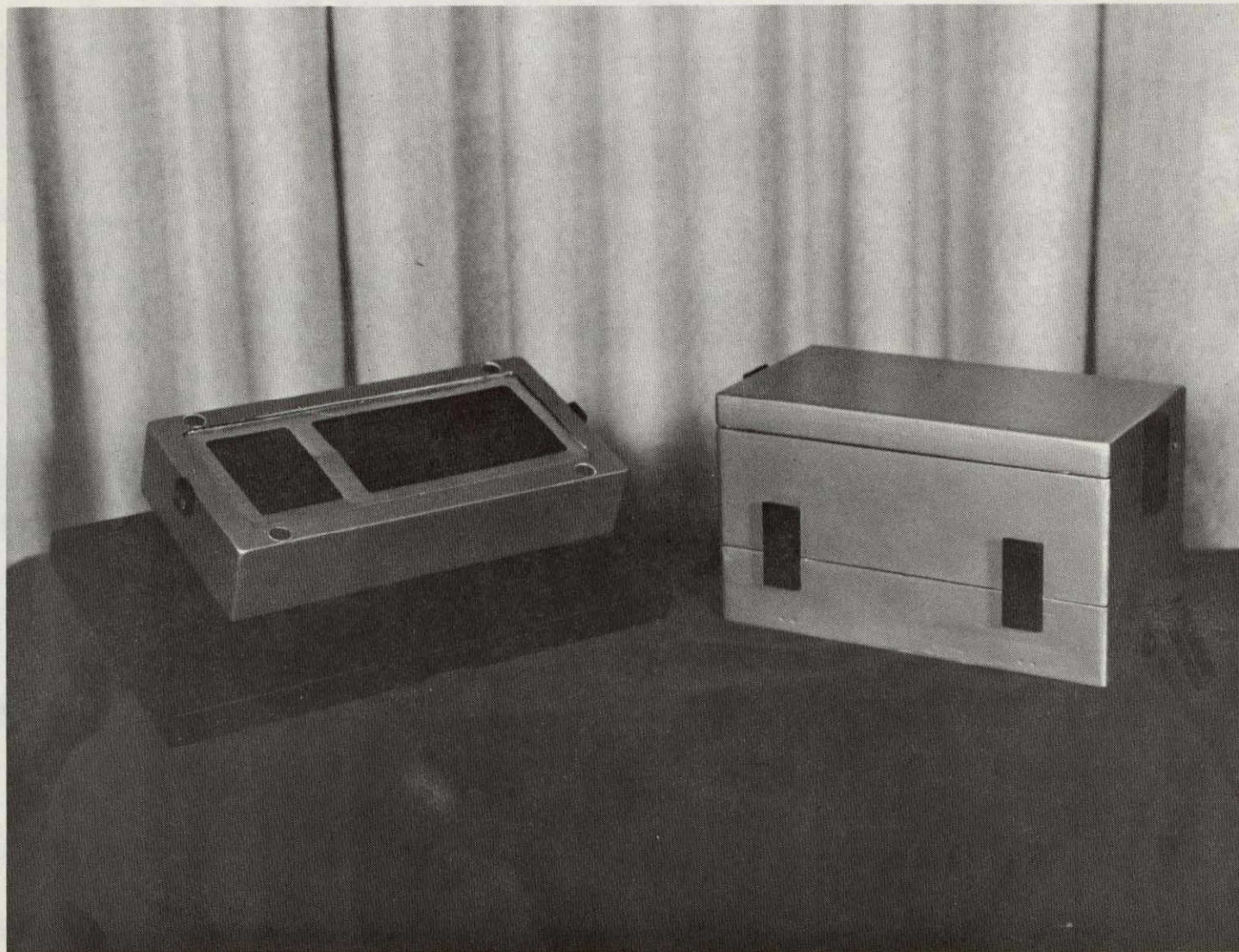


Figure 4.3.1-6. Lunar Subassembly Mock-up

Figure 4.3.1-7 shows the mock-up of the Lunar Subassembly with the two Type A MEEDs deployed for exposure. In the final design, each MEED will be protected from radiation until the unit has been pointed toward the sun; then light covers, similar to camera film-pack slides, will be pulled to start the exposure (see Protocol, Section 4.3.10.1). The simulated wand, mounted at right-angles to the MEED surface, provides the astronaut with a positive indication of perpendicularity of the solar radiation. The MEEDs are ready for exposure when the circular shadow of the wand tip is concentric with the base of the wand.

The clamp used to attach the Lunar Subassembly to the LM leg brace is shown in Figure 4.3.1-7. A side view of the original mock-up version of the clamp is shown in Figure 4.3.1-8. Several features of the clamp design have been revised based on experience gained in deploying the mock-up. The original clamp provides a strong friction-based grip on the brace. The revised clamp will include a spring-action (as shown in Figure 4.3.1-9) to accommodate possible variations in the diameter of the LM brace. Some difficulty was experienced in closing the original clamp prior to locking it during mock-up deployment. The design was revised to include an over-center spring-action which allows the clamp to be cocked during positioning, and then causes the clamp to automatically close when it is positioned on the LM brace. This feature is shown in Figure 4.3.1-9. The modified clamp hardware is shown in Figure 4.3.1-10.

#### 4.3.1.3 MOUNTING

The results of calculations (Appendix B) show that the soft mounts cannot be made deep enough to attenuate significantly the maximum anticipated shock load of 78 "g's" for 25 milliseconds. The mounts cannot attenuate the lower level, longer duration acceleration indicated by Table 4.3.1-2; however, a system designed to withstand the shock requirements will easily meet the acceleration requirements.

The primary purposes of the soft mounts will be to retain the assemblies under the shock loading and to attenuate the vibrations defined approximately in Table 4.3.1-1.

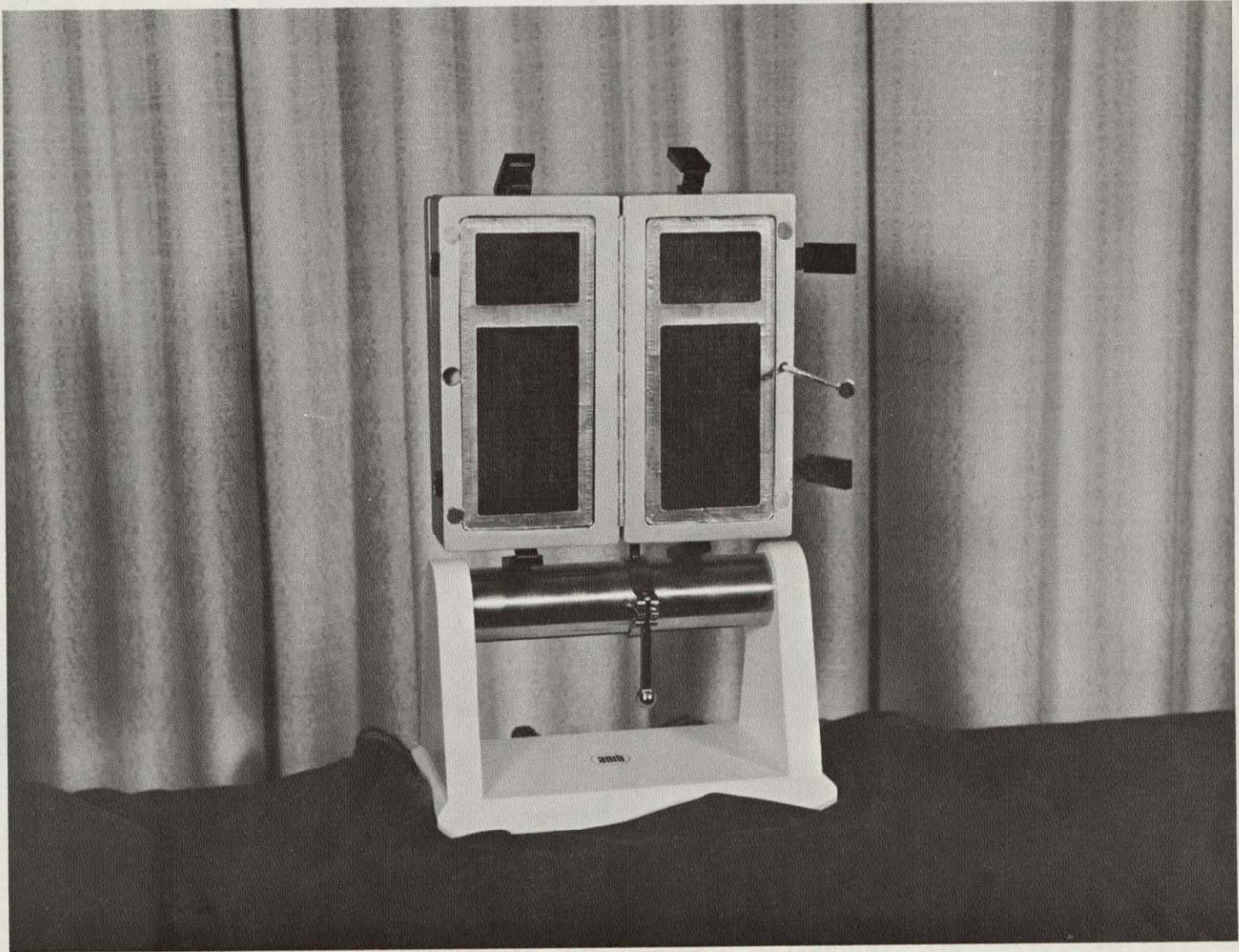


Figure 4.3.1-7. Mock-up of Deployed MEED.

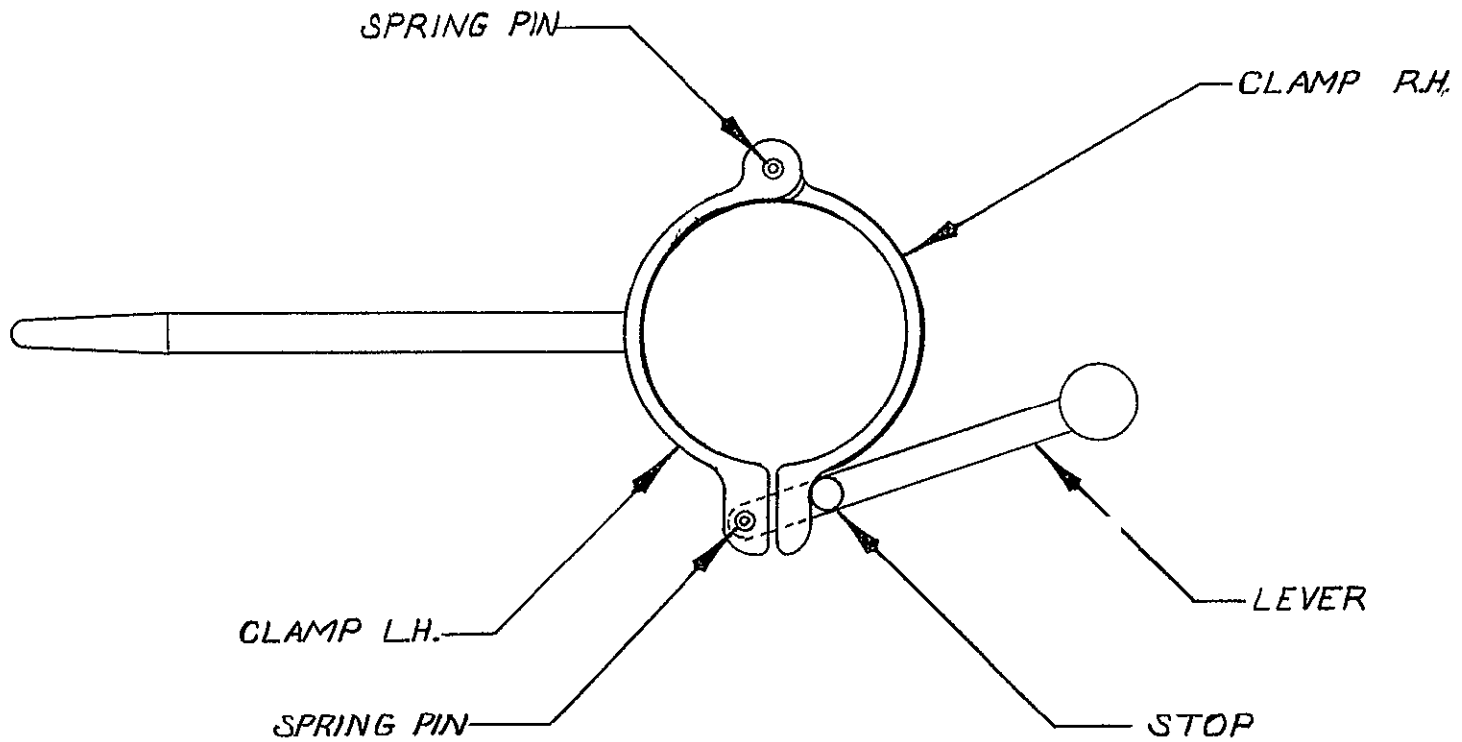


Figure 4.3.1-8. MEED Clamp Assembly

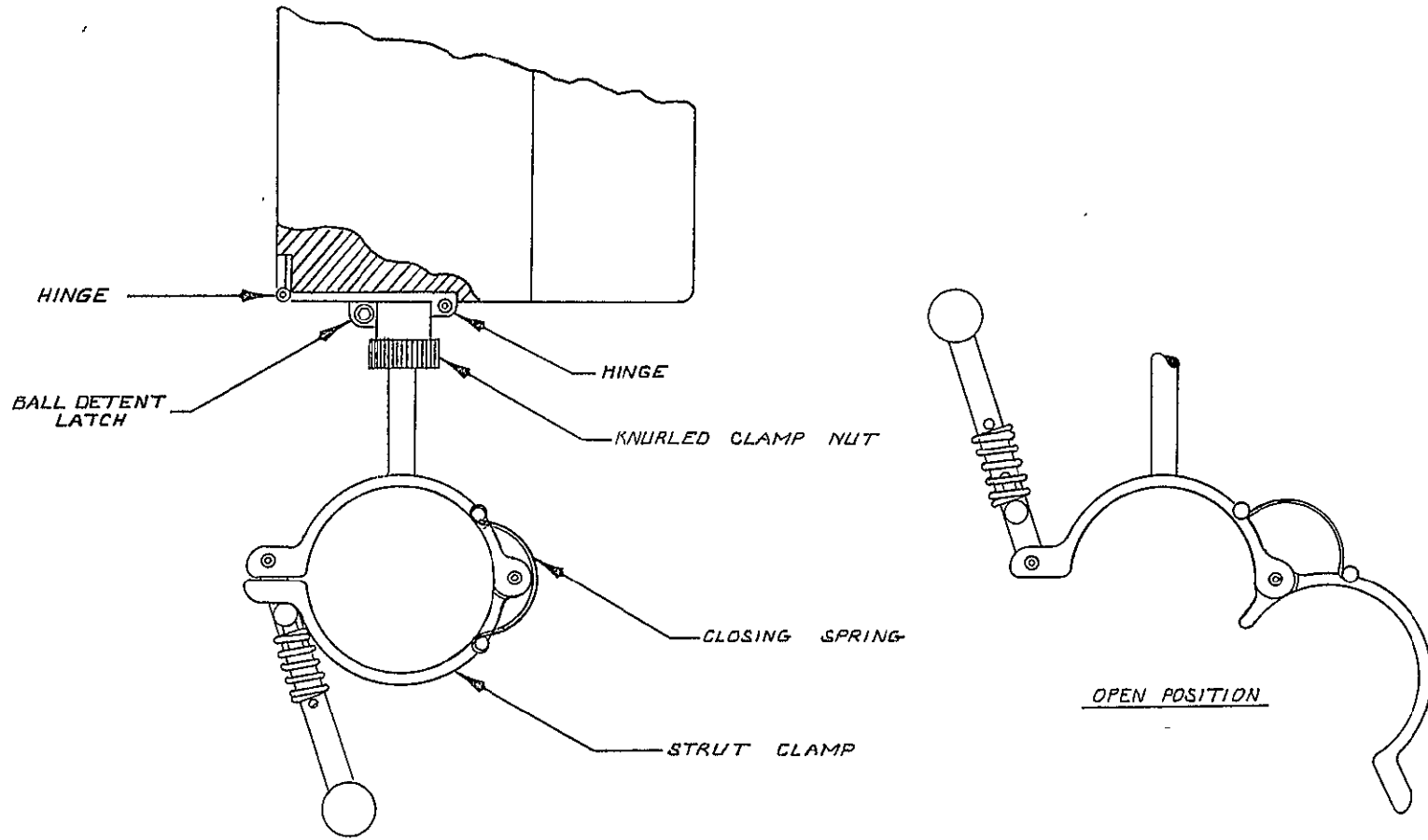


Figure 4.3.1-9. MEED Modified Strut Clamp Assembly



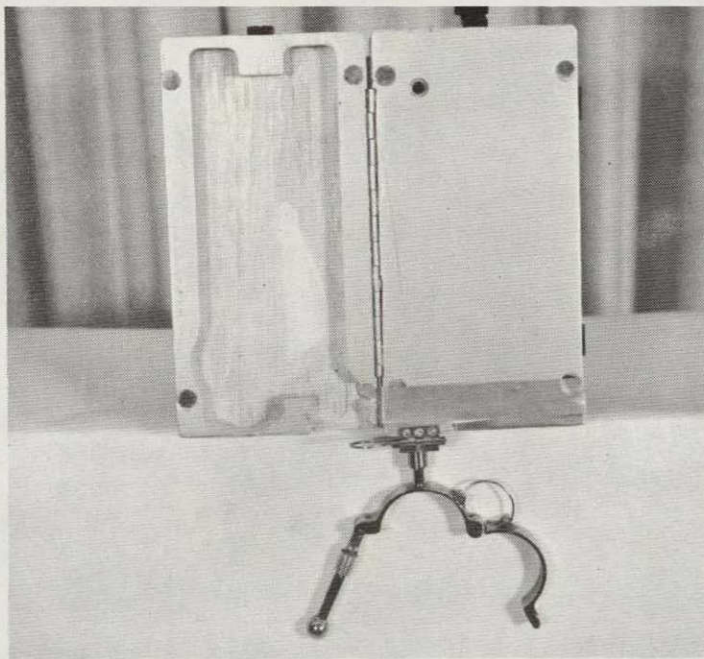
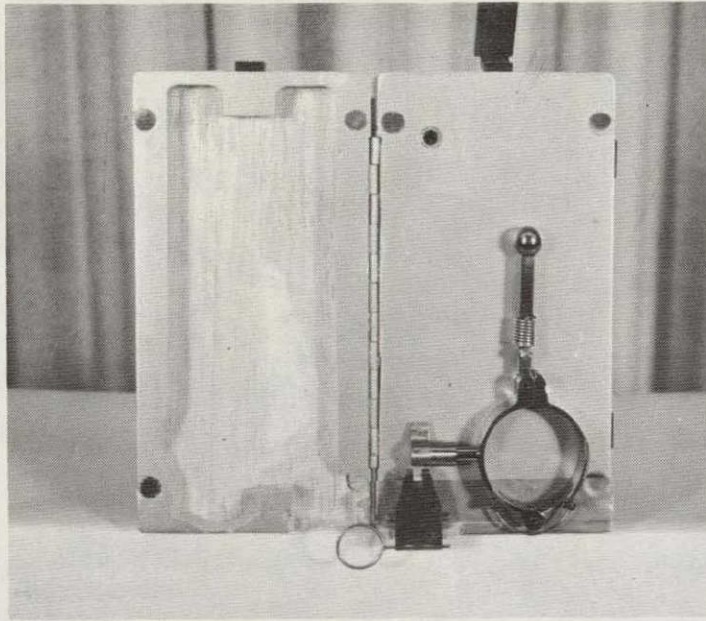


Figure 4.3.1-10. Modified Mock-up Clamp Assembly

The Flight Assembly and the Lunar Subassembly must be able to withstand 78 "g's" for 25 ms in any duration. This corresponds to a force of 354 kg (780 lbs) through the center of mass of the Flight Assembly in any direction. Three potential problem areas must be investigated for the situation where the force is perpendicular to the plane of the mounts. These are 1) an excessive unit load on the soft mounts, 2) a force great enough to separate the cuvette from its contact with the neutral density filter, and 3) an excessive pressure between the cuvettes and the neutral density filters.

The results of the calculations of Appendix B indicate that each soft mount must carry a load of approximately 86.5 kg (195 lbs), an amount which results in mounts of reasonable size. The results of other calculations (Appendix B) show that a shock pressure of less than one psi will exist between cuvettes and the neutral density filters, and that a pressure of the same magnitude is required to prevent separation between the cuvette and the neutral density filter if the direction of the load is reversed.

The results of calculations (Appendix B) show that a side load of 354 kg (780 lbs) passing through the center of mass of the Flight Assembly will cause maximum loads of 475 lbs (216 kg) on each mount. This is the maximum load requirement on the soft mount and sets the load to which the mount was designed.

The selected vibration isolator (soft mount) is the Model HTO-3 (Lord Manufacturing) which is made of steel and silicone elastomer. The unit has a natural frequency in translation of approximately 20 cps (4 mounts to support Flight Assembly). At this frequency, the magnification of vibration will be approximately 2.5 to 1. Vibrations will be heavily damped at all frequencies above 30 cps. This selection is dependent upon the nature of the supporting structure that is available for mounting the unit in the Command Module and the LM. The vibration isolator finally selected will depend upon mechanical factors resulting from this structural interface.

#### 4.3.2 MEED

The MEED consists of a tray loaded with cuvettes, radiation and temperature indicating devices, and the required radiation filters. The final design of the MEED is shown in Figure 4.3.2-1.

##### 4.3.2.1 REQUIREMENTS

The following requirements apply to the MEED design:

- Window covering must cause a minimum attenuation of the solar ultraviolet intensity.
- The system must maintain a pressure of  $14.7 \pm 2$  psia throughout the experiment.
- The burst pressure of the MEED must be adequate to provide a high overall factor of safety.
- The MEED must keep the biological sample temperatures at  $20^{\circ} \pm 5^{\circ} \text{C}$ .
- Provide approximately one-fourth of its surface area in a vented chamber that will hold vented cuvettes.
- Provide approximately three-fourths of its surface area in a sealed chamber that will hold sealed cuvettes.
- Maintain mechanical integrity under shock loads of 78 "g's" for 25 milliseconds.
- Maintain mechanical integrity and its experiment performance requirements under shock loads of 45 "g's" for 25 milliseconds.

##### 4.3.2.2 DESIGN FEATURES - MEED

The MEED (Figure 4.3.2-1) is comprised of a tray that has an aluminum base and cover, a quartz plate window to admit solar radiation, and a filter pack to restrict the wavelength and intensity of the solar radiation.

#### 4.3.3 TRAY

The general arrangement of the MEED tray components (the cover, base, quartz plate, bolts, nut plate, and the seals) is shown in Figure 4.3.2-1. Hardware components from an earlier but similar design that was entirely sealed are shown in the photograph of Figure 4.3.3-1.

The quartz plate is contained between the cover and the base which are bolted together. The quartz plate is separated from the cover and the base by thin layers of elastomeric material surrounding the elastomeric seals. The thickness of the quartz plate for the single-window design was established by calculation and checked by burst tests

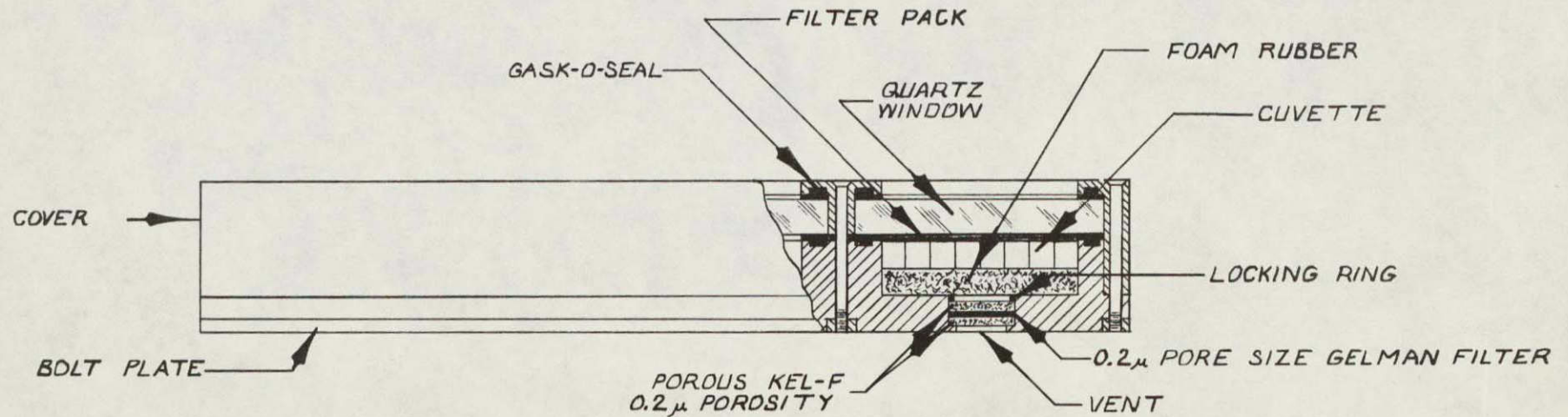
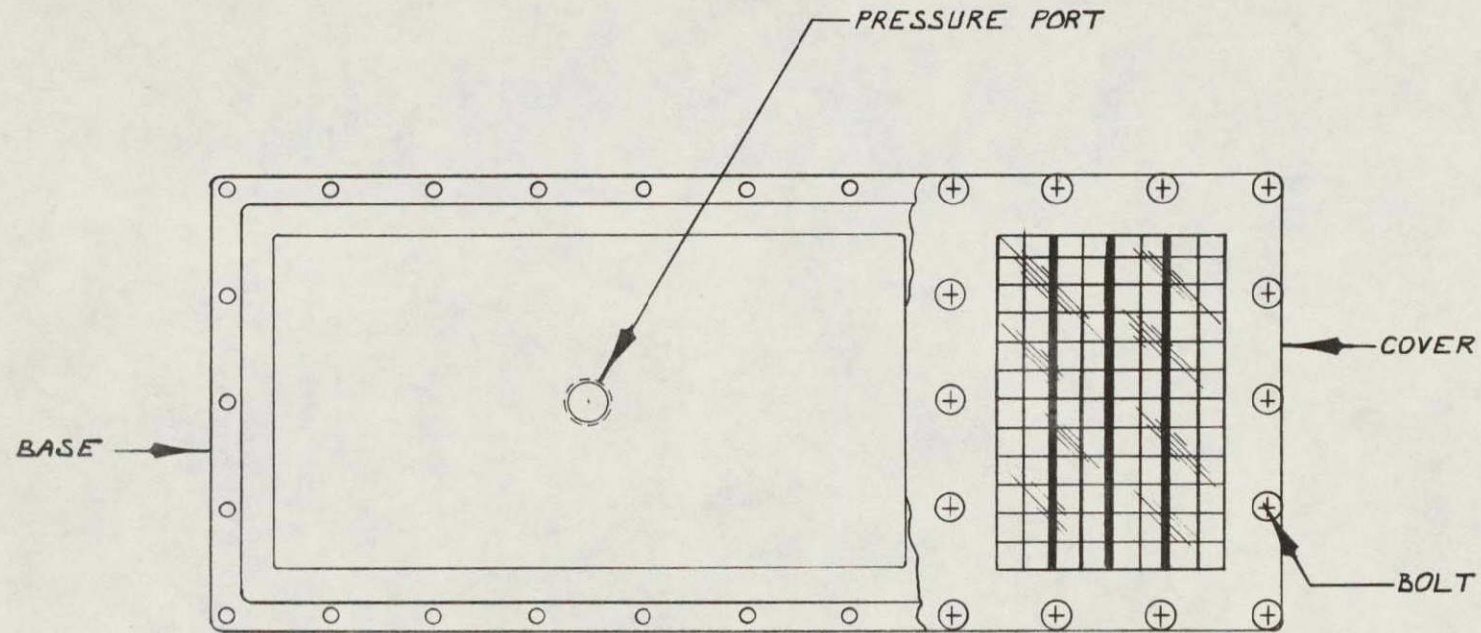


Figure 4.3.2-1. MEED Design Features

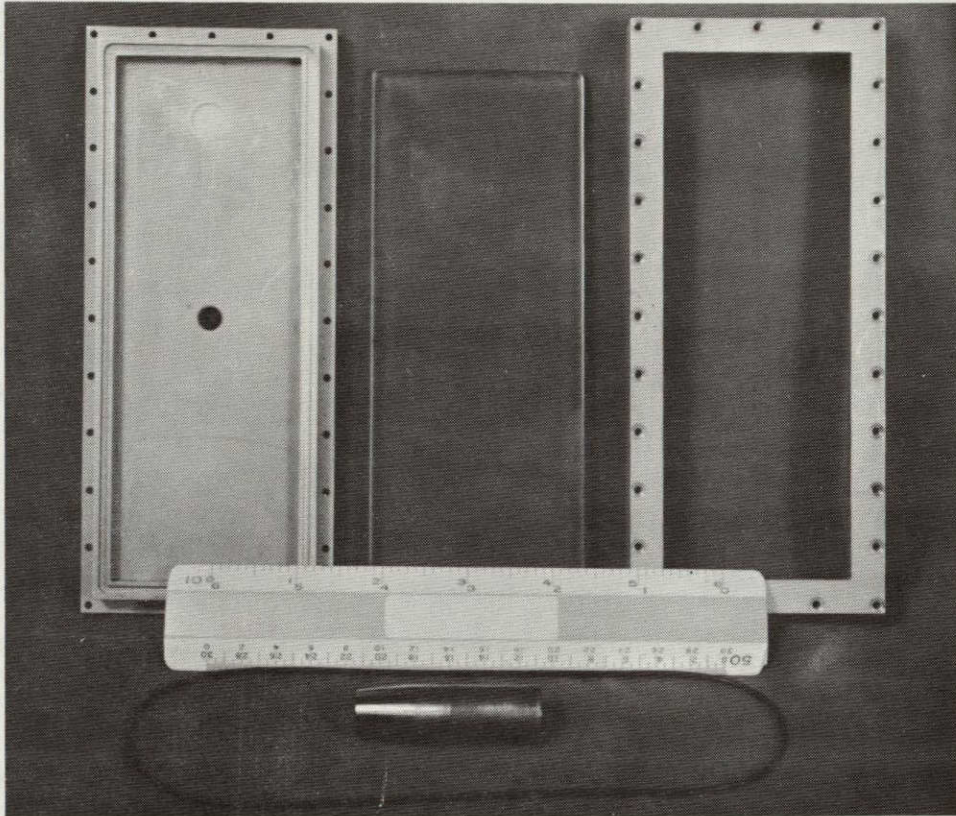


Figure 4.3.3-1. MEED Tray Components

(for calculation, see Appendix B). The 6.2 mm (0.250 in.) thick plate has a calculated factor of safety of over 8 to 1. Burst tests were performed using two plates of a commercial grade of plate glass and a plate of quartz. The burst pressures of the glass were  $9.1 \text{ kg/cm}^2$  (131 psig) and  $13.1 \text{ kg/cm}^2$  (161 psig). These represent safety factors of 9 and 11 respectively. The quartz plate burst at  $15.2 \text{ kg/cm}^2$  (216 psig) with a safety factor of 14.

The seal locations are shown in Figure 4.3.2-1. The seals on the top and bottom of the quartz plate are Gasko seals (Parker Seal Company) molded in place. The seal between the quartz plate and the MEED base is the primary seal. Gas that diffuses through the primary seal material must pass by the Gasko-seal on the top of the plate, the "O" ring between the cover and the base, or small "O" ring seals around the centrally located 3 bolts. Thus, there is full redundancy in the tray sealing system.

Pressure will be maintained in the MEED tray by increasing the pressure to approximately 2 psi above ambient pressure during assembly, and allowing it to decay no more than 4 psi to a value 2 psi below ambient pressure. The pressure decay is due to diffusion leakage through the redundant seals. The increase in pressure on assembly will occur automatically due to the slight pumping action of the secondary "O" ring between the case and the cover.

An analysis was performed to determine the volume of air expected to escape by diffusion through the seal elastomers. The volume of air that is required in the tray to keep the pressure in the range of  $14.7 \pm 2$  psia was approximately 7 cc.

Leakage testing was performed on a MEED tray of the design shown in Figures 4.3.3-1 and 4.3.3-2.

Testing was performed on an "O" ring seal instead of a Gasko-seal because of the relatively high cost of tooling required for the latter. An analysis of the seal problem showed that either an "O" ring seal or a Gasko seal can be used to seal the tray, but that gas diffusion losses through the Gasko seal are expected to be approximately one-half of the leakage through a standard "O" ring. The Gasko seal requires approximately 40 lb. (7.1 kg/cm) compression

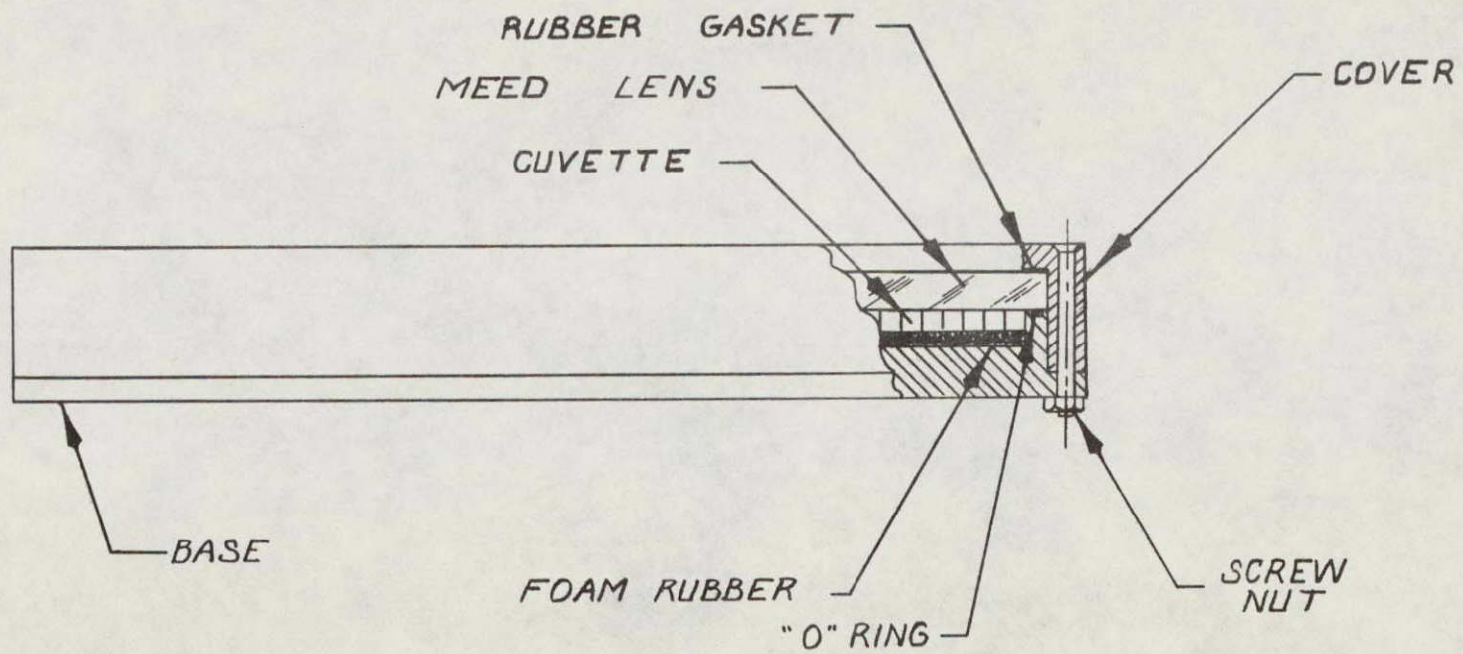
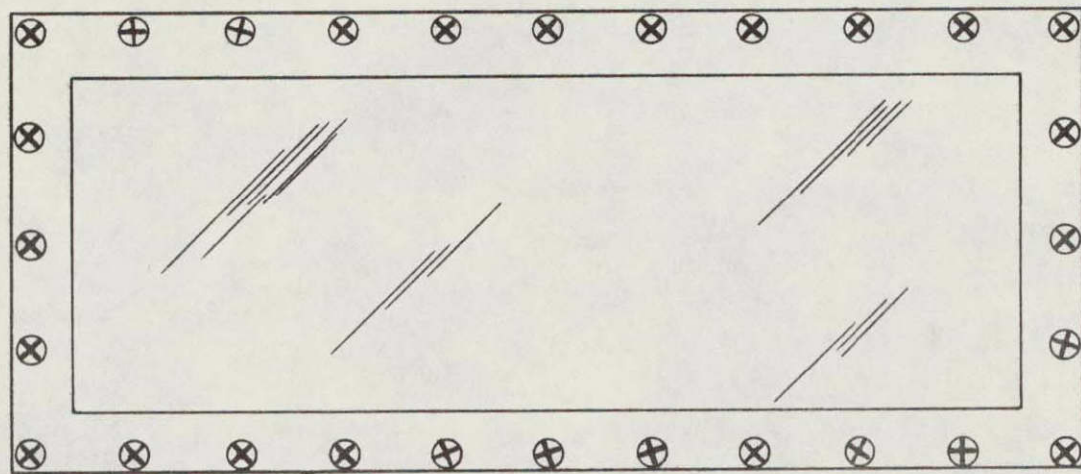


Figure 4.3.3-2. MEED Tray Assembly

force per linear inch of seal, while the "O" ring requires 6 lb per inch (1.1 kg/cm). An adequate number (28) of bolts was provided in the design to insure the higher loading required by the Gasko seal (see Calculations, Appendix B). Figure 4.3.3-3 is a photograph of the drilling jig used for the hardware of Figure 4.3.3-1.

The tray tested has a single primary seal between the glass plate and the tray base. The "O" ring was 1.6 mm (1/16 in) in diameter and was lubricated with silicone grease prior to assembly. The "O" ring groove dimensions were standard for a static seal and resulted in an "O" ring squeeze of 0.5 mm (0.020 in). The "O" ring groove was milled into the tray base using the tooling shown in Figure 4.3.3-4. A surface finish of RMS 32 was specified; however, inspection showed that the resulting surface was somewhat rougher than specified.

Two leak tests were performed. In the first test the tray was pressurized to approximately 50 psia with helium, and a leak test was performed using a CEC Helium Leak Detector (Mass Spectrometer). No leakage was detected. The ~~second~~ test comprised the pressurization of a tray to 50.2 psig (3.5 kg/cm<sup>2</sup>) and subjecting it to absolute pressure of less than 0.1 mm of mercury for 48 hours. No visible change in the charging pressure of 50.2 psig was detected.

On the basis of the leak testing, it was concluded that the configuration of the "O" ring seal is satisfactory, and that no unusual precautions have to be observed to limit the leakage losses due to diffusion through the seal material.



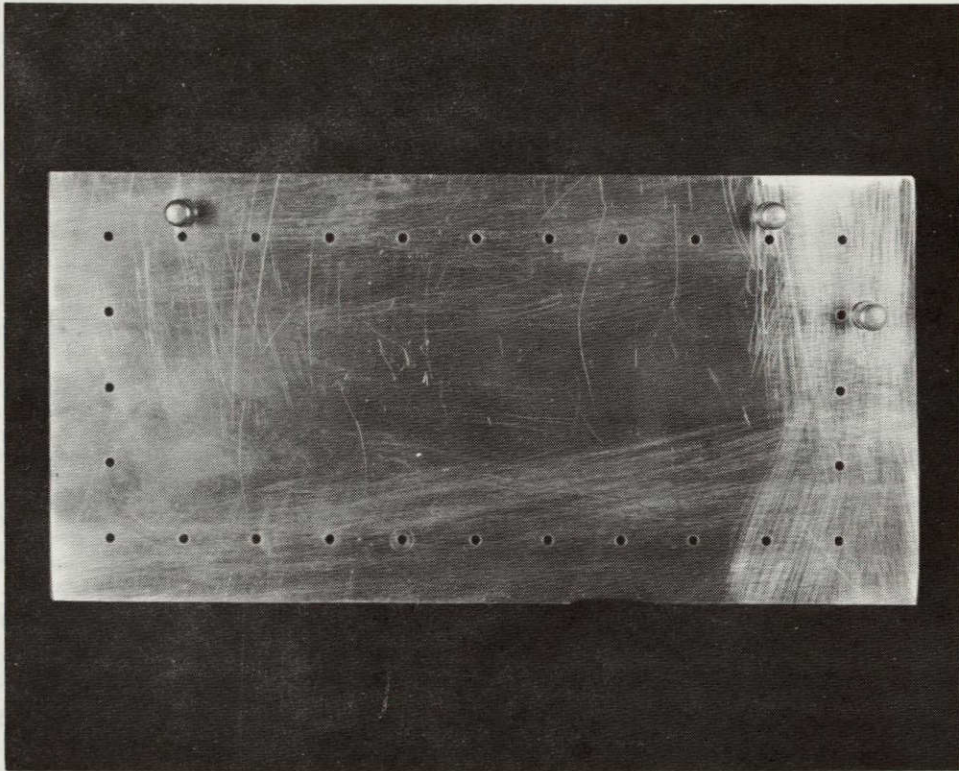


Figure 4.3.3-3. MEED Tray Drill Jig

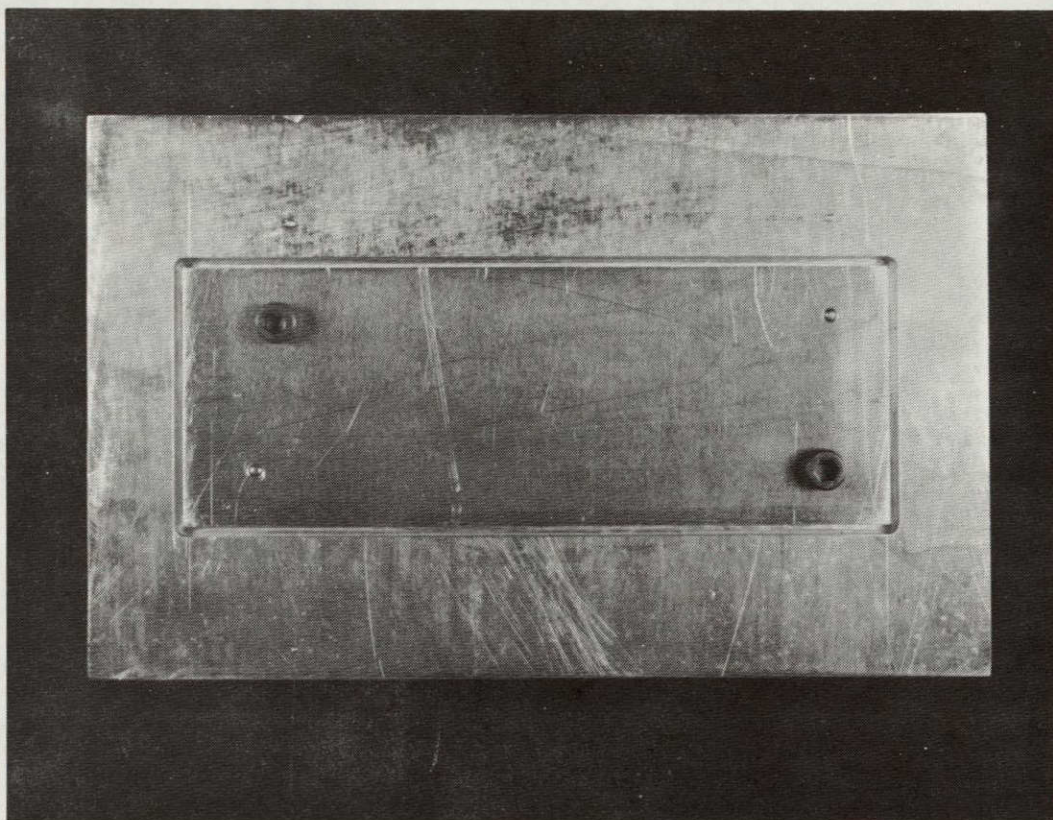


Figure 4.3.3-4. "O" Ring Groove Tooling

#### 4.3.4 CUVETTE

The biological sample container design was developed during the concept selection portion of this study. An early concept comprised a series of wells machined into a solid plate with a quartz cover over the plate. The design problems of sealing between the samples, control of the internal pressure, and retrieval of the samples for analysis eliminated this concept from further consideration.

Individual sealed wells with redundant seals (see Section 4.2.1.4) that contain separate quartz cuvettes were also given consideration. A more suitable arrangement was one in which the biological samples were held in cuvettes which were in turn contained in a sealed tray. This became the baseline concept for the tray-cuvette combination.

The three types of cuvettes that are required for the MEED experiment are: 1) cuvette Type A, which is unvented and holds a liquid culture; 2) cuvette Type B, which is unvented and holds a dry culture; and 3) cuvette Type C, which is vented through a microbiological filter and holds a dry culture. The requirements for these cuvettes and a discussion of the results of feasibility testing that has been performed are included in the following sections.

##### 4.3.4.1 GENERAL REQUIREMENTS

The cuvette requirements are as follows:

1. The cuvette shall be square in cross section and as close to  $0.25 \text{ cm}^2$  in top surface area as space permits.
2. The cuvette design shall eliminate the formation of air bubbles.
3. The window on the top of the cuvette must be transparent to ultraviolet radiation in the 250-300 nanometer wavelength range.
4. The cuvette materials must meet program safety requirements.
5. The cuvette must be capable of being broken by a sharp point to permit collection of the same after the experiment.
6. The sides of the cuvette must be opaque to ultraviolet radiation.
7. The cost of the cuvette must be as low as possible because of the large number of cuvettes required for the program.

#### 4.3.4.2 SEALED CUVETTE REQUIREMENTS (TYPES A AND B)

1. The seal must completely contain the biological samples with a pressure difference of up to  $\pm 4$  psi ( $0.28 \text{ kg/cm}^2$ ) across the walls.

2. The design must permit the cuvette to expand slightly with any expansion of the sample without increasing the internal pressure more than 2 psi ( $0.14 \text{ kg/cm}^2$ ).

3. The Type A cuvette shall hold liquid cultures of from 25 to 50 cubic millimeters.

4. The Type B cuvette shall hold dry cultures in a shallow layer.

#### 4.3.4.3 VENTED CUVETTE REQUIREMENTS (TYPE C)

1. The cuvette must completely contain the microbial samples while allowing gases to flow relatively freely in and out of the cuvette as dictated by the external pressure environment.

2. The cuvette is required to hold dry cultures in a shallow layer.

#### 4.3.4.4 CUVETTE MATERIAL STUDIES

The optical requirements for the cuvette window contrast sharply with those of the cuvette walls. The window must transmit ultraviolet radiation in the 250 nm to 300 nm range, while the sides must be opaque to this radiation. The baseline concept and the initial experimentation were based on cuvettes made entirely of quartz. Quartz cuvettes were made that fulfilled the physical requirements of the cuvette, but they were costly due primarily to the labor involved in cutting, polishing and fusing the material.

When considering the materials to be used in the construction of the cuvettes, other than quartz glass, two parameters must be considered:

1. Material having a high percent transmission of ultraviolet light for the window.

2. Material having a low percent transmission of ultraviolet light for the bottom and sides to prevent scattering of ultraviolet to adjacent cuvettes. Quartz, although it possesses high ultraviolet transmission properties, is rather costly, and is difficult to work with. Conversely, suitable plastics having the spectral qualities outlined would be preferable because they can be fabricated by injection molding and are thus much less expensive.

Consequently, an effort was initiated to survey the field of

available commercial plastics as candidates for cuvette material. Table 4.3.4-1 lists the plastic candidates and their percent transmission at 250 nm and below. The samples were placed in a cuvette holder and read on a Beckman DK2a spectrophotometer using air as a reference and a hydrogen lamp as an ultraviolet light source. Figure 4.3.4-1 shows the spectrophotometer sample holder with a sample in place.

From Table 4.3.4-1, it is obvious that KEL-F would be an excellent choice for the cuvette windows (next to quartz) and that any of the polymer plastics (polyethylene, lexan, teflon, etc.) would be suitable for the sides and bottom of the cuvette. Polymer plastics, due to their molecular structure, are excellent ultraviolet screening materials and are used in sunglasses, etc. Their low transmission percentages are not surprising. The average thickness of those materials tested is about 1/32 inch. Thinner materials will, of course, have higher percentages of transmission with a corresponding decrease of strength.

KEL-F has some limitations in its fabrication qualities, particularly in thick layers. The material must be rapidly cooled during fabrication to maintain its amorphous state which is the state in which it is transparent. Slow cooling will cause a crystalline structure in the interior of the sheet of material that is milky in appearance, and relatively opaque to ultraviolet radiation. Fortunately, the amorphous KEL-F is easy to obtain in the thickness required for cuvette windows. Further experimentation will be required to establish the degree of control of cooling rate required to fabricate complete cuvettes from KEL-F by the injection molding process.

The conclusions reached as a result of the materials studied were:

1. The only suitable plastic for the cuvette windows is KEL-F.
2. KEL-F is qualified as a material for cuvettes that are to be irradiated at the lower levels of intensity.
3. Other materials that meet the transmission requirements for the cuvette windows are fused quartz, and synthetic sapphire (not tested).
4. The ideal cuvette is made of two materials. A window material with high transmissibility, and a wall material that is opaque to ultraviolet radiation and can be readily and inexpensively manufactured

Table 4.3.4-1  
 PERCENT TRANSMISSION OF CANDIDATE PLASTICS  
 (DK2a Spectrophotometer - Air Reference)

<u>Candidate</u>	<u>% Transmission @ 250 nm &amp; Below</u>
Air (Reference)	100%
Quartz <i>1.5</i>	93%
Polystyrene	< 1%
Cellulose Acetate	< 1%
Teflon (FEP)	0%
Polyethylene	0%
Lexan	0%
Teflon (TFE)	0%
Plexiglas (lucite)	0%
KEL-F	> 50%

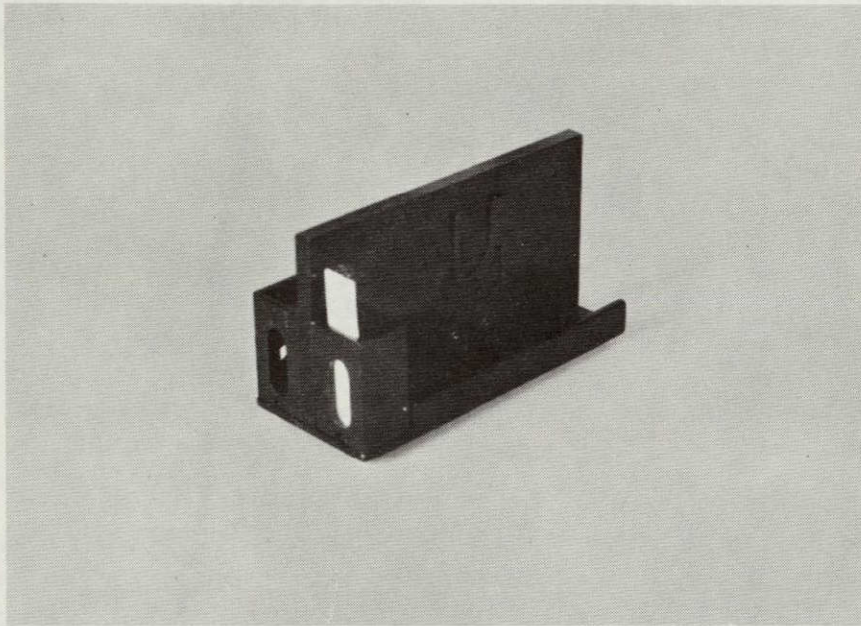


Figure 4.3.4-1. Spectrophotometer Holder

by methods such as injection molding. Thus, considerable attention was given to composite cuvettes in the design and feasibility testing phases of the study.

#### 4.3.4.5 SEALED CUVETTE - LIQUID SAMPLE

The baseline sealed cuvette concept was a crushable all-quartz cuvette, sealed to retain the microbial samples. Quartz cuvettes were fabricated and tested to establish the nature of the fabrication and performance problems. Cuvettes made of plexiglas and quartz, and of KEL-F were also fabricated and tested. The details of these investigations are contained in the following paragraphs.

##### 1. Quartz Cuvette Design and Fabrication

A design for the quartz cuvette is shown in Figure 4.3.4-2. Several cuvettes were made to this general design with widths up to 5 mm. Figure 4.3.4-3 comprises three views of a typical cuvette. The cuvette was fabricated by ultrasonically machining a matrix of several cavities in a quartz plate of proper thickness. A plate of polished quartz of the correct thickness for the cuvette covers (0.4 mm) was then fused to the plate in a high temperature oven, thus covering the matrix of cavities. The two loading holes were drilled into the corners of the base of each cavity. Individual cuvettes were then cut from the matrix, followed by a minor amount of grinding to achieve squareness.

The fabrication process described above was time consuming, because of the hardness of quartz and the high temperature required for fusing the cover to the cuvette body plate. Dimensional tolerance requirements also contributed to the labor required to make the quartz cuvette.

##### 2. Quartz Cuvette - Seal Tests

The quartz cuvette was tested to determine the problems related to loading with biological samples and sealing against leakage. When the cuvette was filled and sealed according to the protocol (Appendix D), excess bubbles were formed inside the cuvette due to air coming from the cuvette solution and the wax seal. Figure 4.3.4-4 is a 20X magnification of an air bubble along the inside edge of a filled quartz cuvette. When the filled cuvette was placed in the desiccating jar and pumped down, to 9 psi (18.6 inches mercury), the wax seals blew out. Figure 4.3.4-5 shows the desiccation vessel apparatus. The samples are placed in the vessel, sealed



## NOTES:

① MAKE TOP PLATE FROM G.E. TYPE 151 FUSED SILICA. BODY TO BE QUARTZ

② POLISH BOTH SIDES OF TOP PLATE

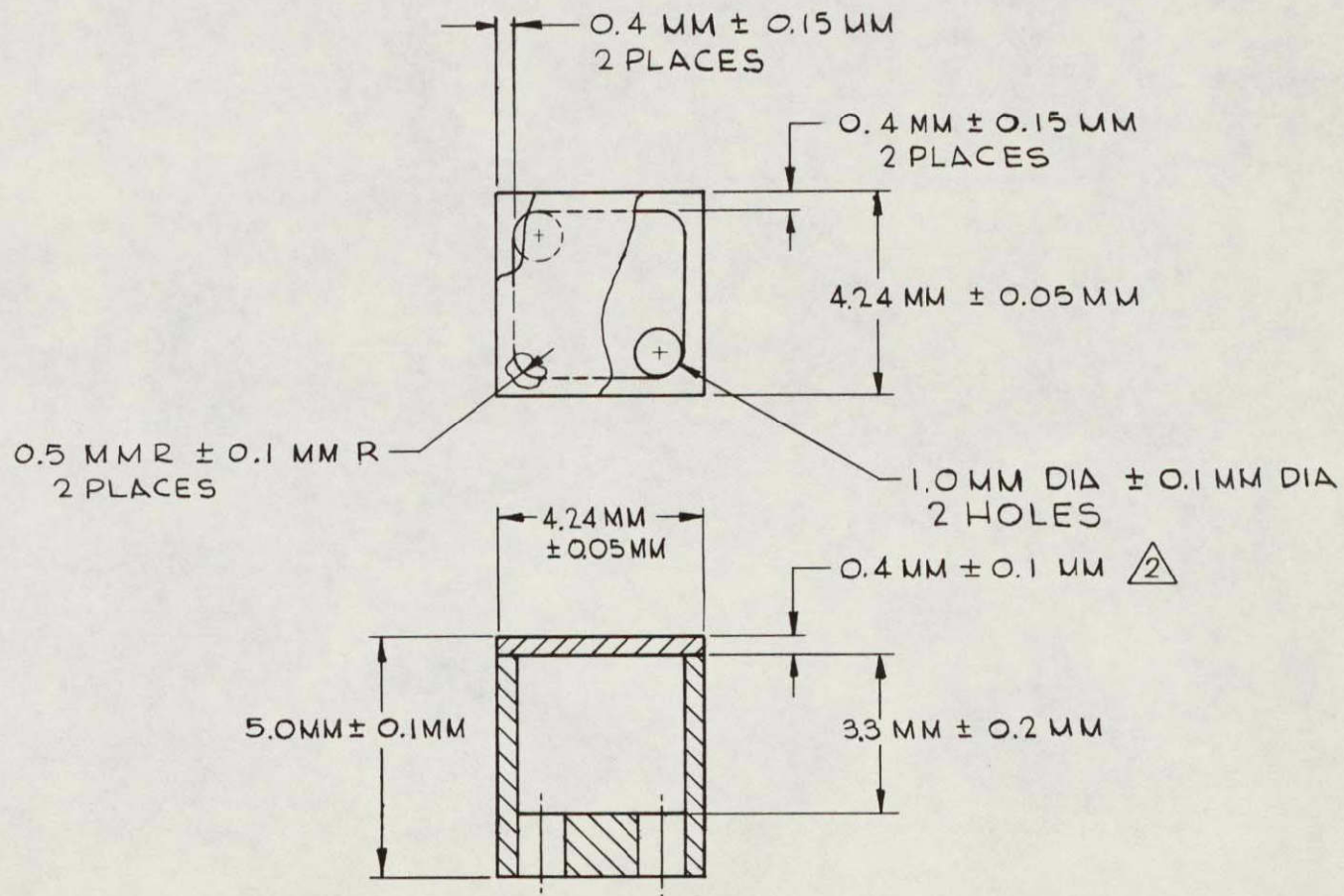


Figure 4.3.4-2. MEED Quartz Cuvette Assembly

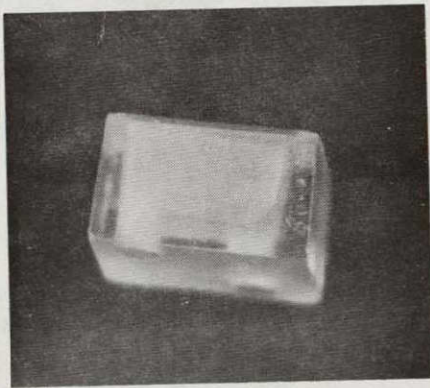
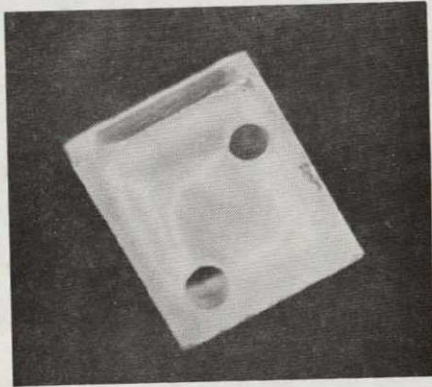
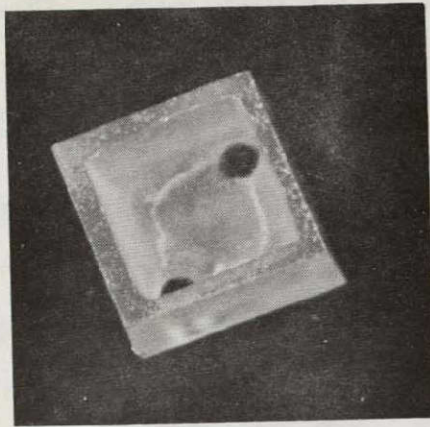


Figure 4.3.4-3. Quartz Cuvettes

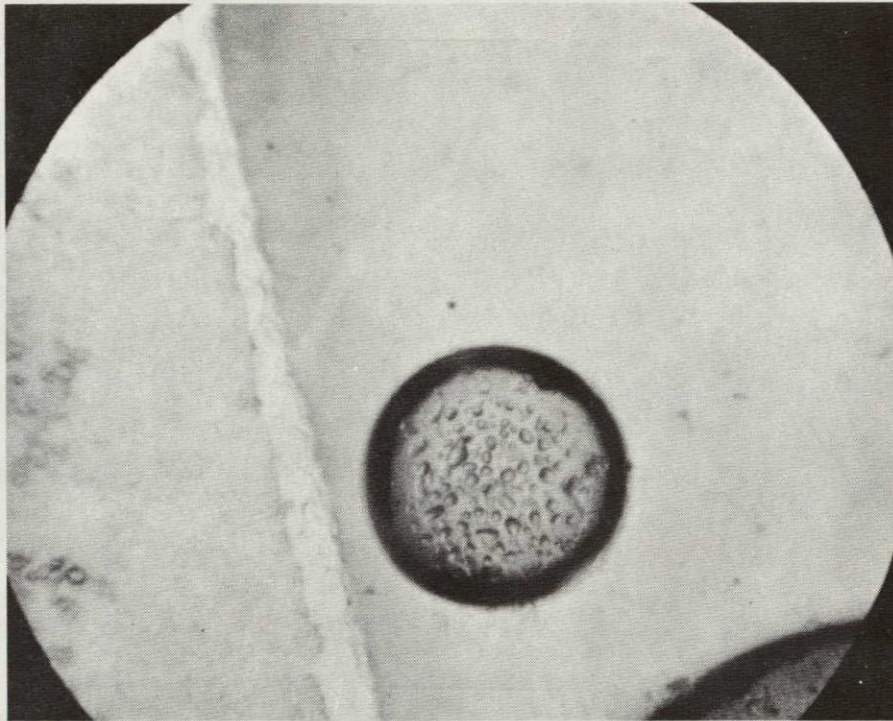


Figure 4.3.4-4. Air Bubble in Cuvette Fluid

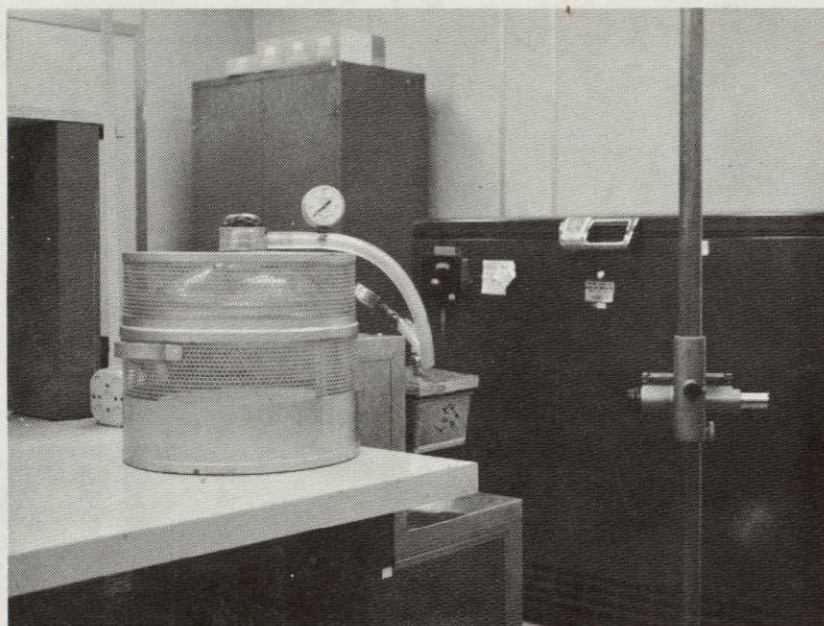


Figure 4.3.4-5. Desiccation Apparatus

and covered with the safety cage. The vessel is connected to a Welch vacuum pump with an in-line gauge. The telescope is used to observe the solutions and cuvettes during de-aeration.

The anticipated pressure differential across the cuvette seal is  $\pm 2$  psi. Testing the wax seal with a six psi pressure drop was a more stringent test than required but it uncovered two significant problems: 1) there was not adequate mechanical strength in the wax seal and 2) the biological sample fluid should be de-aerated as much as possible without damaging the microbes prior to loading. Base on these tests the seal was redesigned to provide a locking feature (see Section 4.3.4.4), and the protocol was revised to include de-aeration of the sample fluid.

The problem of bubble formation has not been fully explored. De-aeration will minimize the formation of bubbles that come out of solution. No tests have been performed to insure that minor outgassing of the microbes will not cause small bubbles to form.

The conclusions reached on the bubble formation problem areas are as follows:

- a. All free air must be removed during the filling of the cuvette.
- b. Bubbles will not form due to pressure change during the actual Apollo mission, since the cuvettes are enclosed in the sealed MEED tray. The bubbles were discovered when the sample cuvette was placed under full vacuum to test the seal integrity.
- c. Air will not normally come out of solution under controlled temperature and pressure conditions. The biological

sample fluid should be de-aerated if possible prior to loading to reduce the chances of small bubble formation.

d. Testing should be performed prior to the design of flight hardware to determine whether small bubbles will occur due to the gases formed by the microbes. The formation of bubbles of significant size from this source under controlled temperature and pressure conditions is not considered to be likely.

### 3. Quartz Cuvette - Siliclad Test

The cuvette was coated with Siliclad, a silicone preparation made by Clay-Adams, in an effort to reduce the tendency of air to stick to the sides of the cuvette during filling. The Siliclad was placed on the inside walls and baked on at 100°C. The test showed that the treatment did reduce air retention. The use of Siliclad does not appear to be essential, however, as cuvettes can be filled bubble-free without it.

Following the Protocol for Loading of the Quartz Cuvette (Appendix D) will result in a de-aerated, properly filled cuvette. Prior to filling, the quartz cuvettes will be cleaned and sterilized in accordance with the Sterilization Protocol (Appendix D).

### 4. KEL-F PLASTIC CUVETTE

Several cuvettes were made of KEL-F plastic to simplify the fabrication process and improve the cuvette seal. Figure 4.3.4-6 is a sketch of the cuvette design. The cuvette is square in cross-section on the outside. The inside cavity was made circular in cross-section to reduce fabrication complexity, but the final design of this unit would be square both inside and out.

The cuvette assembly comprises the basic body with the sample cavity, an insert that snaps into place and provides a fill hole, and a cap to insure the seal. Loading is accomplished by filling the cuvette to the bottom of the fill hole, filling the fill hole and the space above with

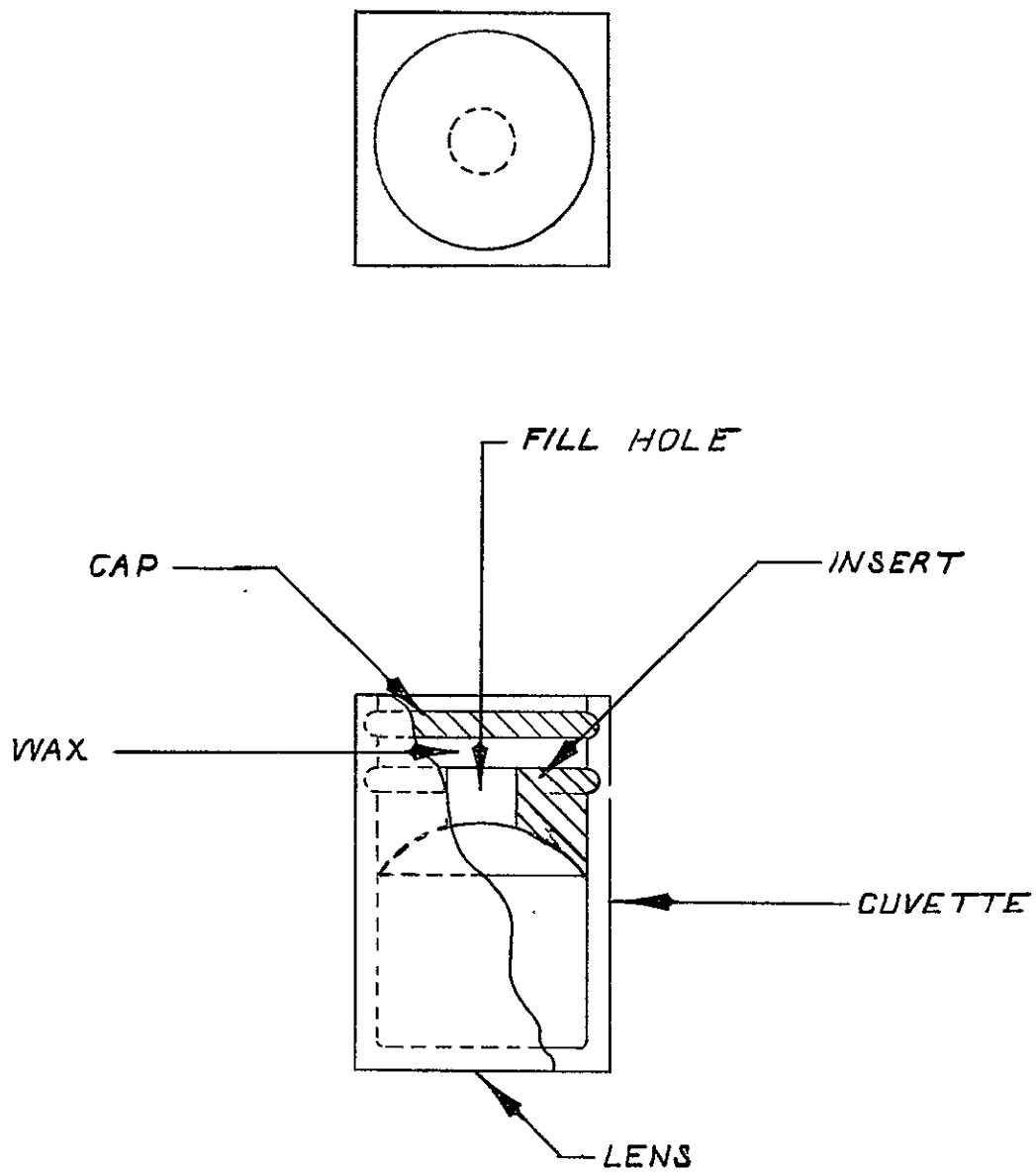


Figure 4.3.4-6. KEL-F Plastic Cuvette Design

low-melting-point wax and pressing the cap into place. Loading tests were performed on the cuvette and all steps proceeded as designed. The insert and cap snapped into position easily and the space between was completely filled with sealing wax. Figure 4.3.4-7 comprises several views of the components of the KEL-F cuvette. View b shows the window that admits the ultraviolet light. The machining marks in this surface are somewhat accentuated by the photographic lighting, and become less visible when the cuvette is filled with water. The dull appearance of the KEL-F is due primarily to the roughness of the surface, although some degree of opacity is due to crystalline KEL-F structure. Both the inside and outside surfaces of the light transmitting cover require additional polishing, however, before this cuvette would be satisfactory for use.

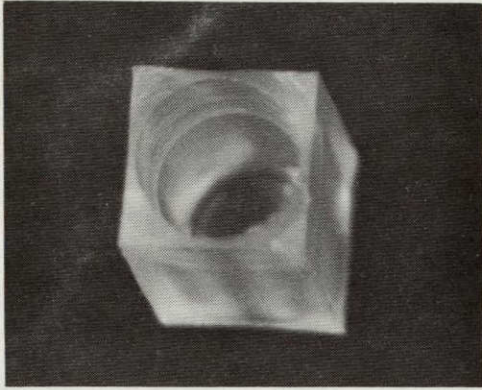
On the basis of these investigations, it was concluded that the window cover for the cuvette should be fabricated separately from the cuvette body and then cemented to the body.

#### 5. Plexiglass Cuvette with Quartz Window

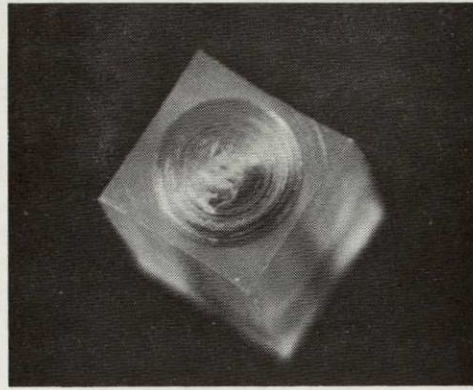
The development of the cuvette was continued by the design and fabrication of a two-material cuvette. This unit comprised a plexiglas cuvette body and a quartz window. One version of the combination cuvette is shown in Figure 4.3.4-8. The window is bonded to the body with epoxy cement and then the cuvette is oven-dried to eliminate any volatile components. The cuvettes actually tested had the walls reduced from 0.020 in (0.5 mm) to 0.012 in (0.3 mm).

The filling hole is chamfered from both the inside and outside to provide a lock for the sealing wax. Figure 4.3.4-9 is a photograph of the cuvette filled with water and with the hour-glass shaped wax seal in place. The cuvette was placed in a vacuum jar and the jar was evacuated three times to less than one psi. No evidence of leakage or loosening of

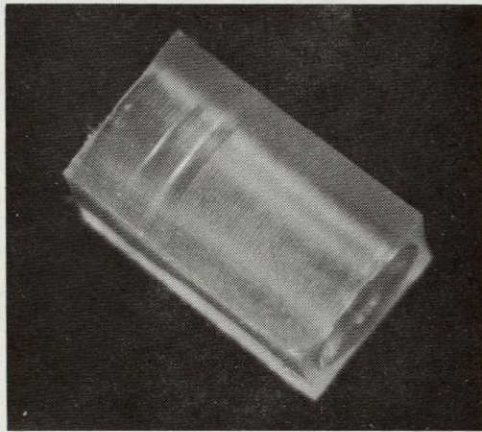




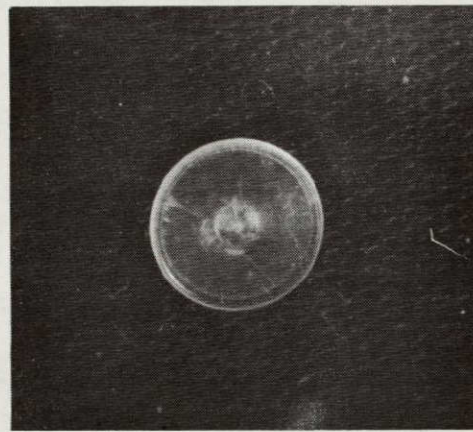
a. Bottom View - Body



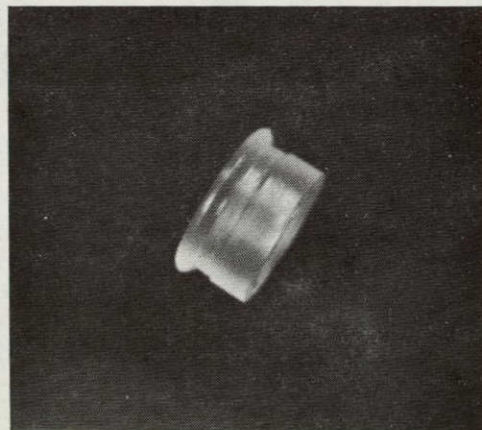
b. Top View of Body



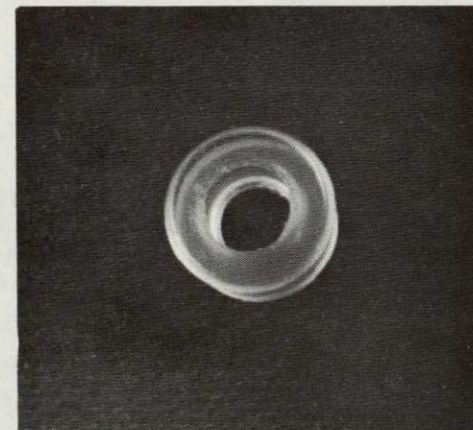
c. Slide View - Body



d. Cap



e. Side View - Insert



f. Top View Insert/Filling Hole

Figure 4.3.4-7. KEL-F Cuvette Components

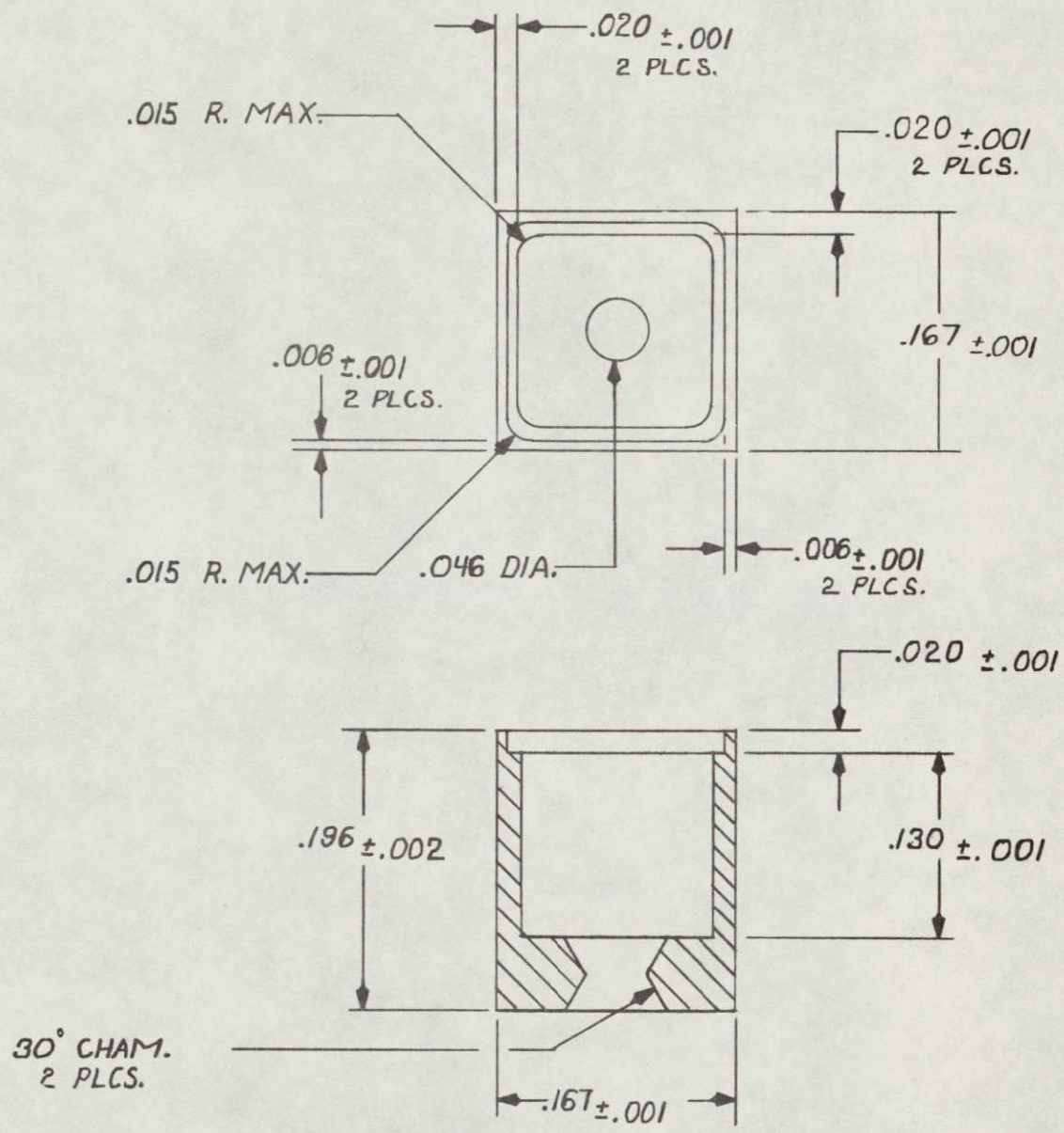


Figure 4.3.4-8. Plexiglas Cuvette with Quartz Window



Figure 4.3.4-9. Plexiglas Cuvette with Wax Seal

the seal occurred. Figure 4.3.4-10 comprises 3 views of the thin-walled plexiglas cuvette body that shows construction details of the cuvette body.

An alternate design with a redundant seal is shown in Figure 4.3.4-11. A snap-in cap seal is included in addition to the hour-glass shaped wax seal. The plexiglas cuvette with quartz window and simple hour-glass seal (Figure 4.3.4-8) is considered to be the basic design for the Type A (liquid sample) cuvette. Figure 4.3.4-11 is a practical but somewhat more complex design that is available for use if sealing problems develop.

The designs of Figures 4.3.4-8 and 4.3.4-11 meet the requirements of the sealed Type A cuvette. The walls are essentially opaque and the windows are extremely transparent to ultraviolet radiation. The seal is positive and yet simple and will withstand a pressure differential of at least one atmosphere. The cuvette walls (at 0.12 inches - 0.3 mm) are thin enough to permit the pressure to approximately equalize when fluid expansion occurs in the microbial samples. The cuvettes are fragile enough that they can be crushed to extract the microbial sample when the experiment is completed (Unloading Protocol, Appendix D). The cuvette body can be injection molded at low cost.

#### 4.3.4.6 SEALED CUVETTE - DRY SAMPLE

The sealed cuvette with the dry microbial sample is shown in Figure 4.3.4-12. This cuvette is similar in construction to the sealed cuvette for liquid samples. It has a quartz cover that is cemented to an injection molded plexiglas body. The dry sample will be deposited on a thin layer of Millipore filter material which in turn is supported by a porous KEL-F block. The closure of the cuvette is accomplished by a snap-in plate that contains the double-chamfered filling hole. The seal is made by pouring wax in the hour-glass shaped filling hole and the space above the filling hole. The option to include a second snap-in cap as a redundant

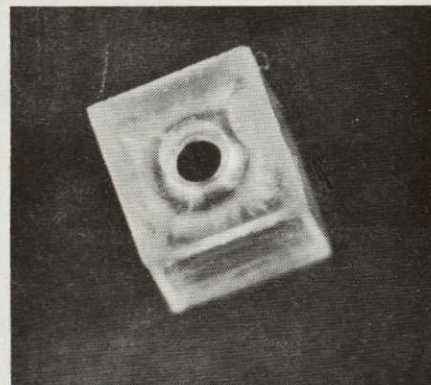
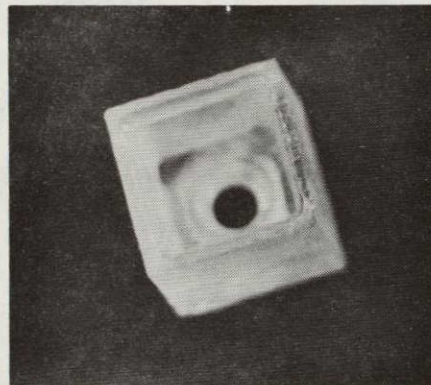
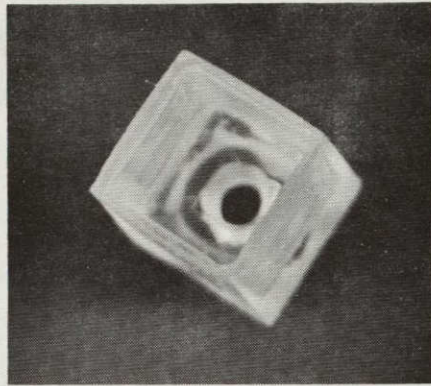


Figure 4.3.4-10. Body of Plexiglas Cuvette

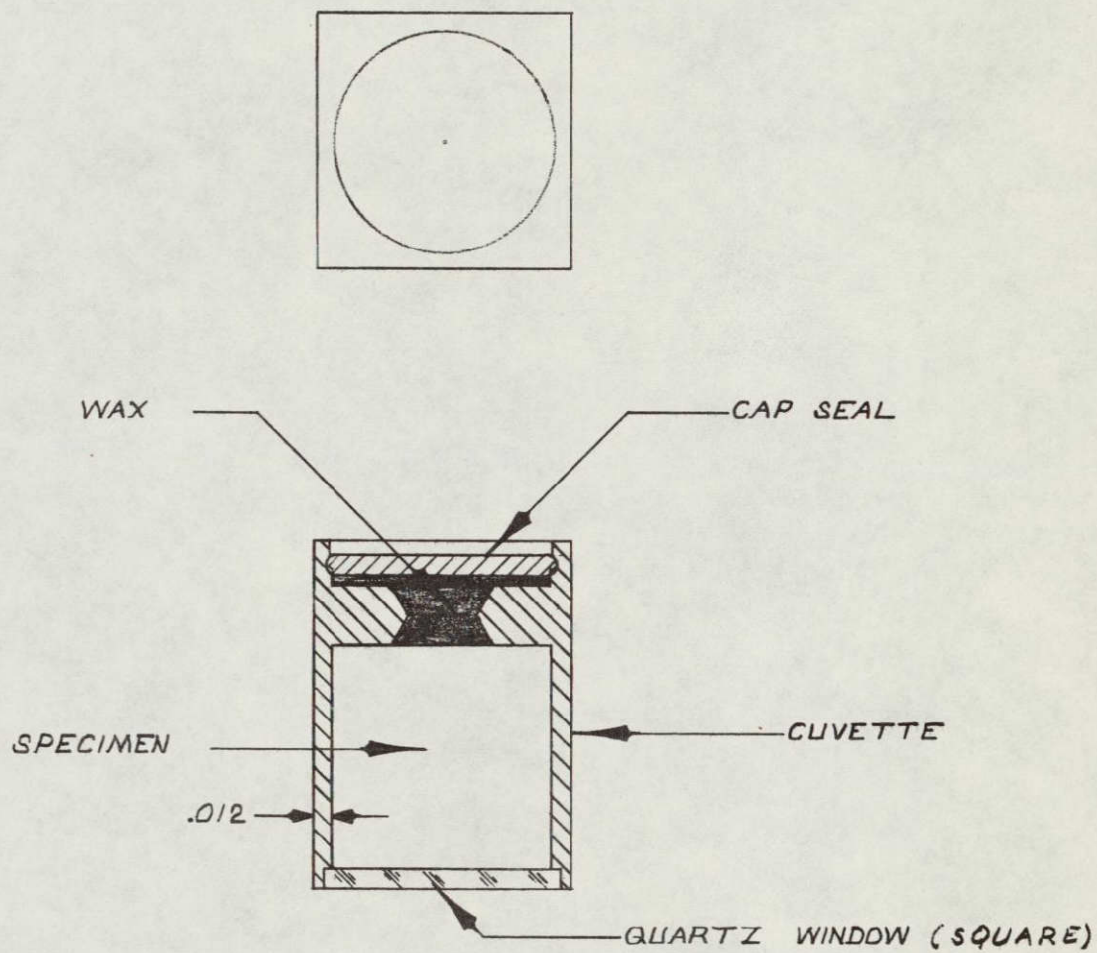


Figure 4.3.4-11. Alternate Design, Plexiglas Cuvette

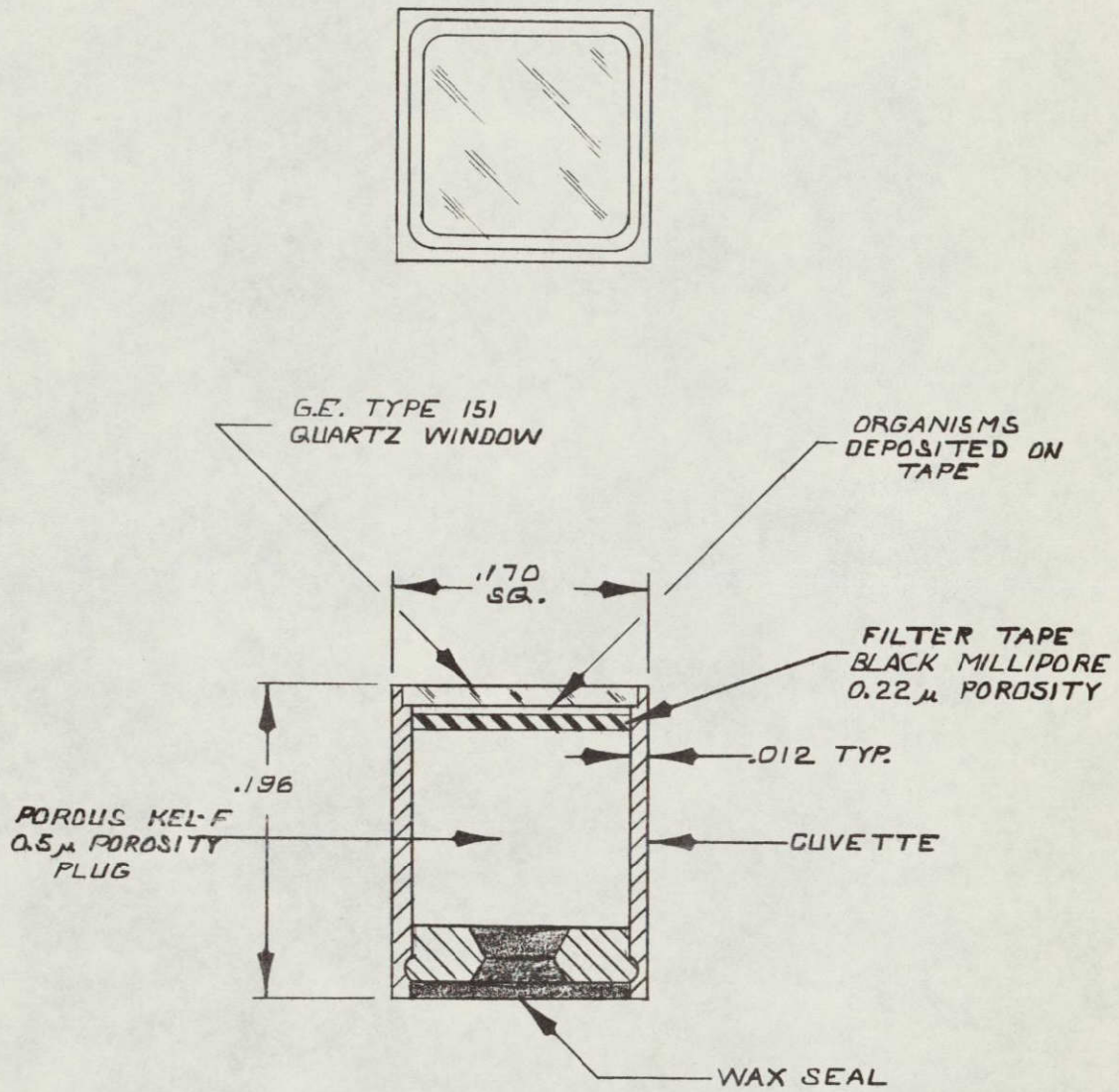


Figure 4.3.4-12. Sealed, Dry Sample Cuvette

seal is available also in this design.

The dry sample sealed cuvette design was simulated by modifying a KEL-F cuvette made with a circular cross-section cavity. An exploded view of this unit is shown in Figure 4.3.4-13, and the assembly is shown in Figure 4.3.4-14.

The major problems associated with the use of this cuvette will be the time required to deposit the dry sample on the Millipore filter, and insuring a secure fit of the filter against the walls of the cuvette.

#### 4.3.4.7 VENTED CUVETTE FOR DRY SAMPLES

One of the significant tests to be made on microbial samples in the proposed experiments for the MEED is the exposure of the samples to the hard vacuum of the lunar surface. Vacuum exposure may occur before, during and after the MEEDs are exposed to the solar radiation.

The dry sample vented cuvette is similar in construction to the equivalent sealed unit except that no wax seal is required (Figure 4.3.4-15). The requirement that the unit be vented is met by the use of the Millipore filter (0.22 micron filter) and the backup filter of porous KEL-F. A simulated vented cuvette is shown in Figure 4.3.4-16.



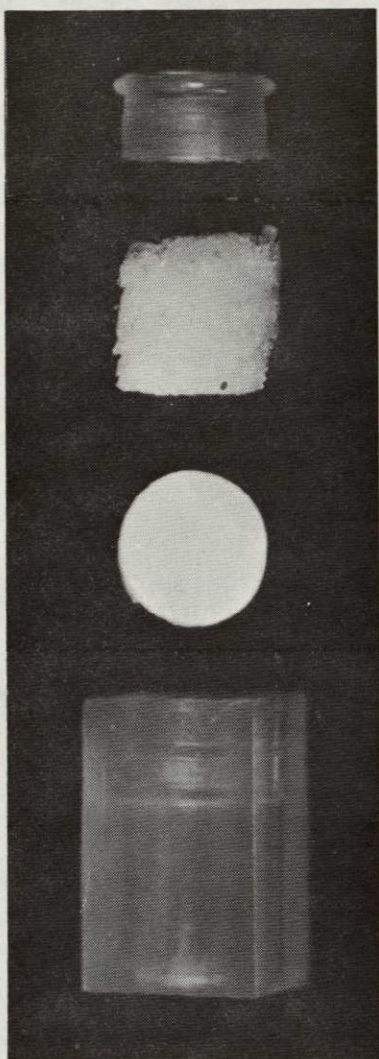


Figure 4.3.4-13. Exploded View, Simulated Dry Sample Cuvette

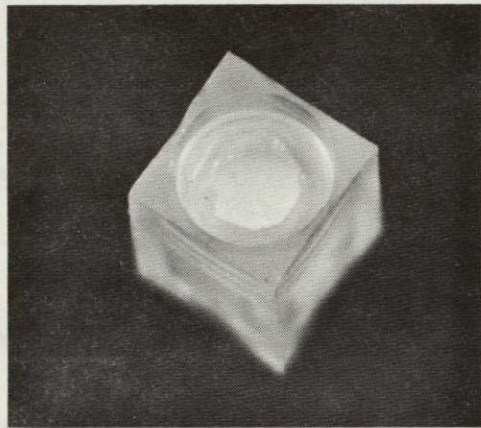


Figure 4.3.4-14. Assembled Dry Sample Cuvette

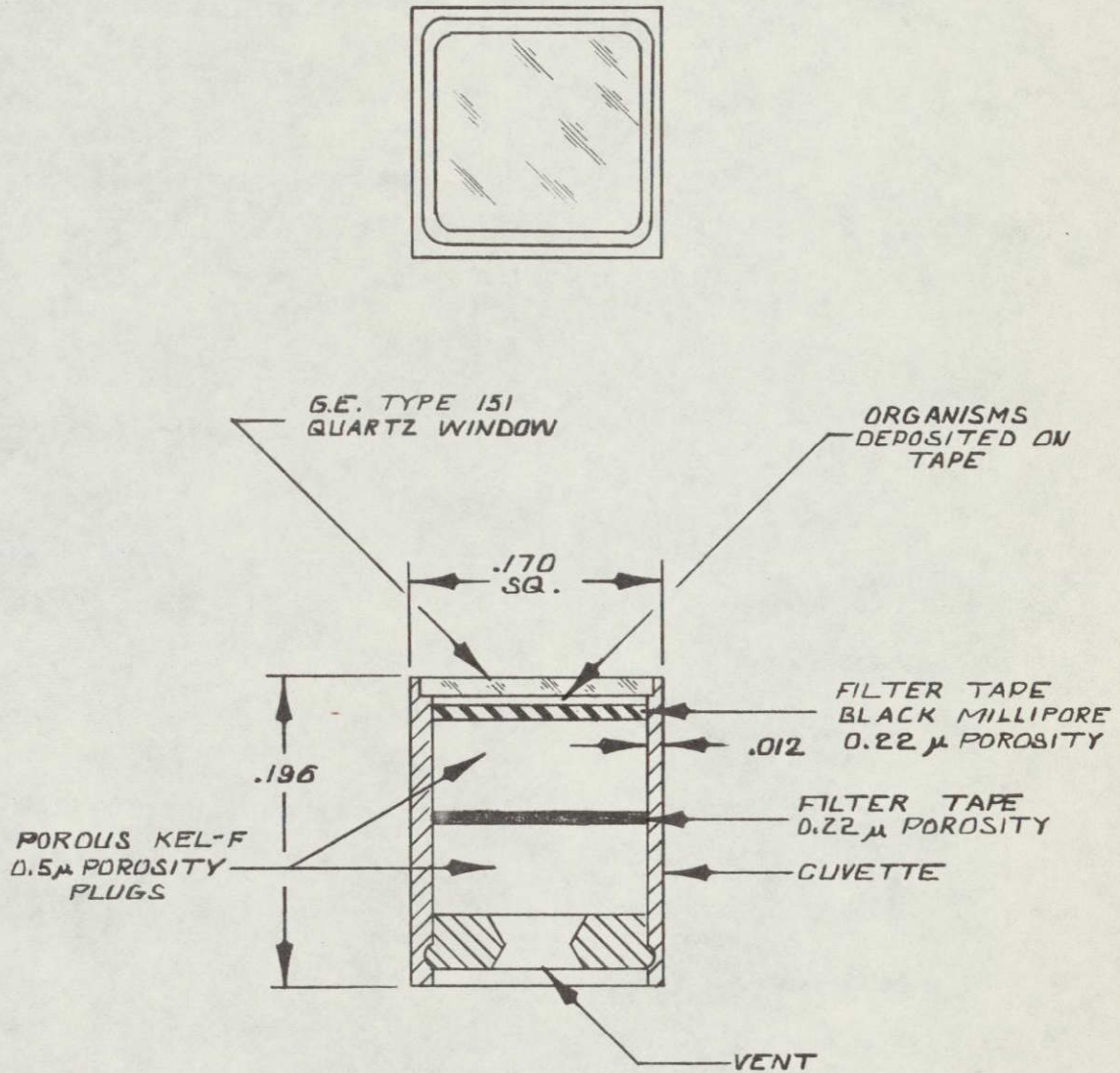


Figure 4.3.4-15. Vented, Dry Sample Cuvette

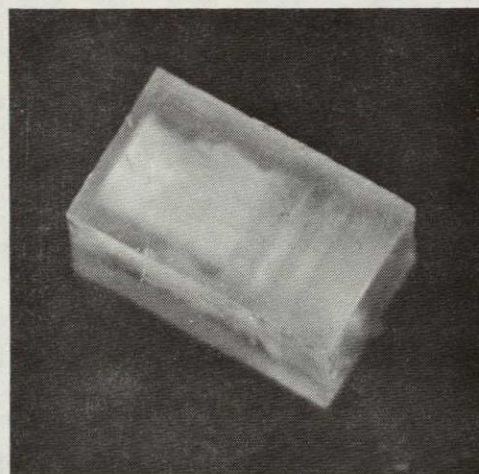
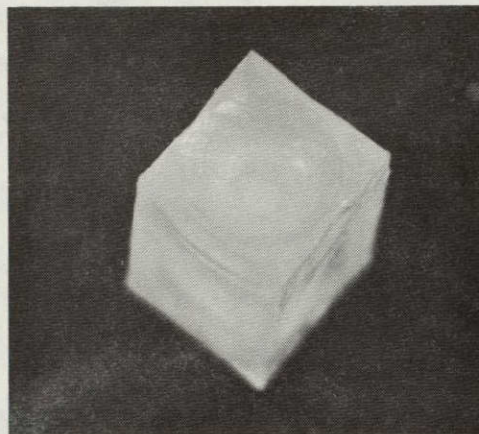


Figure 4.3.4-16. Dry Sample, Vented Cuvette

#### 4.3.5 RADIATION FILTERS

##### 4.3.5.1 REQUIREMENTS/OBJECTIVES

The optical filter system to be considered includes all elements through which radiation must pass prior to interception by the biological sample. These elements must pass a maximum amount of UV radiation at specified wavelengths. For an exposure time of ten minutes, it is desired that the filter system have transmissivity peaks at 254, 260, 280, and 300 nanometers with sufficient half bandwidth so that energy levels ranging from 10 to  $10^5$  ergs per sample chamber are available.

##### 4.3.5.2 DISCUSSION

The UV absorption of DNA peaks at approximately 260 nm and falls to about 50% of the peak value at 240 nm and 280 nm. The absorption for a typical protein peaks at 275 nm with a 50% spread of about 40 nm. The relative germicidal effectiveness of UV peaks at about 260 nm and falls to 50% at about 230 nm and 280nm; by 300 nm it is less than 5%. The total UV dosage desired for a given experiment will depend upon the type of effect under investigation and the type of sample. Interference filters with peak responses anywhere in the UV range are available to select the particular wavelength of interest. Figure 4.3.5-1 shows the total energy impacting on a square centimeter of sample area during a 10-minute exposure period for various realizable bandpass filters. A 25 nm 1/2 peak bandpass filter transmits about 1-1/2 orders of magnitude more energy than a 10 nm filter. Using the following 50% survival exposures (see Figure 4.3.5-2)

Fungi	$1.5 \times 10^5$ ergs/cm <sup>2</sup>
Spore Formers	$1.8 \times 10^4$ ergs/cm <sup>2</sup>
Viruses	$2.2 \times 10^3$ ergs/cm <sup>2</sup>

useful wavelengths for 50% survival of possible experiment samples are:

	Bandpass (1/2 peak)		
	10 nm	15 nm	25 nm
Fungi	--	260-300	240-300
Spore Formers	290-300	220-300	200-300
Viruses	220-300	200-300	200-300

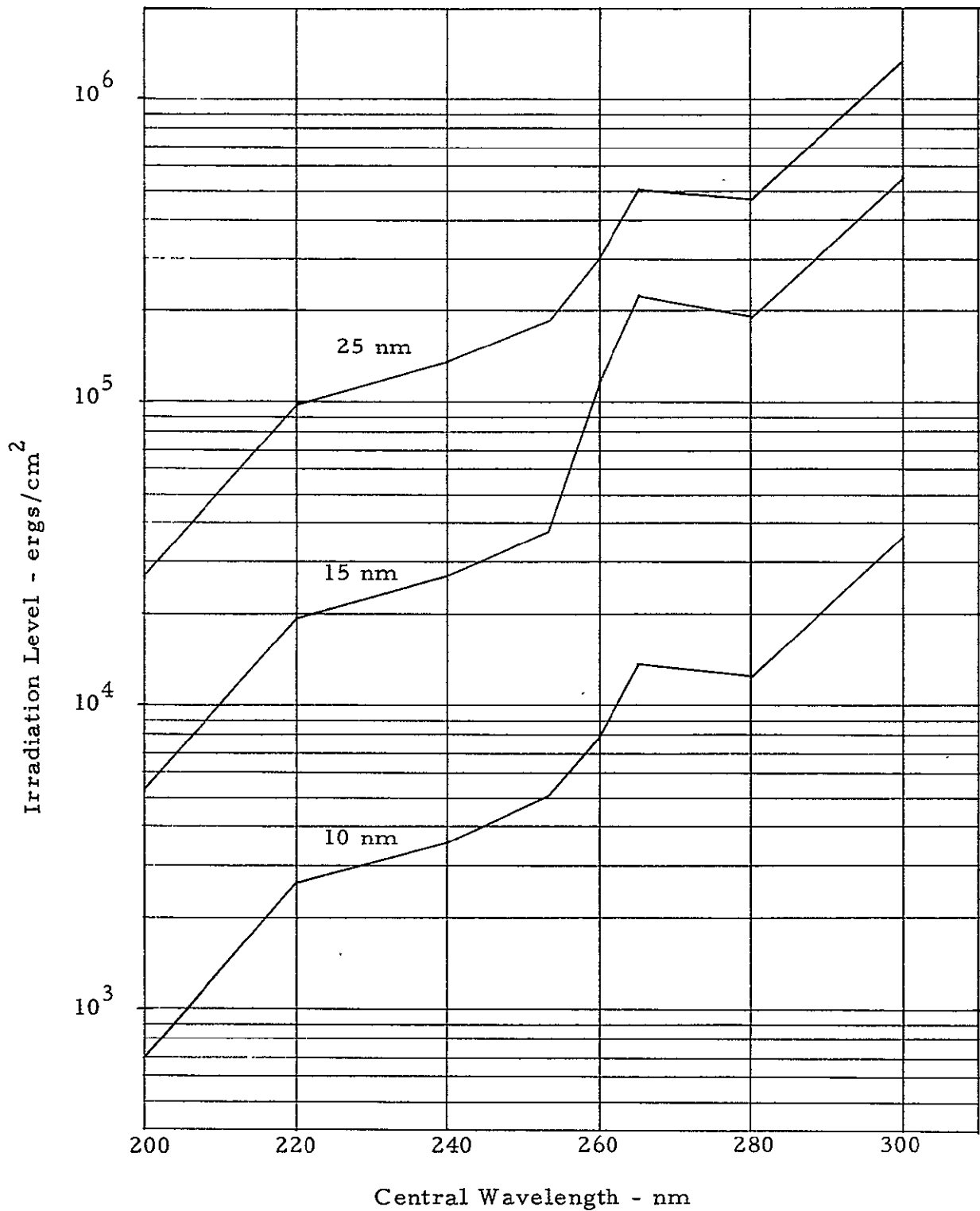


Figure 4.3.5-1. Approximate Irradiation on Sample for Various Filter Half-Peak Bandwidths: Exposure Time = 10 Minutes

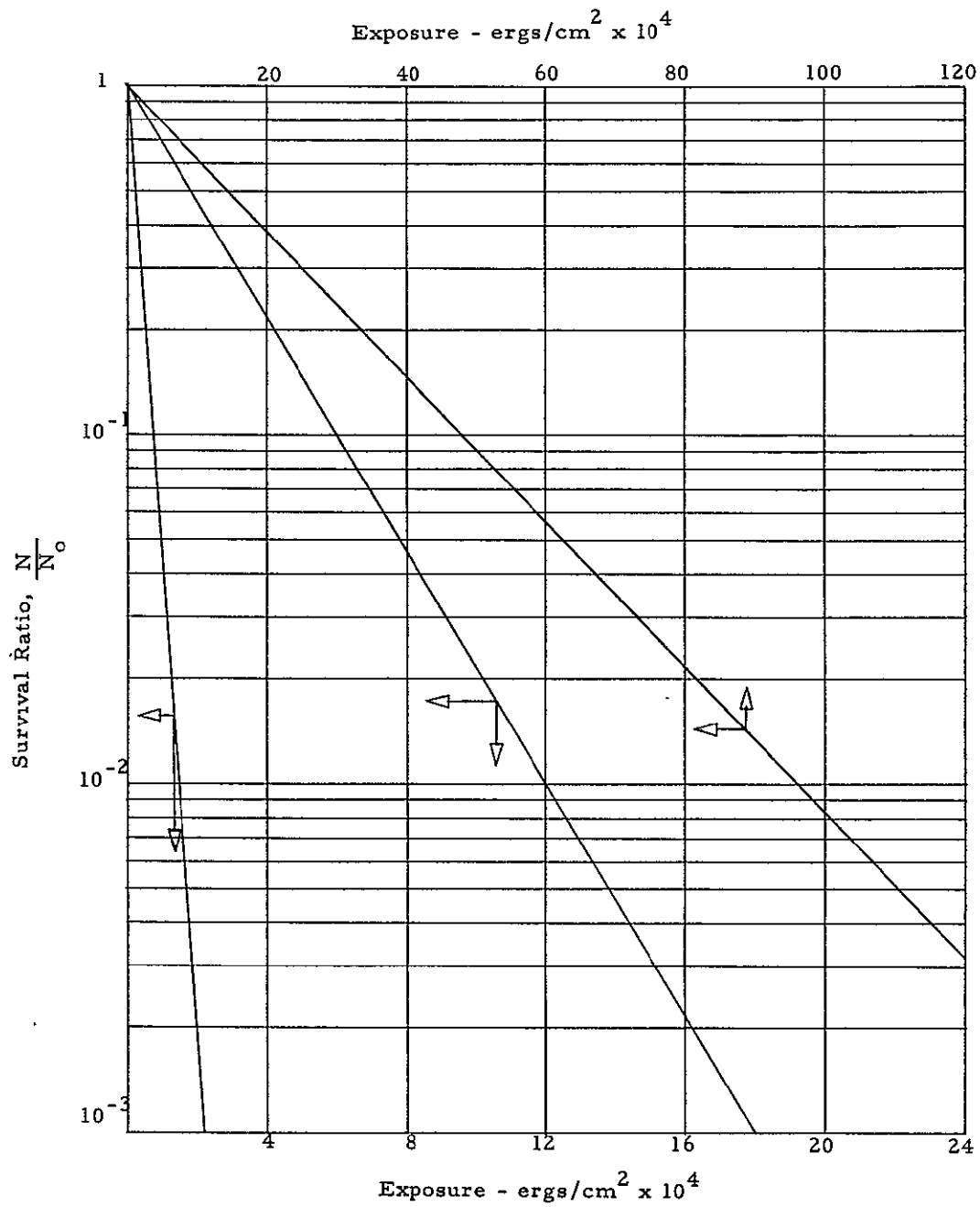


Figure 4.3.5-2. UV Exposure Required to Kill Various Kinds of Organisms  
 (from Ultraviolet Radiation by Lewis Koller, John Wiley & Son, 1965, Sec. Edition, p. 243)

Both DNA and protein exhibit a half-peak bandwidth of 40 nm so that the use of 25 nm bandwidths permits selective irradiation of the DNA or protein spectrum. When higher energy levels are desired, use of 50 nm 1/2 peak bandwidth filters will produce approximately 10 times the levels shown for the 25 nm values. The total energy available in the 200 to 300 bandpass is about 12,000,000 ergs/cm<sup>2</sup> of which approximately 6-10 x 10<sup>6</sup> ergs/cm<sup>2</sup> could be directed on the samples.

When a high degree of selectivity is desired, such as separating 253.7 nm from 265 nm wavelength radiation, the use of the 10 nm 1/2 peak bandwidth filter is necessary. For example, only about 10% of peak 253.7 nm wavelength energy will be present as 260 nm wavelength energy when using a 10 nm bandwidth filter centered at 250 nm. It would appear that experiments of this type would be limited to viruses. However, the possibility remains that this degree of selectivity can be employed on spore formers as well.

It appears that very narrow bandpass filter systems centered around 254 nm may limit the ability to achieve high enough UV irradiation to result in survival ratios below 50%. Jagger<sup>(1)</sup> indicates that for fungus spores the maximum number of mutations (about 30%) occurs for survival ratios of about 5%. For a survival ratio of 50% the number of mutations is about 3%. A filter system with a 1/2 peak bandpass of 25 nm will pass only enough UV to achieve fungus survival ratios of about 20-30% when system losses are included. It may be necessary to use the wider bandpass system for experiments specifically designed to evaluate mutations. This type of problem is most prevalent at the shorter wavelength of 254 nm because of the reduced solar irradiance available. It is also most apparent when dealing with fungi because of their higher resistance to UV dosages. When the solar spectral irradiance data of Figure 4.3.5-3 is combined with typical transmission curves for a 25 nm and a 10 nm 1/2 peak bandpass filter, the spectral energy distribution of Figures 4.3.5-4 and 4.3.5-5 are obtained. The first order filter (25 nm

---

(1) Jagger, John, Introduction to Research in Ultraviolet Photobiology, Prentice Hall, 1967, p. 68.

(2) Data taken from F.S. Johnson, Space Materials Handbook, LMSC, Jan. 1962, and JPL.



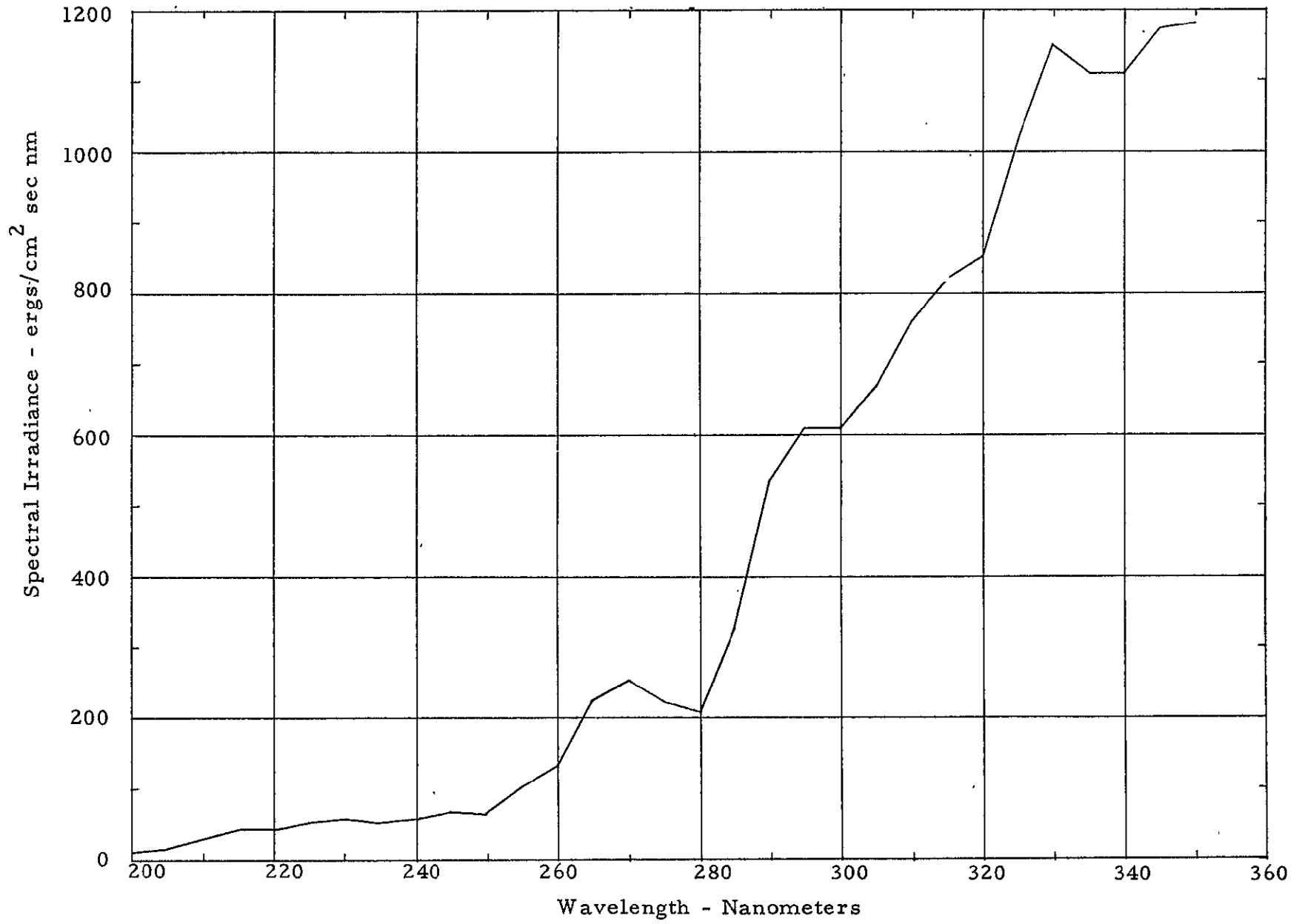


Figure 4.3.5-3. Solar Spectral Irradiance (Composite Data)

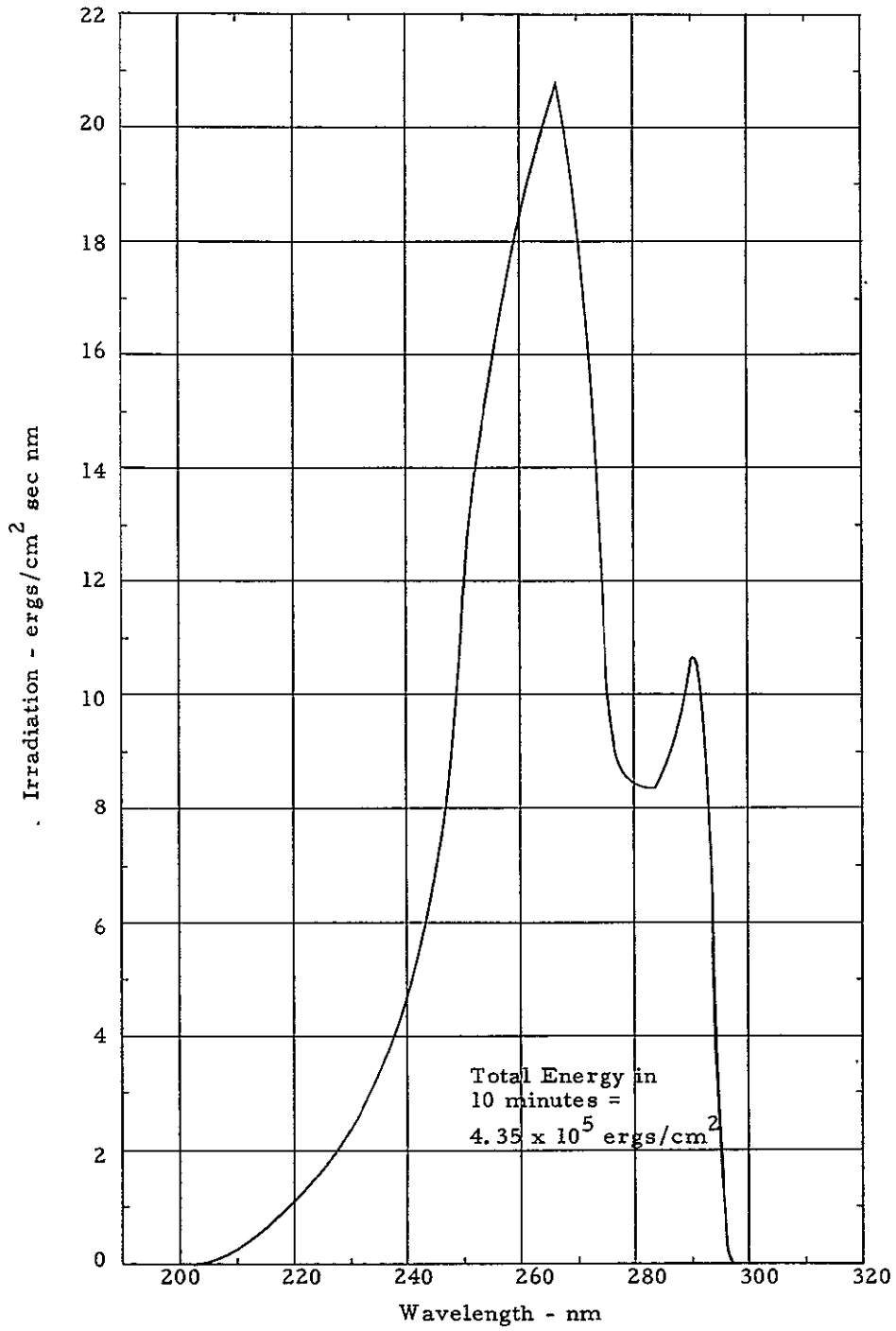


Figure 4.3.5-4. Solar Spectral Irradiation Passing through Interference Filter with Half-Peak Bandwidth = 25 nm

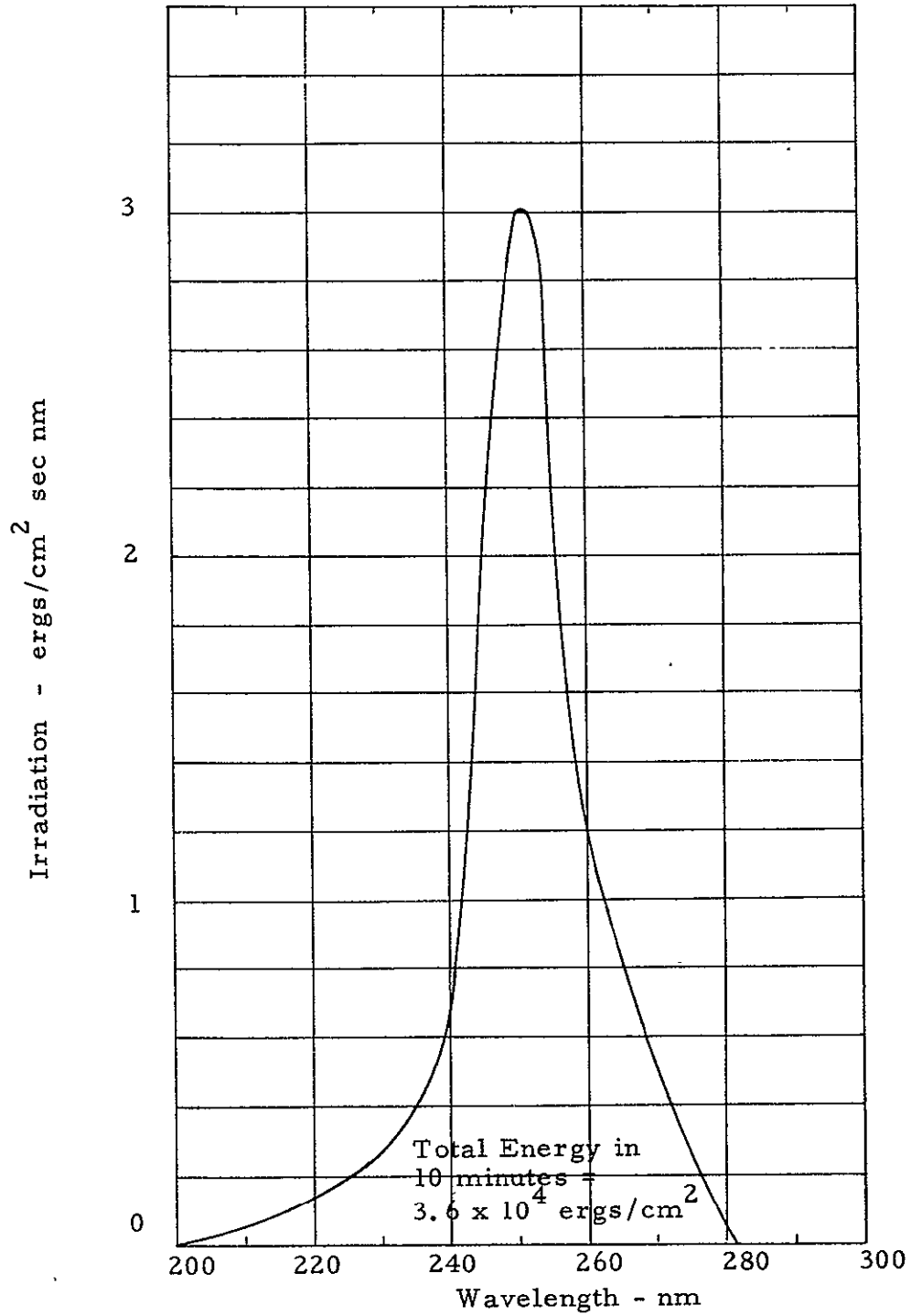


Figure 4.3.5-5. Solar Spectral Irradiation Passing through Interference Filter with Half-Peak Bandwidth = 10 nm

bandpass) by itself has a peak transmissivity at 253.7 nm. However, when combined with the non-uniform solar distribution, the peak in the transmitted energy shifts slightly to the longer wavelengths. The narrow 10 nm bandpass filters experience less shift in the peak of the transmission band. Both figures do not include the effects of a MEED cover glass or the cuvette cover glass. The choice of cover glass will have an influence on the level of sample irradiation and the location of the peak intensity.

Quartz glass, such as G.E. 151 Fused Silica, has a spectral transmittance shown in the following table.

UV Transmittance of 151 Fused Silica, 1 cm thickness  
(Manufacturer's data, excluding surface reflection losses)

Wavelength nm	Internal Transmittance %
220	92
240	95
260	98
280	100
300	100

The fact that the transmittance of the quartz is only slightly dependent on wavelength would amount to a negligible shift in the location of the peak irradiance of the biological sample.

One other material potentially useful as cuvette covers is KEL-F. Measured transmittance of this material is given below.

Measured UV Transmittance of KEL-F, 0.76 mm thickness

Wavelength nm	Transmittance (including surface reflection losses) %
235	35.0
240	40.5
250	49.5
260	56.5
270	62.0
280	66.0
290	70.0
300	73.0

Although the transmittance is substantially lower than Quartz, it could be used as a combination cover "glass" and "neutral" density filter for experiments requiring reduced irradiation. The non-uniform spectral transmittance of KEL-F may cause a slight shift in the peak transmitted energy. Additional reductions in energy level are easily achieved with commercially available neutral density filters. Figures

4.3.5-6 and 4.3.5-7 show the measured transmittance of two interference filters and their combination with Quartz and KEL-F. Air was used as a reference for these measurements. One of the filters (10-33-3) was supposed to peak at about 253.7 nm but actually peaked at about 257 nm. The other filter (10-65-8) peaked at the proper wavelength (280 nm). It is important to mention here that ultimately the various filters/covers combinations will have to be tested to insure that the desired spectral distribution and energy levels are in fact achieved for the various experiments.

#### 4.3.5.3 FEASIBILITY OF FILTER SYSTEM

At the present time, it appears as though there will be no problems in achieving the basic requirement of energy levels ranging from 10 to  $10^5$  ergs per sample chamber. Certain combinations of desirable conditions may present some problems, e.g., low bandwidth, short wavelengths, and high level of irradiation (low survival ratios). It is also difficult to achieve high irradiation levels while also achieving high selectivity of wavelengths such as separating 254 nm from 260 nm irradiation. Combining some of the elements of the filter pack such as the interference filter and the neutral density filter, thus reducing the number of "glass" interfaces, could help to reduce transmission losses. A reevaluation of the above potential problems should be done when specific wavelengths and energy level combinations have been determined.

#### 4.3.5.4 RADIATION FILTER MODEL

Figure 4.3.5-8 shows a model of the radiation filter system which may be used to experiment with UV exposures of biological samples. This model contains 4 Type A cuvettes. Above the cuvettes is a piece of KEL-F, an interference filter (10-65-8) with a transmittance peak at 280.0 nm, and a quartz cover glass. The transmission characteristics of these three filter pack elements are shown in Figures 4.3.5-6 and 4.3.5-7.

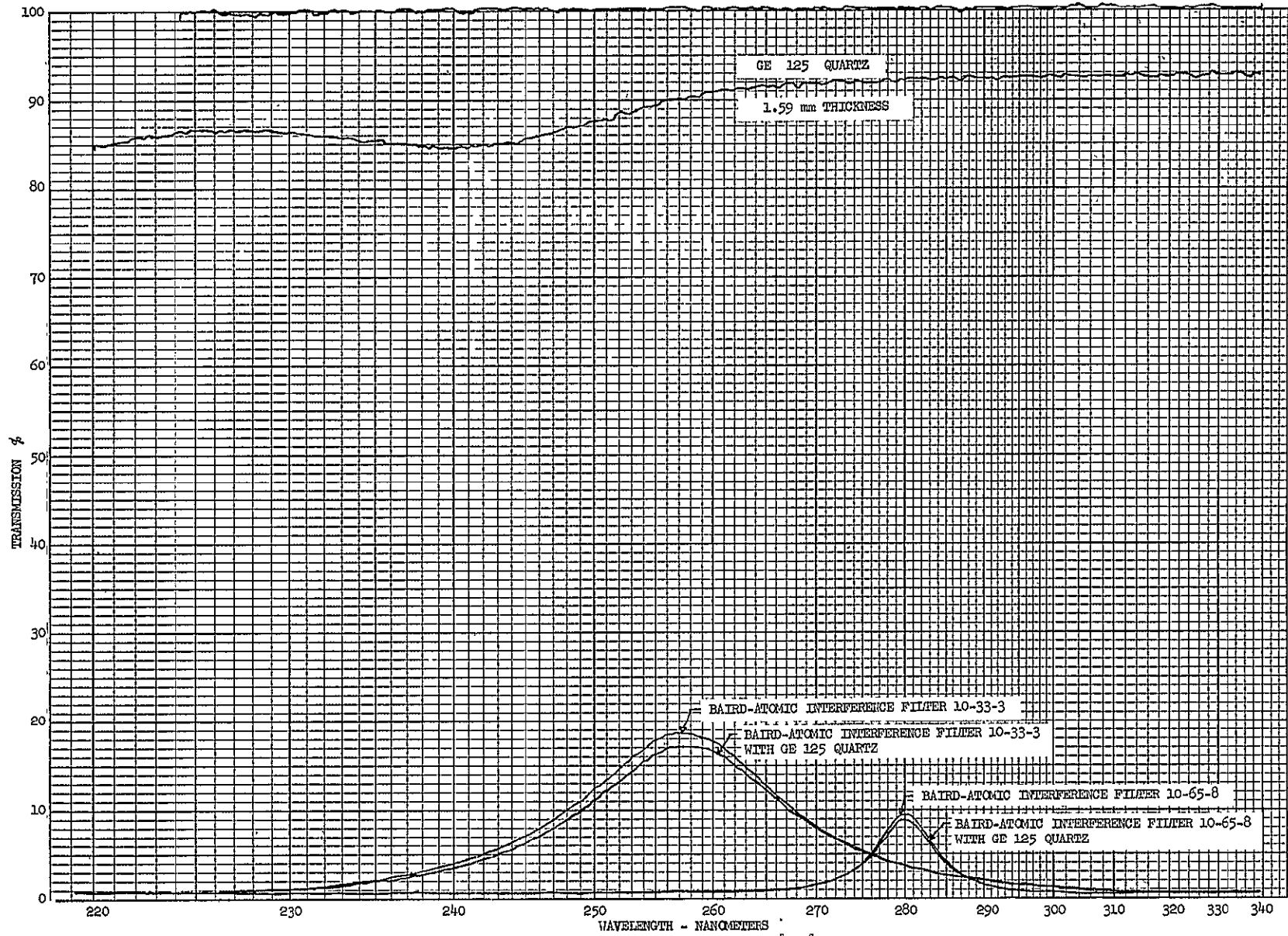


Figure 4.3.5-6. Measured Transmission Characteristics of Interference Filters and Quartz Glass

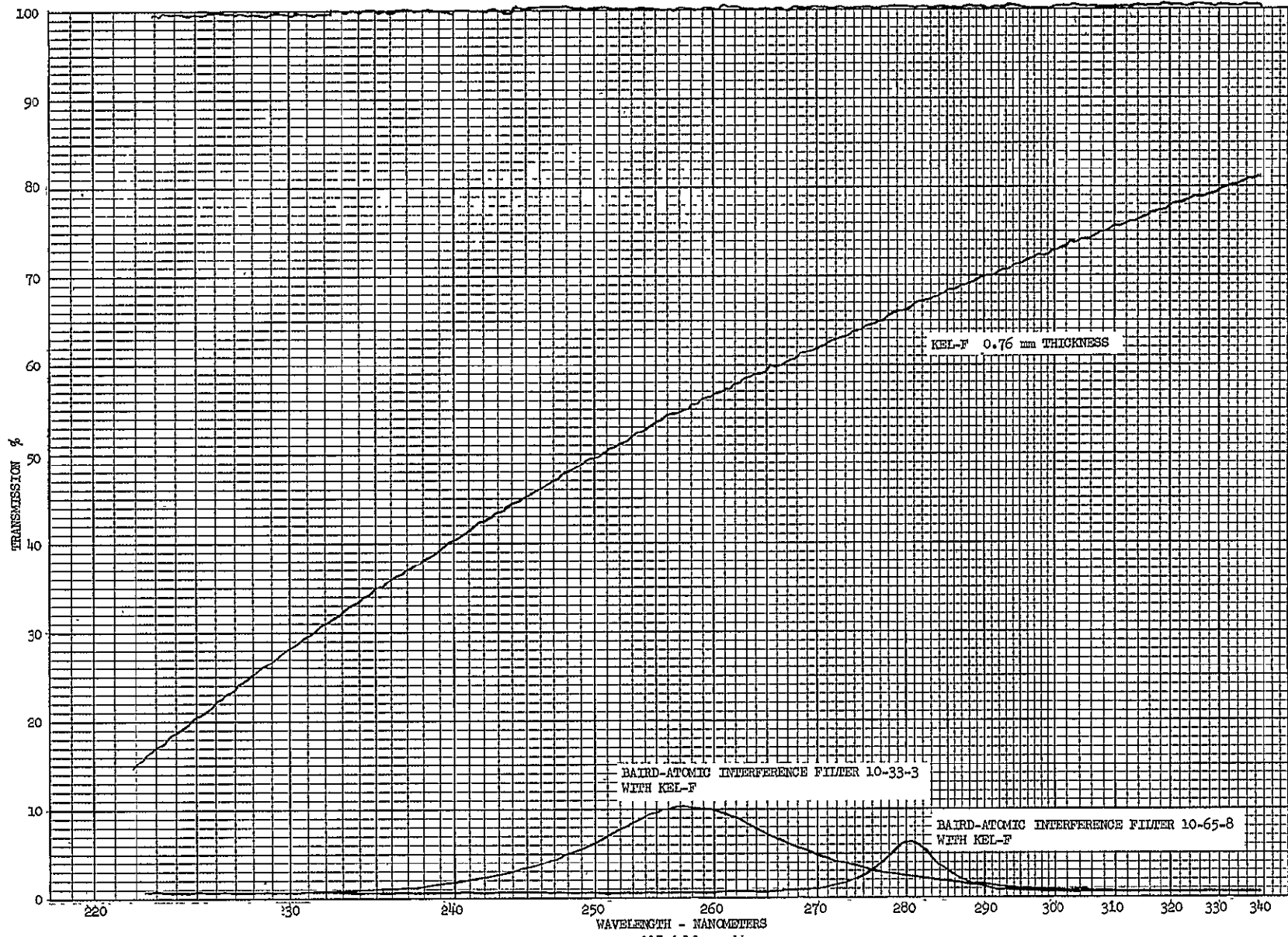


Figure 4.3.5-7. Measured Transmission Characteristics of Interference Filters and KEL-F

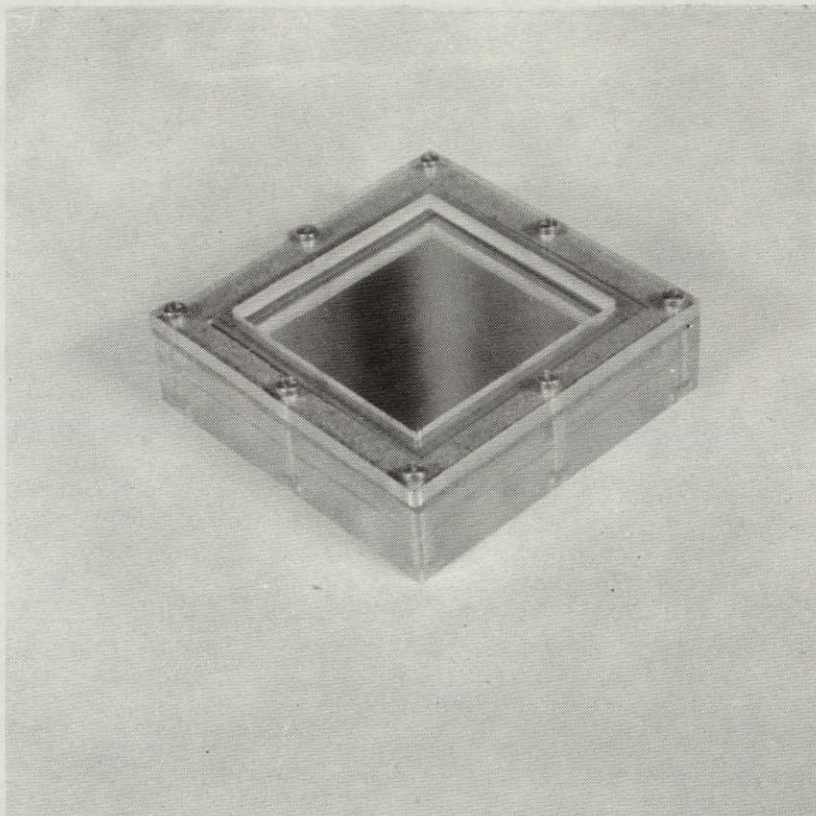


Figure 4.3.5-8. Radiation Filter Model



#### 4.3.6 TEMPERATURE RANGE INDICATOR

##### 4.3.6.1 INTRODUCTION

The MEEDs exposed to radiation and the control MEEDs located at MSC Houston, in the Command Module, and on the lunar surface will have varying temperature environments. The biological samples for each MEED will be subjected to temperature ranges that depend on the external temperature environment of the MEED in which they are located.

The function of the temperature indicators for the MEED is to provide a positive indication of the maximum and minimum temperatures that the biological samples are exposed to during the entire Apollo mission.

The target requirement for the accuracy of measurement is  $\pm 2^{\circ}\text{C}$  and the mechanical environment to which the indicator is subjected is the same as that for all of the components of the MEED.

Three types of temperature indicators were investigated during this study: 1) the organic solvent melting point indicator, 2) the liquid crystal indicator, and 3) the bimetallic temperature indicator. The first two types depend upon the melting point of the material and a change in the color of the material respectively. These approaches show considerable promise for maximum temperature indications. No principle has been uncovered that will permanently indicate the minimum temperature encountered that is based on chemical or physical changes in the material. The bimetallic element can be used however to indicate both maximum and minimum temperatures.

The microbial sample temperature will be somewhat different under each combination of radiation wavelength and intensity. The variations in temperature between cuvettes will be much smaller than the variations in temperature that will occur with time. The planned temperature indicator design for the MEED will thus comprise a reasonably accurate measurement at one location in the MEED tray. The temperatures at all other points will be determined by calculations based on calibration tests run prior to the MEED experiment. This data will be obtained during the development of the Lunar Subassembly in the environmental test that simulates solar radiation, space vacuum, the surrounding radiation environment of the lunar surface and cold space.

#### 4.3.6.2 ORGANIC SOLVENT MELTING POINT INDICATOR

A popular technique for indicating temperature maximums has been the use of "pyro-cones", non-ferrous alloys which melt down at particular temperatures. Unfortunately, such indicators are designed for high temperature work in the red-hot regions and above. In addition, these cones indicate maximum temperature. The requirement in this application is for a maximum-minimum indicator.

A technique suitable for the MEED would be the use of organic solvents whose melting points are in the temperature range prescribed. Refer to Table 4.3.6-1 for a list of readily available organic compounds and their respective melting points. All of the organic compounds on this list have been checked out in Dangerous Properties of Industrial Materials, Irving Sax 1963, and all of them are generally safe for use. Unfortunately, the melting point techniques are applicable for maximum temperature indications only.

Organic solvent melting points as temperature indicators can be employed in two ways:

- a. Change in color due to dye dissolution upon melting.
- b. Change in crystallographic geometry upon melting and recrystallization.
- a. Change in color due to dye dissolution upon melting.

This technique is straightforward and quite simple.

Place the organic compounds having the desired melting points in an oven and melt them. While molten, fill the appropriate containers, i. e., cuvettes, each with a different solution. Place the filled cuvettes in a refrigerator and allow the contents of each to solidify. Of course, the volume will decrease upon solidifying. Place in each cuvette one grain of Rhodamine B stain.

When the temperature exceeds the melting point of the particular organic compound, it will melt and the dye will go into solution imparting a red color to the entire contents. Whether or not the organic compound melts and solidifies several times more, the red color will remain following the initial melt. Refer to Figure 4.3.6-1. The white vial on the right has never been above its melting point since the addition of Rhodamine B; the dark vial (red) on the left has been above its melting point following the addition of Rhodamine B.

Table 4.3.6-1

## MELTING POINTS OF ORGANIC COMPOUNDS

<u>Organic Compound</u>	<u>Melting Point °C</u>
Monoethanolamine	10-12
Aracel B	11-14
p-Xylene	13
1,2,3,4-Tetrahydroquinoline	15-16
Atlas NNO	15-16
Phenyl cellosolve	15
Span 20	15
Trichlorobenzene	15-17
Cyclopropanecarboxylic acid	17-19
Glaurin	17-18
Sodium lactate	17
Sodium manganate	17
Phenylhydrazine	18-19
Butyl stearate	19
Tridodecylamine	20-22
Triethanolamine	21
Octanophenone	21-22
Triphenyl phosphite	22-24
Phenyl laurate	23-25
2,4,6-Trichloropyrimidine	23-25
Aminomethylpropanol	24-28
Tolunitrile	25-27
Tertiary butyl alcohol	26
Diethanolamine	26-28
Cyclohexyl stearate	28-29
Octadecane	27-28
o-Cresol	29-31
Quinoxaline	31-32
p-Cresol	32-35
Tetradecanol	35-37
N, N-Dimethylbenzamide	44-44
2, 6-Dimethylphenol	45-47

Data from "Handbook of Chemistry and Physics", 1961

Table 4.3.6-1 (continued)

<u>Organic Compound</u>	<u>Melting Point °C</u>
3, 4-Dimethylaniline	50-52
Thymol	50-52
Methyl stearate	50-52
Diphenylamine	52
Dimethyl oxalate	53-55

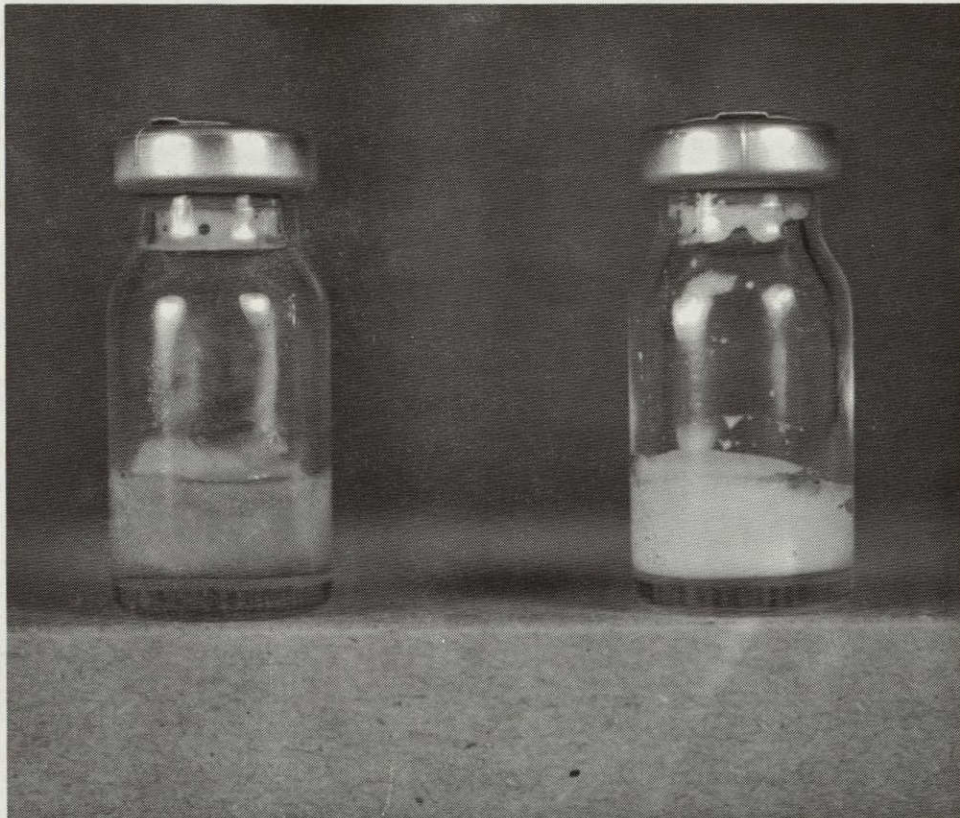


Figure 4.3.6-1. Melting Point Indicator

This technique is irreversible; however, all of the cuvettes or vials must be kept stored below the lowest melting point of the organic compounds selected as indicators. The all-stained cuvette having the highest melting point indicates the maximum temperature reached.

b. Change in Crystallographic Geometry Upon Melting and Recrystallization

This technique is not as simple as the previous one and requires keen microscope observation. Place the organic compounds having the desired melting points in separate beakers and add about 25 ml of acetone to each and dissolve completely. Using separate pasteur pipettes, place a drop from each beaker on a microscope slide and store at a temperature below the lowest melting point of the organic compounds. Store until the acetone has separated, dropping out the organic compounds as microcrystalline deposits. When these deposits melt at that particular melting point and then resolidify, macrocrystals will be formed which are readily observed on a low power microscope.

In Figure 4.3.6-2, the top photograph is a particle of tetradecanol formed by dissolution in acetone and subsequent deposition as microcrystalline material. The bottom photograph is another particle of tetradecanol that has melted and resolidified following the acetone deposition. The geometric order and macrocrystalline structure of the particle are of interest. Thus by observing the organic compounds with a low power microscope, one can determine if melting has occurred following deposition. As before, the slides containing the deposited organic compounds must be stored at a temperature below the lowest melting point.

4.3.6.3 LIQUID CRYSTAL TEMPERATURE INDICATOR

Another technique for recording maximum temperature is the use of liquid crystals. Derivatives of cholesterol, cholesteric liquid crystals flow like a liquid and at the same time exhibit the optical properties of a crystal by scattering light selectively. When white light shines on liquid crystals, they will reflect colored light. The crystals reflect only one wavelength at each angle, and the reflected beam is circularly polarized. When light comes from several directions at once, a different wavelength is reflected at each angle, and the resulting mix of different colors is seen as the



Figure 4.3.6-2. Tetradeanol

irridescence.

The specific organization that gives rise to the scattering is a helical variation in the direction of molecular ordering. Figure 4.3.6-3 shows the probable molecular order. Most of the molecules in this system lie parallel in any one region; when the temperature varies, this direction changes in an orderly manner, thus causing a shift in molecular structure. This results in a different color at the same angle. The wavelength of the color produced by the temperature change can be as large as 100 nm shift/ $^{\circ}\text{C}$ . The response time of a liquid crystal system averages to be 0.1 seconds, which is much faster than for most standard thermometry techniques. Because the colors scattered by liquid crystals are unique for a specific temperature, quantitative temperature measurement is possible to  $\pm 0.1^{\circ}\text{C}$ .

Figure 4.3.6-4 exhibits a few of the several possible liquid crystal systems that can be modified to meet the requirements of a particular job requirement.

The MEED, of course, requires a "memory system", i. e., a system that will record temperature readings and will not be reversed following the conclusion of the experiment.

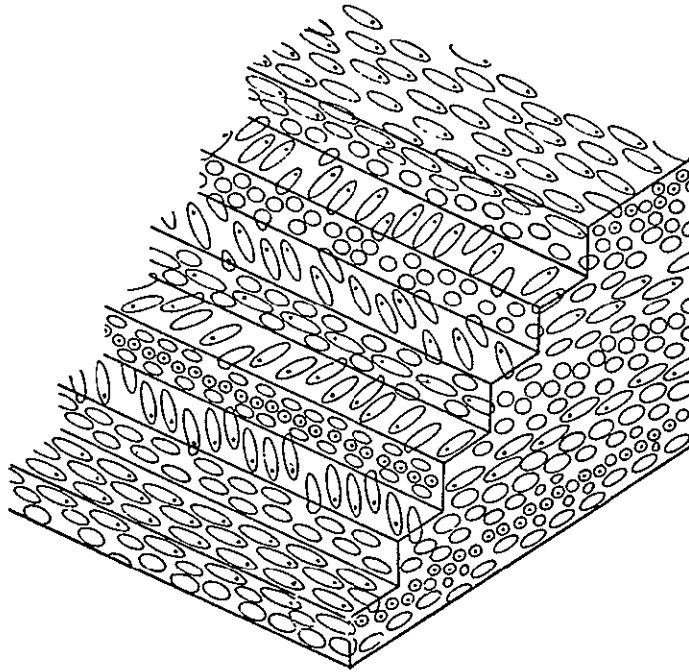
Although liquid crystal systems are reversible and are designed mainly for on-site observation, Liquid Crystal Laboratories, Turtle Creek, Pa., has developed a "memory" liquid crystal solution which has been tested in the laboratory. A solution designed for  $42^{\circ}\text{C}$  indication was tested in this study.

The technique for using these solutions in the laboratory is quite simple.

- a. Place a drop of the memory liquid crystal solution on a microscope slide and cover with a cover slip.
- b. Press down on the cover slip to spread out the solution to obtain a thin film or smear; the smear will have an iridescent-greenish cast.
- c. Place the slide on a hot plate set for  $42-45^{\circ}\text{C}$ ; the smear will change color to blue-black.
- d. When cooled down, the smear will not revert to green.

\*Figure taken from Reference 2





The molecular packing of the cholesteric structure. This figure represents the molecular arrangement of the cholesteric phase. Notice that there is no order in the molecular position. However, the direction of the long axis of the molecule is fixed. The diagram represents a cutaway section of a film, the plane surface being the upper layer. If we look at the right-hand side, we will see that different aspects of the molecules are presented so that they create a periodicity in the index of refraction. This can also be seen on the steps in the front of the cutaway. The black dot on the molecule describes the complete helix.

Figure 4.3.6-3. Liquid Crystal Molecular Order

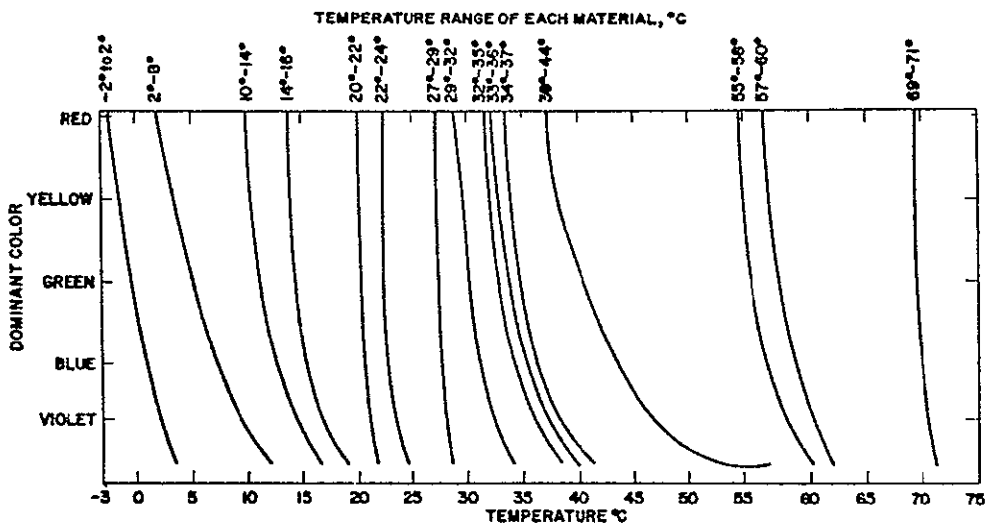


Figure 4.3.6-4. Liquid Crystal Systems

amb tests indicate, however, that this memory liquid crystal solution is unstable when vibrated. When subjected to low frequency fields such as 100 cps, the molecular structure apparently shifts back to a normal configuration such as before the application of heat; likewise, the color changes from blue-black back to green. Liquid crystal solutions are highly susceptible to oxidation and breakdown from ultraviolet light and would have to be shielded from the same when exposed to direct sunlight.

#### Bibliography

1. Liquid Crystals Instruction Booklet, Liquid Crystal Industries 1969, Turtle Creek, Pa.
2. "Liquid Crystals in Nondestructive Testing", James Fergason, Applied Optics, Vol. 7, No. 9 (Sept. 1968).

#### 4.3.6.4 BIMETALLIC TEMPERATURE INDICATOR

The bimetallic principle can be used in two basic ways to provide temperature maxima and minima. One method comprises the use of small curved bimetallic strips which expand and break a frangible connecting link when a given high or low temperature is reached. The problem with this approach is that each element can only detect that its critical temperature has been exceeded. Thus several elements of varying preset temperature points are required at both the high and the low temperature extremes.

The second method comprises a coiled bimetallic strip similar to those used on commercial bimetallic thermometers. The coiled strip expands and moves a needle to indicate temperature. This type of unit can be used as a recording temperature range indicator by adding a scribing point that scratches a sensitive layer of material in a circular arc as the bimetallic strip expands and rotates.

A rudimentary breadboard model of a bimetallic temperature range indicator was assembled and Figure 4.3.6-5 shows the bimetallic element which is anchored at the periphery. Heating of the element causes the shaft in the center to rotate which in turn rotates the disk that is behind the bimetallic indicator. The rotating disk with the scribing ball is shown in Figure 4.3.6-6. In this view, the cover, which is coated with blueing has been opened. The scratch mark that was caused when the bimetallic element was heated can be seen over an arc of approximately  $120^{\circ}$ . The same scratched arc can be seen from the outside of the indicator cuvette in Figure 4.3.6-7.

No effort was made to calibrate the breadboard model. A degree of feasibility has been shown by the model but the following problems remain to be solved during the indicator development period:

1. The indicator and its container require a degree of miniaturization. The length of the side would be reduced from approximately 24 mm to 16 mm (4 cuvettes). All other dimensions would be reduced approximately proportionately.

2. The bimetallic element would be fabricated from one of the newer high-energy bimetallic materials to provide an adequate arc of movement over the  $10^{\circ}\text{C}$  range anticipated within the MEED.

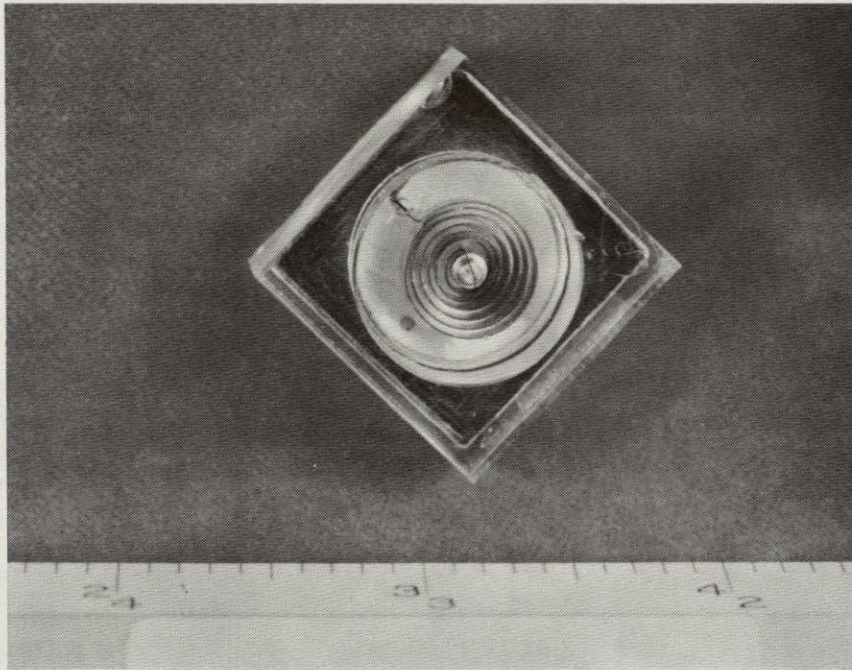


Figure 4.3.6-5. Bimetallic Temperature Indicator Element

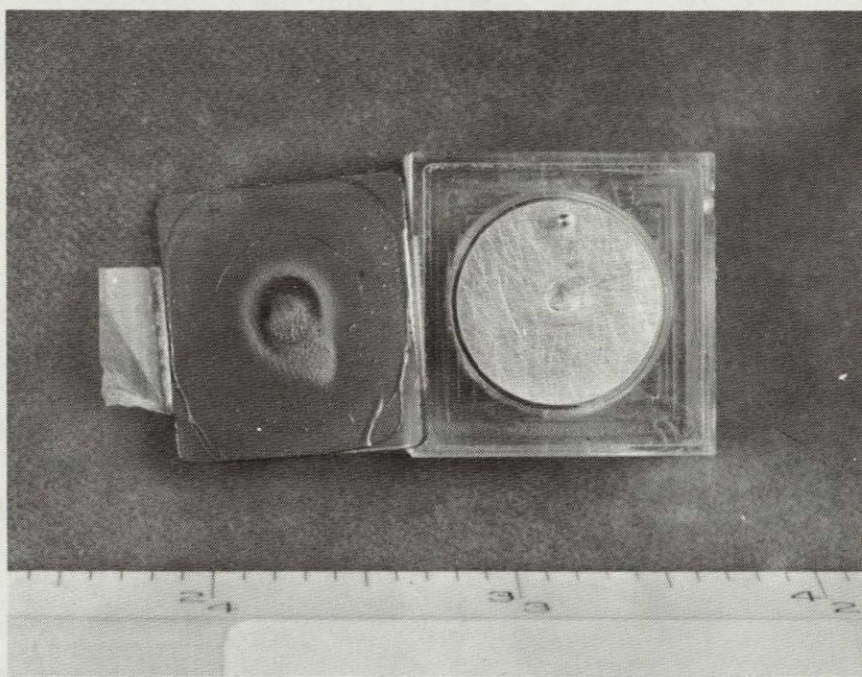


Figure 4.3.6-6. Bimetallic Indicator with Cover Open

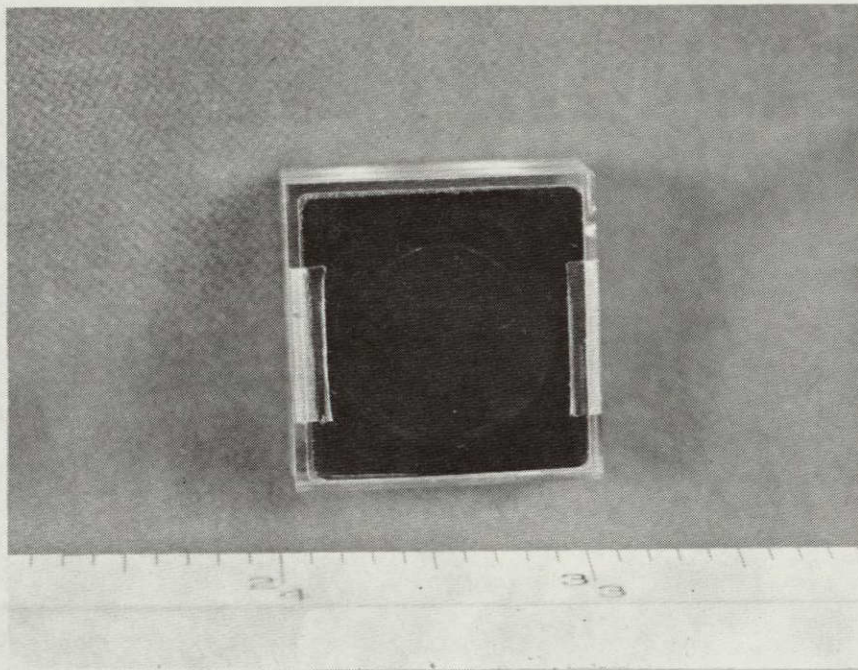


Figure 4.3.6.7. Bimetallic Indicator Trace Due to Temperature Change

3. The bimetallic element will have to be constructed with wide enough elements that it provides adequate force to scratch the selected film without hysteresis.

4. The scribing point will have to be sharp enough to trace the motion, yet smooth enough to prevent sticking on the quartz window.

5. Tests will be required to insure that vibration and shock do not cause movement of the scribe. The final unit may be filled with a viscous, inert fluid if shock loads cause a false reading. Simple tests of the breadboard indicate that shock will not be a significant problem.

Discussions were held with the Taylor Instrument Company concerning the development of a bimetallic temperature range indicator. The proposed unit utilized one of the recently developed high-energy bimetals, but would require additional miniaturization.

The conclusion reached on the basis of the study was that the temperature indicating unit lies within the present technology, but that some development will be required to produce a low-hysteresis unit.



#### 4.3.7 RADIATION LEVEL INDICATOR (ACTINOMETER)

##### 4.3.7.1 INTRODUCTION

The MEED will employ the potassium ferrioxalate chemical actinometer as a method for measuring the total ultraviolet energy irradiating the MEED test systems.

For lunar research, the chemical actinometer has many distinct advantages over a physical actinometer or thermopile:

- Reduced size
- Reduced weight
- No support assemblies
  - Power supplies
  - Electrical power
  - Recording apparatus
- Simplicity of operation

For several years, the standard chemical actinometer available to the laboratory was the uranyl oxalate chemical actinometer. However, this actinometer has several disadvantages, mainly:

- Low sensitivity
- Decreased precision at low light intensities
- Complex laboratory technique

In 1956, Hatchard and Parker developed a new sensitive chemical actinometer known as the potassium ferrioxalate chemical actinometer. The results of their work have resulted in the replacement of uranyl oxalate by potassium ferrioxalate as a standard chemical actinometer. The advances of potassium ferrioxalate as a chemical actinometer are discussed below in detail:

- The sensitivity is about one-thousand times greater than that of uranyl oxalate.
- The quantum efficiency (the ratio of rate of decomposition to light intensity (expressed as moles/einstein) is constant and independent of light intensity.
- It is as precise as uranyl oxalate under all conditions and more precise for measuring low light intensities.
- It has a long wavelength range with uniform quantum efficiencies up to 500 nm.
- The stability of the actinometer solutions and photolysis products is improved.
- Ease of operation
- Sensitive to wide ranges of total radiation dose values.

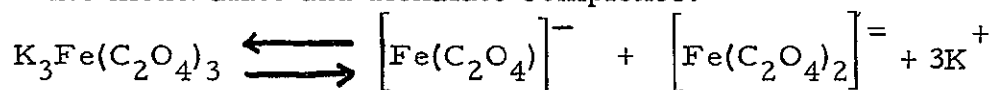
The potassium ferrioxalate actinometer has specific advantages for the MEED application. At all wavelengths below 510 nm, it has been established by Hatchard and Parker that accurate temperature control is unnecessary when using the potassium ferrioxalate actinometer provided that the depth and concentration of the potassium ferrioxalate actinometry solution is chosen so that light absorption is high.

Studies have shown that a one centimeter optical depth of 0.006 M potassium ferrioxalate actinometer solution will absorb 99% or more of the light of wavelengths up to 390 nm (Figure 4.3.7-1). In the region of our interest, i.e., 250 nm to 300 nm, a one millimeter optical depth of 0.006 M potassium ferrioxalate absorbs 100%. As a result, only one millimeter is required as a nominal optical depth for the final cuvette design for the MEED. For longer wavelengths, where the percent absorption drops off, the 0.15 M solution is preferable. Refer to the protocol for the method of synthesis of these actinometer solutions.

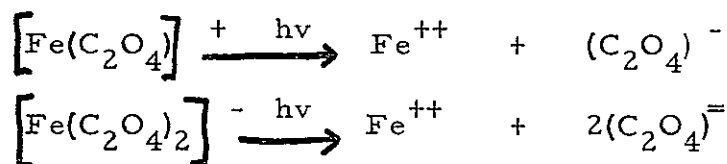
The quantum efficiency of the potassium ferrioxalate actinometer is constant for varying concentrations of ferrioxalate. At 0.006 M and above, light absorption is complete.

#### 4.3.7.2 CHEMISTRY

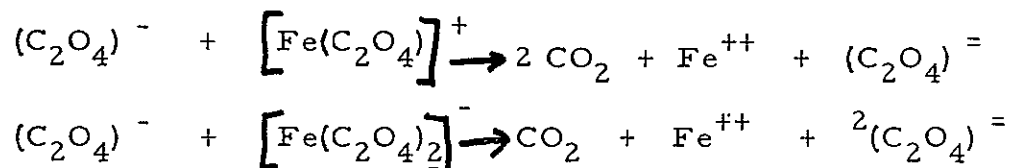
The actinometric or photolyte solution consists of 0.006 M potassium ferrioxalate,  $K_3Fe(C_2O_4)_3 \cdot 3H_2O$ , in 0.1 M sulphuric acid,  $H_2SO_4$ . In an acid solution, the dioxalate-ferric ions are largely dissociated into monoxalate and dioxalate complexes:



On exposure to ultraviolet light, the following reactions occur:

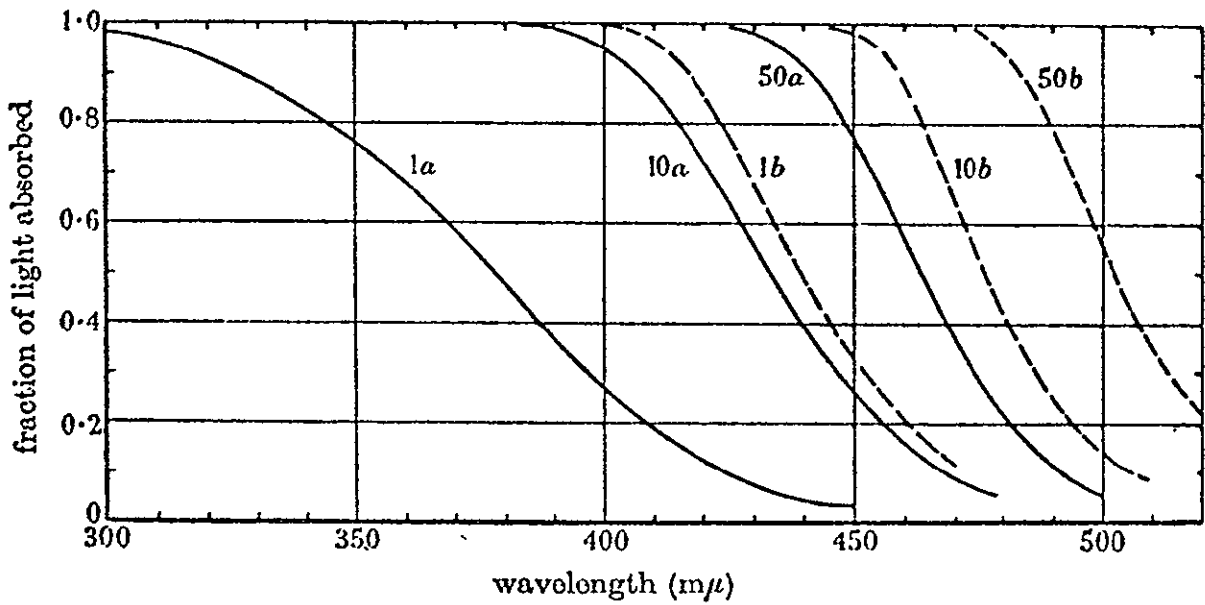


then,



After irradiation, a solution of phenanthroline is added to the actinometer

\*Data from C.G. Hatchard and C.A. Parker

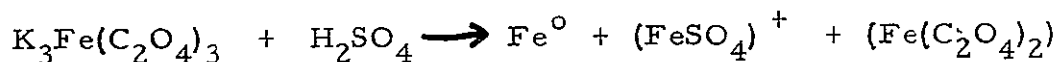


Light absorption by recommended actinometer solutions. Curves 1*a*, 10*a* and 50*a* are for 0.006 M-potassium ferrioxalate in 0.1 N-sulphuric acid with optical depths of 1, 10 and 50 mm respectively. Curves 1*b*, 10*b* and 50*b* are for 0.15 M-potassium ferrioxalate in 0.1 N-sulphuric acid at the same optical depths respectively.

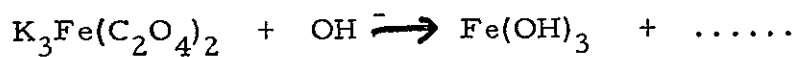
Figure 4.3.7-1. Actinometer Solution Absorption

solution, forming a colored complex with the reduced (ferrous) iron. The concentration of the iron-phenanthroline complex can be determined by measurement of its absorption at 510 nm.

The effect of varying the sulphuric acid concentration has been studied. Between 1.0 N and 0.01 N, the quantum yield varies slightly and it is maximum at 0.1 N, the standard concentration chosen for optimum actinometry. At high acidities, i. e., 10 N H<sub>2</sub>SO<sub>4</sub>, the quantum yield drops a great deal as a result of the dissociation of potassium ferrioxalate to ferric iron and its related sulphate complexes.



The products, in turn, act as "inner filters" and decrease the transmission of ultraviolet light through the actinometer solution, thus lowering the quantum efficiency. Conversely, the actinometric solution should not be neutral; should it shift from neutral to just slightly alkaline, excessive amounts of ferric hydroxide would be formed and precipitated.



In the interests of good chemistry, 0.1 N H<sub>2</sub>SO<sub>4</sub> is an acceptable concentration to insure a satisfactory quantum efficiency as well as a safeguard against pH shift to an alkaline situation.

#### 4.3.7.3 MATERIALS AND METHODS

Following the synthesis of the potassium ferrioxalate as prescribed under the protocol, a calibration curve was made for our particular spectrophotometer. Referring to Table 4.3.7-1, it is observed that the standard deviation is between 0-.02, which indicates that the data is linear as expected. Referring to Figure 4.3.7-2, a straight line denoting linearity is also observed.

Parker notes that 1.81 x 10<sup>-6</sup> moles of Fe<sup>++</sup> in the 20 ml test solution should have an optical density of 1.0. From the curve made in the amb laboratory, 1.81 x 10<sup>-6</sup> moles of Fe<sup>++</sup> has an optical density of 1.08, which corroborates the amb calibration effort with the Beckman DK 2a spectrophotometer.

Table 4.3.7-1

## ACTINOMETER CALIBRATION TABLE

Beckman DK-2a Spectrophotometer

Calib. Soln Vol.	Conc. Fe <sup>++</sup>	Optical Density	O. D. / 0.5 ml	Std Deviation
0 Control	0	0 (blank)	0	$\bar{X} = 0.12$
0.5	$0.2 \times 10^{-6}$ moles	0.13	0.13	0.01
1.0	$0.4 \times 10^{-6}$ moles	0.25	0.12	0
1.5	$0.6 \times 10^{-6}$ moles	0.36	0.12	0
2.0	$0.8 \times 10^{-6}$ moles	0.48	0.12	0
2.5	$1.0 \times 10^{-6}$ moles	0.59	0.11	0.01
3.0	$1.2 \times 10^{-6}$ moles	0.73	0.14	0.03
3.5	$1.4 \times 10^{-6}$ moles	0.84	0.11	0.01
4.0	$1.6 \times 10^{-6}$ moles	0.97	0.13	0.02

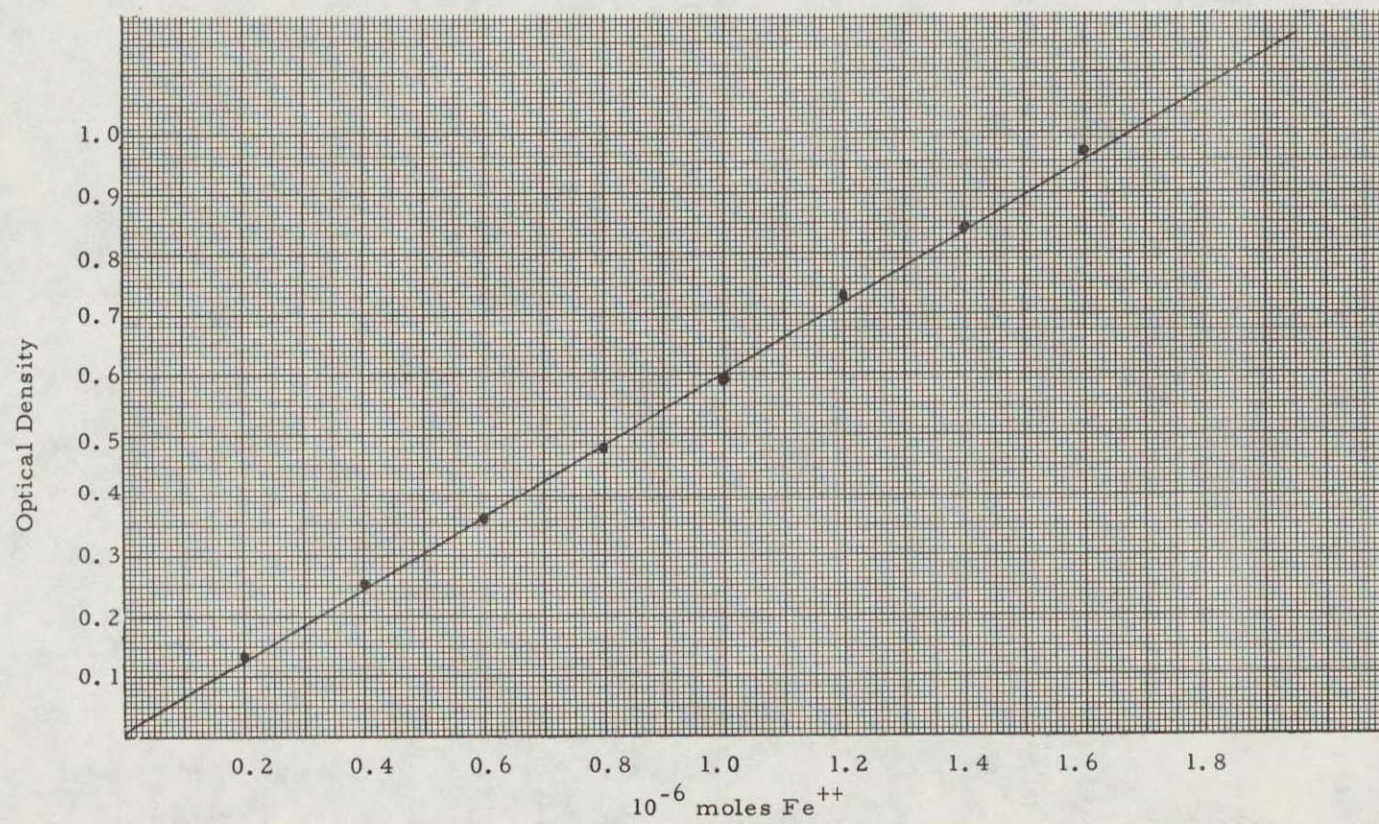


Figure 4.3.7-2. Calibration Curve

The MEED directive states that the peaks of interest are 254, 260, 280 and 300 nm. Once the actinometry solutions are checked out and the ultraviolet light source is calibrated, then studies at the peaks of interest, i. e., 254 nm in the short wave, will be done using Baird-Atomic ultraviolet bandpass filters.

To test the efficacy of the actinometer solutions prepared in the amb laboratory, it was necessary to provide for a "standard" ultraviolet light. It was then decided to provide for two "standard" ultraviolet light sources, to test the actinometer solutions at both ends of the ultraviolet spectrums, i. e., long and shortwave ultraviolet sources.

Following the investigation of the ultraviolet light sources, a shortwave bandpass filter for 250 nm (from Baird-Atomic, Cambridge, Mass.) was studied. For the preliminary investigations, the following apparatus was obtained:

#### Shortwave Apparatus

"Mineralight" ultraviolet source UV S-12

Baird-Atomic Bandpass Filters

250 nm

280 nm

#### Longwave Apparatus

B-100 "Blak-Ray" ultraviolet source

KENRAD 100W CA4 Mercury-vapor lamp

Roundel longwave filter

#### Miscellaneous Apparatus

1 x 4 cm Beckman Standard Spectrophotometric Cuvettes

5 x 5 x 3 mm MEED prototype quartz cuvette

Interval timer

OB red safelight

#### 4. 3. 7. 4 TEST PROCEDURE

The actinometer solution (photolyte) is placed in four 1 x 4 cm Beckman cuvettes at a distance of 1 meter from the ultraviolet light source; the cuvettes are irradiated by the ultraviolet light source prescribed. Following irradiation, the contents of the cuvettes are pooled; 1 to 5 ml samples are diluted, accordingly, with the appropriate reaction solutions and evaluated on the DK 2a

Spectrophotometer at 510 nm. All of the above is done in a darkroom with OB (red) safelights only.

#### 4.3.7.4.1 ACTINOMETER TESTS

##### 4.3.7.4.1.1 LONGWAVE LIGHT SOURCE (B-100 BLAK-RAY)

When the preliminary checkout of the actinometry solution was made, the B-100 (unfiltered) was turned on and off between exposures and it was noted that on successive exposures it became more difficult to restart the lamp. It was also noted that excessive amounts of visible light were given off by the B-100 lamp. The four and five-minute exposures had less energy levels than the two- and three-minute exposures and the one-minute exposure had no energy level at all (refer to Table 4.3.7-2).

Reviewing the ultraviolet literature, it was found that when a mercury vapor lamp is turned off and then on, ignition is difficult unless the lamp is permitted to cool; mercury vapor lamps require at least two minutes of warmup before maximum-constant intensity output is obtained; excessive turning on/off mercury vapor lamps decreases their intensity output and shortens their life.

From the above, it is not difficult to explain the anomalies observed:

- a. 1 minute - when the lamp was turned on for 1 minute, it did not reach an "optimum" intensity value before it was turned off.
- b. 2 to 3 minutes - for these two time periods the lamp was on long enough to warm up and become effective over the different exposure times.
- c. 4 to 5 minutes - when the lamp was turned off after the 3-minute exposure, it was hard to restart and some flickering was noticed; when the lamp did start, it apparently was below intensity and never reached maximum because of the heat and restarting cycle.

Referring to the manufacturer of the B-100 Blak-Ray (Ultra-Violet Products, San Gabriel, Calif.), transmission curves for the filtered and unfiltered B-100 Blak-Ray were obtained.

Figure 4.3.7-3 reveals that the spectrum of the unfiltered B-100 Blak-Ray lamps has peaks from the visible blue spectrum at 546 nm down to 200 nm; the same source, when filtered

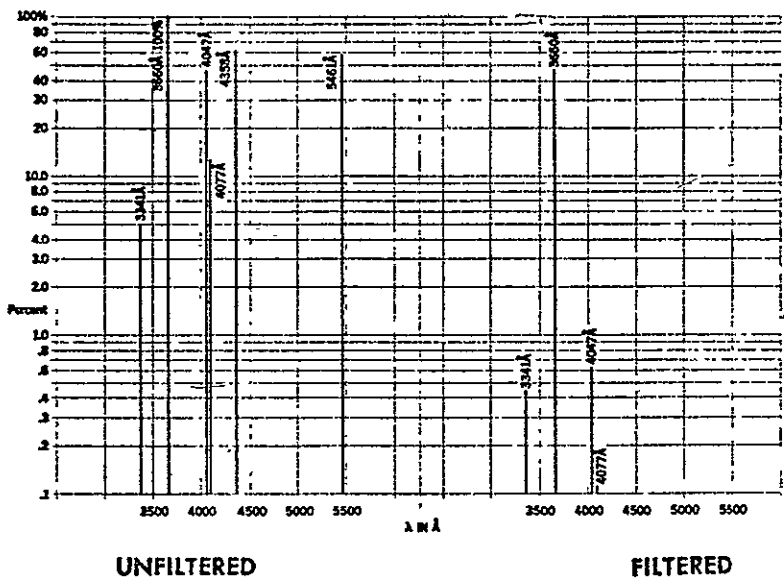


Table 4.3.7-2

PRELIMINARY ACTINOMETRY

D-100 Blak-Ray (unfiltered) 1 Meter from Actinometry  
Solutions (1 cm cuvettes)

<u>Exposure Time</u> <u>(minutes)</u>	<u>O. D. @ 510 nm</u>
1	0.01
2	0.42
3	0.88
4	0.58
5	0.64



This curve is typical of the BLAK-RAY® model B-100A Lamp. With the 3660 A unfiltered line representing 100 per cent, all other lines from the unfiltered Model B-100A source are in relation to it.

The filtered curve demonstrates the decrease in radiation caused by filtering.

Figure 4.3.7-3. Emission Curves, High-Pressure Arc

with a longwave "Roundel" filter, has a narrow spectrum from 400 nm to 300 nm with reduced radiation intensity due to filtering. Refer to Figure 4.3.7-4 for the transmission curve of the "Roundel" longwave filter. To eliminate visible light from the light source and at the same time have a narrow spectrum (300-400 nm) for preliminary investigations, a longwave filter was used.

In conclusion, the following procedures were followed in the investigation of the actinometry solution and the longwave ultraviolet light source:

- a. A new flood-type longwave lamp was obtained for the B-100 Blak-Ray lamp; a flood-type was chosen over the reflector spot to provide an even intensity during tests (Sylvania H44-45M-100 watts).
- b. A longwave "Roundel" filter was used over the new lamp resulting in a 300-400 nm bandpass.
- c. During tests, the lamp was left on continuously and was masked between radiation exposures.
- d. Warm-up time was accounted for.

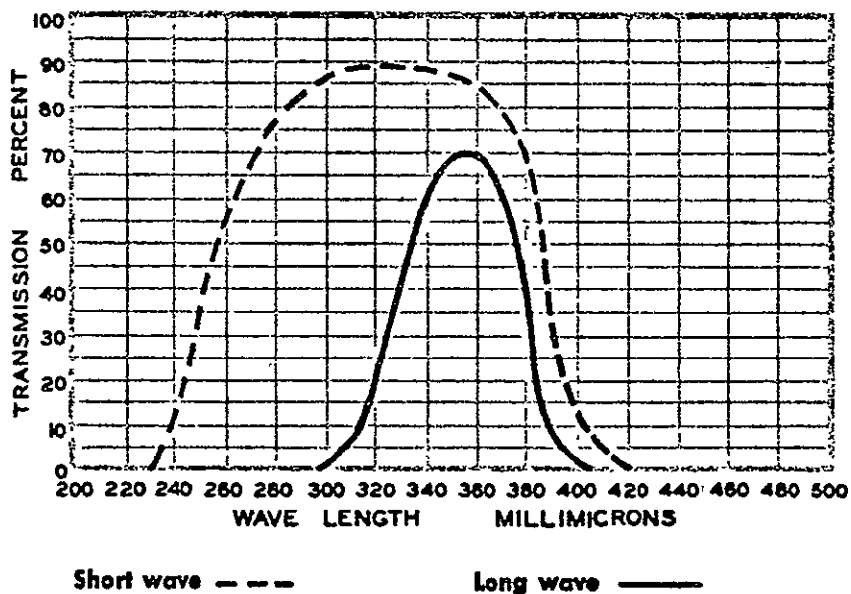
Prior to testing, the ultraviolet transmissivity of the Beckman cuvette must be considered. Referring to Figure 4.3.7-5, it is observed that for the standard Beckman cuvette:

<u>Wavelength</u>	<u>% Transmission</u>	<u>Correction Factor</u>
253.7 nm	72%	1.39
366.1 nm	85%	1.18

The significant point here is that all calibrated values obtained by the actinometer must be corrected for decrease of intensity due to absorption by the Beckman cuvette window. Use the correction factor where deemed appropriate. For our calculations, we will apply the correction factor to the dose rate only since it is the value of greatest interest.

Thus, having a better understanding of the light source and techniques required, it was desired to study the actinometer using the B-100 with/without the "Roundel" longwave to observe the sensitivity of the actinometer to narrow and broad spectrum ultraviolet radiation. The test was performed as prescribed. The B-100 exposure with filter was 5 minutes; the one without the filter was 2.5 minutes due to the increased intensity.

From Tables 4.3.7-3 and 4.3.7-4, it is observed that the dose rate for the unfiltered B-100 Blak-Ray lamp is 4X that of the



The two transmission curves shown are for long wave and short wave filters as generally used with BLAK-RAY and MINERALIGHT Lamps. Long wave filters do not tend to vary as much in transmission characteristics as short wave filters. The difficulty of making the short wave nickel-cobalt filters makes precise quality control almost impossible; consequently, new filters may vary from batch to batch. Short wave filters used over a period of time solarize or decrease in transmission at the shorter wavelengths. This characteristic is variable, depending on the batch of material and the intensity of solarizing short wave radiation striking the filter.

Figure 4.3.7-4. Transmission Curves, Longwave and Shortwave Ultraviolet Filters

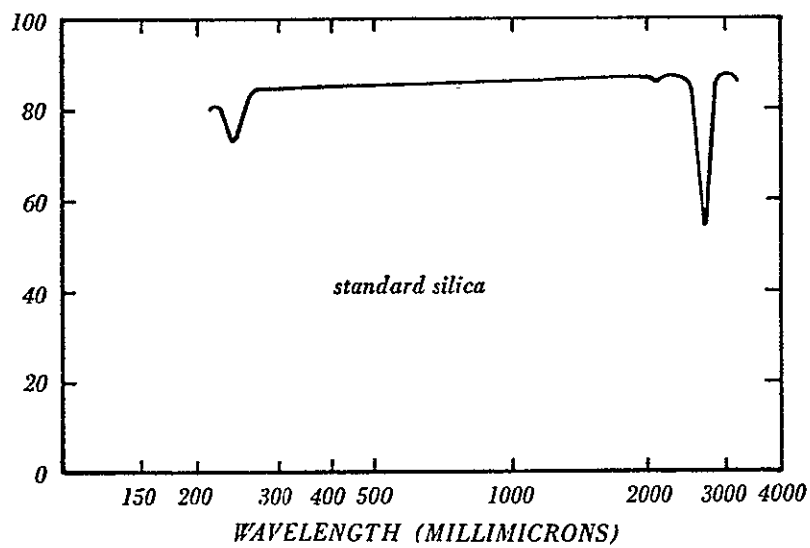


Figure 4.3.7-5. Transmission Spectra, Beckman Standard Cuvet

Table 4.3.7-3

B-100 Blak-Ray with Roundel Filter - 5-Minute Exposure

<u>Sample Volume Reacted</u>	<u>OD @ 510 nm</u>	<u>OD/ml</u>	Std Dev. <u><math>\bar{X} = 0.10</math></u>
1 ml	0.10	0.10	0
2 ml	0.185	0.09	.01
3 ml	0.29	0.10	0
4 ml	0.39	0.10	0
5 ml	0.50	0.10	0

Calculation: Average value is 0.10 O.D./ml

From Calibration Curve  $0.16 \times 10^{-6} \text{ m Fe}^{++}$  formed/ml

Quantum Yield @ 366 nm is 1.26 m/ein

Amount Radiation is  $\frac{0.16 \times 10^{-6} \text{ m Fe}^{++}/\text{ml}}{1.26 \text{ m/ein}} = 1.27 \times 10^{-7} \text{ ein/ml}$

Total Amount Radiation Striking  $(1.25 \times 10^{-7} \text{ ein/ml})$   
 $(3.25 \times 10^{-2} \text{ erg/ein at 366 nm})$   
 $= 4.15 \times 10^5 \text{ ergs/ml}$

For a 4 ml Cuvette  $= 4(4.15 \times 10^5 \text{ ergs/ml})$   
 $= 16.60 \times 10^5 \text{ ergs/4 ml cuvette}$

Dose is  $\frac{16.60 \times 10^5 \text{ ergs}}{400 \text{ mm}^2} = 4.15 \times 10^3 \text{ ergs/mm}^2$

Dose Rate =  $\frac{4.15 \times 10^3 \text{ ergs/mm}^2}{(5 \text{ min}) 300 \text{ sec}} = 14 \text{ ergs/mm}^2/\text{sec}$

Dose Rate - Absorption Corrected =  $(1.18) (14 \text{ ergs/mm}^2/\text{sec})$   
 $= 16.5 \text{ ergs/mm}^2/\text{sec}$

Table 4.3.7-4

B-100 Blak-Ray Without Filter - 2.5-Minute Exposure

<u>Sample Volume Reacted</u>	<u>OD @ 510 nm</u>	<u>OD/ml</u>	<u>Std Dev.</u> <u><math>\bar{X} = 0.195</math></u>
1 ml	0.20	0.20	.005
2 ml	0.40	0.20	.005
3 ml	0.58	0.19	.005
4 ml	0.77	0.19	.005
5 ml	0.97	0.195	0

Calculation: Average value is 0.195 OD/ml

From Calibration Curve  $0.33 \times 10^{-6} \text{ m Fe}^{++}$  formed/ml

Quantum Yield @ 366 nm is 1.26 m/ein

Amount Radiation is  $\frac{0.33 \times 10^{-6} \text{ m Fe}^{++}/\text{ml}}{1.26 \text{ m/ein}} = 2.62 \times 10^{-7} \text{ ein/ml}$

Total Amount Radiation Striking

One ml is  $(2.62 \times 10^{-7} \text{ ein/ml}) (3.27 \times 10^{12} \text{ erg/ein})$   
 $= 8.57 \times 10^5 \text{ ergs/ml}$   
 For a 4 ml Cuvette  $= 4(8.57 \times 10^5 \text{ ergs/ml})$   
 $= 34.28 \times 10^5 \text{ ergs/4 ml cuvette}$

Dose is  $\frac{34.28 \times 10^5 \text{ ergs}}{400 \text{ mm}^2} = 8.57 \times 10^3 \text{ ergs/mm}^2$

Dose Rate is  $\frac{8.57 \times 10^3 \text{ ergs/mm}^2}{(2.5 \text{ min}) 150 \text{ sec}} = 56 \text{ ergs/mm}^2/\text{sec}$

Dose Rate - Absorption Corrected is  $(1.18) (56 \text{ ergs/mm}^2/\text{sec})$   
 $= 66.1 \text{ ergs/mm}^2/\text{sec}$

filtered source. From Figure 4.3.7-3, it is observed that, at 366 nm, the filtered line is 80% of the unfiltered value; at 546 nm, which is visible-blue, the filtered line is zero or completely filtered out, indicating the absence of visible light; at 404 nm and 407 nm, the filter has reduced these lines to less than 1% of their unfiltered value. This data demonstrates that the potassium ferrioxalate actinometer solution, as synthesized and operated in the amb laboratory, is functioning properly and is, indeed, very sensitive to long-wave ultraviolet radiation. In addition, the extreme sensitivity of the actinometer to visible light (i. e., 546 nm) is clearly demonstrated, thus emphasizing the need for a light-tight test facility during actinometry and spectrophotometry.

#### 4.3.7.4.1.2 SHORTWAVE LIGHT SOURCE (MINERALIGHT)

Fortunately, an excellent shortwave ultraviolet light source is available for our purposes. Such a source is the Mineralight UV S-12 (refer to Figure 4.3.7-6). The standard wavelength for shortwave ultraviolet work, i. e., germicidal, is 253 nm. This particular source, when unfiltered, uses 253 nm as the 100% line; the other lines are less than 5%. Because of this excellent narrow spectral characteristic, this lamp will be considered for test as an unfiltered source.

The test procedure for the Mineralight source was identical to that of the Blak-Ray except, due to the low intensity output, a 10-minute exposure time was employed (refer to Table 4.3.7-5).

As was mentioned in Section 4.3.7.1, a 1 mm optical depth of 0.006 M potassium ferrioxalate absorbs 99% of wavelengths less than 300 nm. Since the Beckman cuvette is 10 mm in optical depth, the dose rate calculated represents a 10X dilution due to the first one mm complete absorption of the 10 mm optical depth. The dose rate calculated must be multiplied by 10 to achieve the proper optical correction.

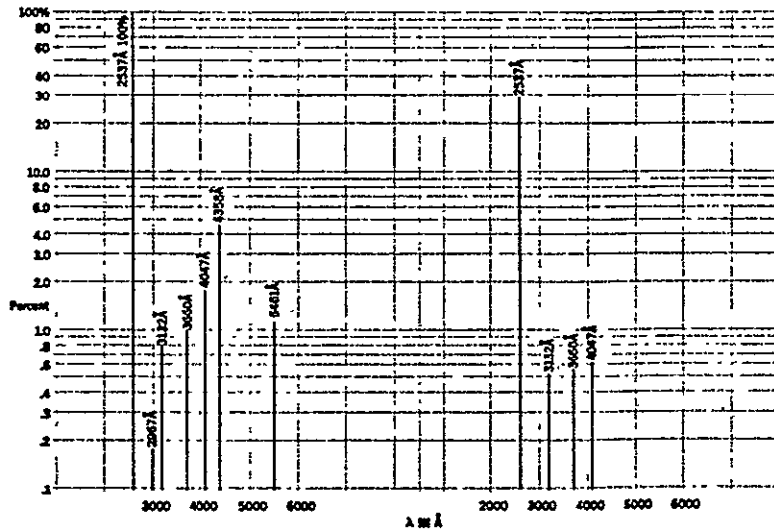
#### 4.3.7.4.1.3 BANDPASS FILTERS

At the present time the amb laboratory has received two shortwave bandpass filters from Baird-Atomic:

10-33-3 - 253.7 nm

10-65-8 - 280 nm





Lamps in this area include MINERALIGHT® Model UVS-11, UVS-12, M-14, and R-51; the C-81 (used in the CHROMATO-VUE® Cabinet C-5) and PEN-RAY® Lamps. The 2537 Å unfiltered line is taken as the 100 per cent line for short wave lamps. All others are in relation to it. The filtered curve illustrates the effect of the filter on a typical unfiltered source.

Figure 4.3.7-6. Emission Curves, Shortwave Ultraviolet Lamps

Table 4.3.7-5

## Mineralight UV S-12 Without Filter - 10-Minute Exposure

<u>Sample Volume Reacted</u>	<u>OD @ 510 nm</u>	<u>OD/ml</u>	<u>Std Dev.</u>
1 ml	0.03	.03	.005
2 ml	0.05	.025	0
3 ml	0.075	.025	0
4 ml	0.095	.024	.001
5 ml	0.12	.024	.001

Due to the low OD values, the 4 ml value will be used.

Calculation:

From Calibration Curve  $0.16 \times 10^{-6} \text{ m Fe}^{++}/4 \text{ ml cuvette}$

Quantum Yield is  $1.26 \text{ m/ein}$

Amount of Radiation is  $\frac{0.16 \times 10^{-6} \text{ m Fe}^{++}/4 \text{ ml}}{1.26 \text{ m/ein}} = 1.27 \times 10^{-7} \text{ ein}/4 \text{ ml}$

Total Amount Radiation Striking  $(1.27 \times 10^{-7} \text{ ein}/4 \text{ ml})$   
 $(4.71 \times 10^{12} \text{ erg/ein at } 253.7 \text{ nm})$

4 ml Cuvette is  $= 5.98 \times 10^5 \text{ ergs}/64 \text{ ml cuvette}$

Dose is  $\frac{5.98 \times 10^5 \text{ ergs}}{400 \text{ mm}^2} = 1.49 \times 10^3 \text{ ergs/mm}^2$

Dose Rate =  $\frac{1.49 \times 10^3 \text{ ergs/mm}^2}{(10 \text{ min}) 600 \text{ sec}} = 2.5 \text{ ergs/mm}^2/\text{sec}$

Dose Rate - Absorption Corrected is  $(1.39) (2.5 \text{ ergs/mm}^2/\text{sec})$   
 $= 3.5 \text{ erg/mm}^2/\text{sec}$

Optical Depth Correction is  $10(3.5 \text{ ergs/mm}^2/\text{sec})$   
 $= 35 \text{ ergs/mm}^2/\text{sec}$

Since the amb laboratory does not have a suitable light source to test the 280 nm bandpass filter, only the 253.7 nm filter will be tested, using the unfiltered Mineralight as a light source. The test procedure is the same as for the Mineralight light source with three exceptions:

1. Due to the low percent transmission of the bandpass filter, 16%, the exposure was increased to one hour.
2. The bandpass filter was placed in front of the cuvettes; the sides and top of the cuvettes were masked so that only filtered ultraviolet light would strike the cuvette from the front 1 meter from the Mineralight.
3. Due to the low response anticipated, the cuvettes were pooled, as prescribed, and a 5 ml sample was reacted.

From Table 4.3.7-6 a value of 5.2 ergs/mm<sup>2</sup>/sec has been calculated. Referring to Figure 4.3.5-6, the percent transmission of the 250 nm bandpass filter, as read on the DK 2 a spectrophotometer in the laboratory, is 16% @ 253.7 nm. From the previous test a value of 25 ergs/mm<sup>2</sup>/sec was calculated for the unfiltered Mineralight. Comparing the unfiltered Mineralight value with that of the bandpass filter:

$$\text{@ 253.7 nm} \quad \frac{5.2 \text{ ergs/mm}^2/\text{sec} (100)}{35 \text{ ergs/mm}^2/\text{sec}} = 15.0\% \text{ transmission}$$

From this calculation, excellent agreement is observed. Comparing the actinometer value of 15.0% to the 16% value of the spectrophotometer yields a 6% discrepancy between the two measurements. From these tests, we have shown that the potassium ferrioxalate actinometer, set up and operated, is acceptable for use as prescribed and/or required.

As a conclusion to the actinometer effort it was decided to conduct a test using the quartz MEED cuvette; its dimensions are 5 x 5 x 3 millimeters. The detailed technique is as follows:

1. Under red light,
  - a. Fill the cuvette with 0.006 M potassium ferrioxalate using a syringe as prescribed.
  - b. For test purposes, seal the cuvette with masking tape instead of the usual wax.
  - c. Place the cuvette one meter from the

Table 4.3.7-6

250 nm Bandpass Filter - One-Hour Exposure

<u>Sample Volume Reacted</u>	<u>OD at 510 nm</u>
5 ml	0.11

Calculation:

From Calibration Curve  $0.18 \times 10^{-6} \text{ m Fe}^{++}$  formed/5 ml

Radiation Amount is  $\frac{0.18 \times 10^{-6} \text{ m Fe}^{++}}{1.26 \text{ m/ein}} / 5 \text{ ml} = 1.43 \times 10^{-7} \text{ ein/ml}$

Total Radiation Striking

Cell is  $(1.43 \times 10^{-7} \text{ ein/5 ml}) (4.71 \times 10^{12} \text{ erg/ein})$   
 $= 6.73 \times 10^5 \text{ ergs/5 ml}$

Dose is  $\frac{6.73 \times 10^5 \text{ ergs/5 ml}}{500 \text{ mm}^2} = 1.34 \times 10^3 \text{ ergs/mm}^2$

Dose Rate is  $\frac{1.34 \times 10^3 \text{ ergs/mm}^2}{(60 \text{ min}) 600 \text{ sec}} = 0.38 \text{ ergs/mm}^2/\text{sec}$

Dose Rate - Absorption Corrected is  $(1.39) (0.38) \text{ ergs/mm}^2/\text{sec}$   
 $= 0.52 \text{ ergs/mm}^2/\text{sec}$

Optical Depth Correction is  $10(0.52 \text{ ergs/mm}^2/\text{sec})$   
 $= 5.2 \text{ ergs/mm}^2/\text{sec}$

Mineralight source with the window facing the source.

- d. Expose for 30 minutes.
2. Following the exposure, for the MEED cuvette:
  - a. Since the MEED cuvette holds 0.05 ml of actinometer solution, then one-tenth of the reaction solutions used for a 0.5 ml sample are required.
  - b. Mix the following:  
9.5 ml of 0.1 N  $\text{H}_2\text{SO}_4$   
2 ml 1, 10 phenanthroline solution  
8 ml buffer solution  
20 ml total. Fill a syringe with 2 ml of this reaction mixture.
  - c. Remove the tape from the MEED cuvette and hold it over a test tube.
  - d. Insert the syringe needle into the upper hole of the MEED cuvette and flush its contents into the tube with the reaction mixture of the syringe.
  - e. Wait one-half hour and evaluate as prescribed.

The aforementioned test was repeated three times. From Table 4.3.7-7, a value of  $34.2 \text{ ergs/mm}^2/\text{sec}$  is obtained. Comparing this value with the one obtained with the 1 centimeter Beckman cuvette and the Mineralight,

$$\frac{34.2}{35} (100) = 97.7\%$$

reveals excellent agreement and readily demonstrates the feasibility of both the MEED cuvette and its actinometer.

#### 4.3.7.5 ULTRAVIOLET SENSITIVE FILM

Another technique for the measurement of the ultraviolet radiation levels is the use of photographic film sensitized to the ultraviolet spectrum. Eastman Kodak has pioneered in this field and has published extensive data. The film-type most compatible for our requirements, i. e., 250-300 nm, is Eastman's "Kodak Spectroscopic Film, Type 103-0". Refer to Figure 4.3.3-7 for the spectral sensitivity of this particular film.

Essentially, Kodak uses basic emulsion types for their scientific films; then for particular spectral requirements, a special

Table 4.3.7-7

## MEED QUARTZ CUVETTE

30 min - UV S-12 Light

<u>Sample Value Reacted</u>	<u>OD @ 510 nm</u>	<u>Average</u>
0.05	0.10	$\bar{X} = 0.12$
0.05	0.13	
0.05	0.135	

## Calculation:

From the Calibration Curve  $0.2 \times 10^6 \text{ m Fe}^{++}$  formed/cuvette

Radiation Amount is  $\frac{0.20 \times 10^{-6} \text{ m Fe}^{++}}{1.26 \text{ m/ein}}$  /cuvette =  $1.58 \times 10^{-7}$  ein/cuvette

Total Radiation Striking Cell is  $(1.58 \times 10^{-7} \text{ ein/cuvette})(4.71 \times 10^{12} \text{ ergs})$   
 $= 7.44 \times 10^5 \text{ ergs/cuvette}$

Dose is  $\frac{7.44 \times 10^5 \text{ ergs/cuvette}}{25 \text{ mm}^2} = 2.9 \times 10^4 \text{ ergs/mm}^2$

Dose Rate is  $\frac{2.9 \times 10^4 \text{ ergs/mm}^2}{(30 \text{ min}) 1800 \text{ sec}} = 16.1 \text{ ergs/mm}^2/\text{sec}$

Dose Rate - Absorption Correction  $(1.06)(16.1 \text{ ergs/mm}^2/\text{sec})$

(GE 125) Quartz, 93% transmission =  $17.1 \text{ ergs/mm}^2/\text{sec}$  requires a 1.06 correction factor)

Corrected Optical Depth is  $2(17.1) \text{ ergs/mm}^2/\text{sec}$

(2 mm depth) =  $34.2 \text{ ergs/mm}^2/\text{sec}$

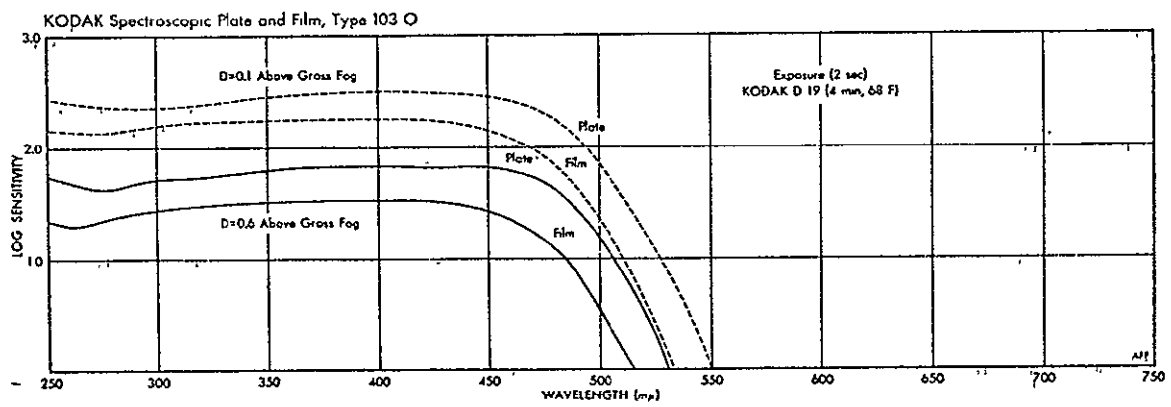


Figure 4.3.7-7. Spectral Sensitivity

sensitizing coating is deposited on the basic emulsion. The sensitive coating can be applied at the Kodak plant or can be done in the laboratory prior to use. Figure 4.3.7-8 summarizes the spectral sensitizings and their respective spectral qualities.

For the requirements of the MEED, however, the use of ultraviolet film is not acceptable:

- Extremely low sensitivity requiring long exposures.
- Must be stored in deep freezer.
- Wide bandpass: 500 nm - 100 nm.
- Shielding required against gamma and beta radiation.
- Complicated processing technique.
  - Removal of sensitizing treatment.
  - Anti-fog treatment.
  - Vigorously-controlled development.
- Low gelatin content of 103-0 film, requires extreme care in handling.
- Film quality is a function of each batch by Kodak.

Kodak does manufacture special films for satellite or deep-space recording systems. Unfortunately, these films are sensitive mainly to shortwave ultraviolet radiations below 250 nm which is unsuitable for the MEED. Such a film is Kodak Special Film Type 101-01.

In conclusion, the ultraviolet film technique would cause several technical design problems and, even if used, would not be as sensitive or accurate as the chemical actinometer.

#### Bibliography

Kodak Plates and Films, P-9, 1967.

Kodak Scientific Products Consumer Catalog, 1970.

Kodak Data Release P-135, 1967.

"A New Sensitive Chemical Actinometer I", C.A. Parker, Proc. Royal Soc. London, 1953.

"A New Sensitive Chemical Actinometer II", C.G. Hatchard and C.A. Parker, Proc. Royal Soc. London, 1956.

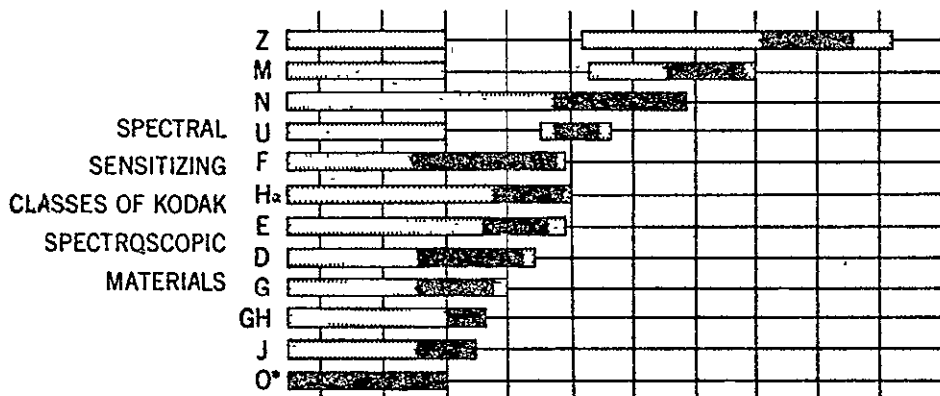
Photoluminescence of Solutions, C.A. Parker, Sievert Publishers, 1968.

Ultraviolet Photo Biology, John Jagger, Prentice-Hall, 1968.

Optical Methods in Biology, E. Slayter, Wiley Inter-Science, 1970.

Ultraviolet Radiation, L. Koller, Wiley, 1967.





\*Class O represents unmodified spectral sensitivity of all spectroscopic emulsions.

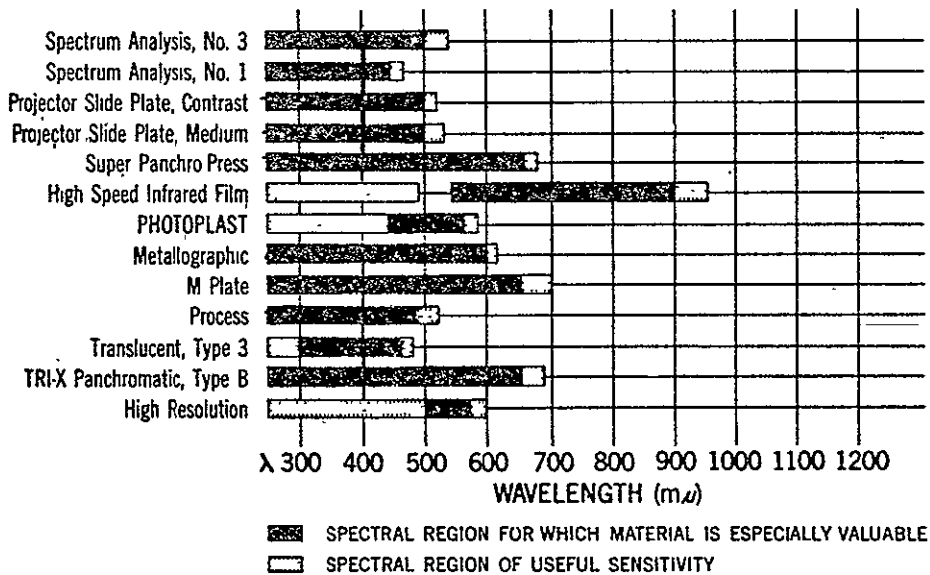


Figure 4.3.7-8. Summary of Spectral Sensitizings

#### 4.3.8 TEMPERATURE CONTROL

##### 4.3.8.1 REQUIREMENTS/OBJECTIVES

The MEED will be subjected to a variety of environments during its life time which begins at the time the cuvettes are loaded with biological samples and ends when the samples are extracted for analysis. During this time the MEED will experience Apollo launch, trans-lunar orbit and return, lunar orbit, lunar EVA, earth entry and recovery. Since at least some of the biological samples will be temperature sensitive, it is required that the samples be maintained at a temperature of  $20 \pm 5^{\circ}\text{C}$ . Also, the MEED is to achieve temperature control without any active elements. During most of the MEED life time, the experiment will be in a temperature controlled environment typically within the above limits. However, there are two time periods during which the surrounding environment is not controlled and the MEED temperature control system must provide the required temperatures. These are during the time the LEM is on the moon (including the time during which the samples are exposed to UV) and during Apollo recovery. The following sections will present the basic temperature control system design concepts and some preliminary calculations to demonstrate performance and feasibility.

##### 4.3.8.2 DESIGN APPROACH

Since the MEED temperature control system is to be completely passive, it is necessary that the biological samples be surrounded by insulation and/or an enclosure capable of regulating the heat exchange between the samples and the surroundings. Further, the enclosure should have an equilibrium temperature as close to the nominal sample temperature ( $20^{\circ}\text{C}$ ) as possible so as not to place unrealistic requirements on the insulation. The primary purpose of the

insulation should be to provide a margin of safety because of tolerances in manufacturing of both the insulation and the radiation properties of the enclosure (and its surface finishes). Heat leaks by conduction will have to be controlled to acceptable levels.

During the time that the biological samples are exposed to UV (10 minutes), the enclosure will be opened and, of course, will be ineffective in shielding against direct solar irradiation which represents the greatest single source of heat input to the MEED. The sides and back of the MEED will still be protected by the enclosure. Temperature control during this exposure period will require a careful selection of radiation surface finishes, coupled with MEED heat capacity, so that the system time constant is sufficiently long to maintain temperatures between 15°C and 25°C for at least 10 minutes. Selection of these parameters will have to be done after the filter system is designed since at least a part of the surface finishes (radiation properties) will be dictated by the filter system.

#### 4.3.8.3 PRELIMINARY PERFORMANCE CALCULATIONS

A preliminary evaluation of performance during the 10-minute exposure period can be obtained by lumping all the elements shown in Figure 4.3.2-1 into one homogeneous mass and subjecting this mass to two extreme environmental conditions which bracket the true condition. The first case ("cold") assumed that the quartz window was opaque to the solar irradiation. In the second case ("hot") the quartz window was assumed to be transparent. The results of the first case showed that it took almost 40 minutes for the lumped mass to cool from 20°C to 15°C. In the second case the temperature rose from 20°C to 25°C in about 3 minutes. The true situation lies somewhere between these extremes. This is discussed further in the following section. The quartz window transmits better than 90% of the solar irradiation from about 250 nm out to about 2.5 microns where it becomes almost total absorbing. However, all of the energy in the quartz transmission band is not transmitted to the cuvettes. The major portion of this energy is reflected from the interference filters back out through the quartz and is lost to space.

During the 10-minute exposure time, the temperatures of the lunar surface (and, hence, the sun angle) will have relatively little effect on MEED temperatures because of the short exposure time. Since the back and sides of the MEED are insulated, the net thermal balance between radiation losses to space from the front surface and the normal solar irradiation will determine performance during the UV exposure time.

Once the UV exposure period has ended, the MEED case will be closed. At least 2 options in operating protocol are available at this time. (1) The MEED may be returned to the LEM at the end of the 6 hour EVA. (2) It may be left outside the LEM until the

end of the last EVA (about 72 hours total time). During the time the MEED is outside the LEM, it will be exposed to solar irradiation and heat exchange with the lunar surface. Estimates of enclosure temperatures have been made for a few surface finishes and sun angles. The results of these calculations are summarized below.

<u>Surface Finish</u>	<u>Sun Angle/Lunar Surface Temperature</u>	<u>Average Enclosure Temperature</u>
white paint	23°/110°F (43°C)	50°F (10°C)
white paint	8°/-20°F (-29°C)	-30°F (-34°C)
aluminum paint	23°/110°F (43°C)	140°F (60°C)
aluminum paint	8°/-20°F (-29°C)	90°F (32°C)
aluminum paint w/white top	23°/110°F (43°C)	88°F (31°C)
aluminum paint w/white top	8°/-20°F (-29°C)	45°F (7°C)

It is apparent from the above preliminary estimates that the enclosure temperatures will vary over a wide range depending upon the local sun angle, and no single surface finish will be capable of maintaining a constant enclosure temperature. An analysis of these conditions will have to be treated as a transient to adequately evaluate the response of the MEED to the changing lunar environment.

The insulation system for the MEED is presently envisioned as a 1/2 inch thick superinsulation blanket of aluminized Mylar. So as not to compress the insulation and reduce its effectiveness, the MEEDs will be supported with low conductance standoffs that unfortunately will have to penetrate the superinsulation. However, an overall vacuum conductance of  $8 - 14 \times 10^{-3}$  Btu/hr appears reasonable. For an external enclosure temperature of 32°C and a starting temperature of the MEED of 20°C, it will take about 72 hours for the MEED to rise to 25°C. Further discussion of this problem is

to be found in the following section.

Information presently available indicates that LEM interval environmental temperatures may vary anywhere between about 13°C to about 32°C during a 6 hour EVA. When the LEM is pressurized, the effectiveness of the MEED insulation drops by about 2-3 orders of magnitude. If the MEED is returned to the LEM at the end of the first EVA and the internal LEM temperature is a constant 32°C, it will take about 1 hour for the MEED to rise from 20°C to 25°C assuming that the MEED case temperature is the same as the LEM interval environment (32°C). No attempt has been made here to allow for the effects of changing LEM temperatures after the LEM environmental control system is turned on.

Performance of the MEED during Apollo recovery is expected to be comparable, except that the MEED case temperature would probably be initially 20°C  $\pm$  5°C thus lengthening the time for the MEEDs to rise from 20°C to 25°C when subjected to an external environment of 32°C. These conditions will have to be re-evaluated during a final design effort when better data are available on the typical environmental conditions existing at these times.

#### 4.3.8.4 THERMAL MODEL ANALYSIS

For purposes of the thermal model analysis, it is assumed that the 10-minute UV exposure would take place anytime during the 72 hours on the lunar surface. The sun angle above the horizon is assumed to be between 8-23 degrees at the beginning of the first EVA. After 72 hours the sun angle will be about 39 degrees higher (or a maximum of about 62 degrees). The lunar surface temperature during this time will rise from about -29°C (-20°F) for a sun angle of 8 degrees to about 99°C (210°F) for a sun angle of 62 degrees. <sup>(1)</sup>

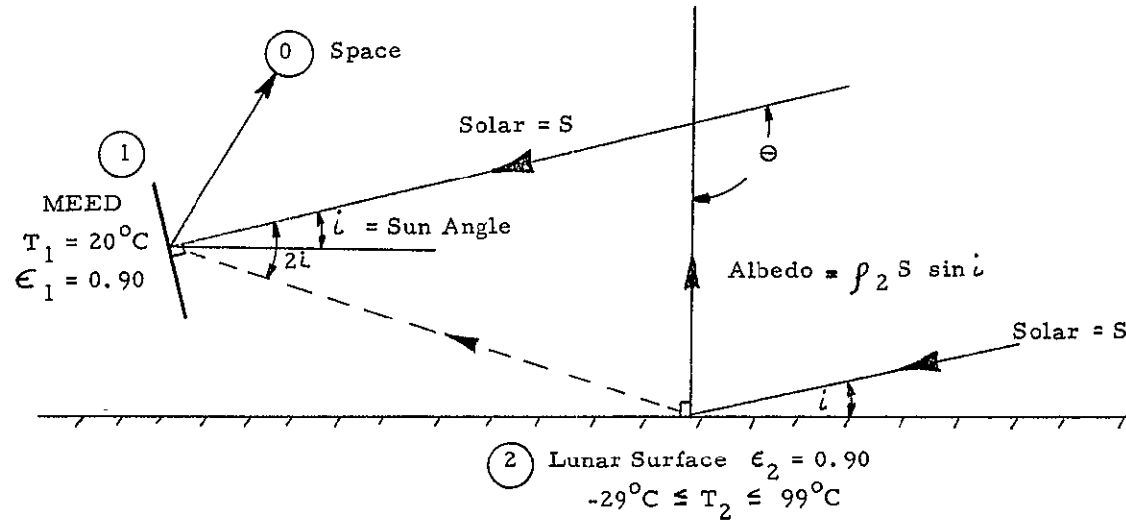
(1) L.D. Stimpson and J. W. Lucas, Revised Lunar Surface Thermal Characteristics Obtained From The Surveyor V Spacecraft, AIAA Paper No. 69-594, AIAA 4th Thermophysics Conference, June 16-18, 1969.

Also, since the exposure of the biological samples requires the incident solar energy to be normal to the MEED, the orientation of the MEEDs with respect to the lunar surface would be different at various times during the 72 hour stay. It would be expected that a "worst" condition would exist at some time during the 72 hour period. Following an approach of Stimpson and Lucas, the thermal balance of Figure 4.3.8-1 is used. Since the MEED is always normal to the solar vector, the direct solar input is a constant. The reflected solar input is a maximum of about 3% of the direct solar input primarily because the lunar reflectance,  $\rho_2$ , is only 0.077, and so the only heat input which varies much is the radiation exchange from the face of the MEED with the lunar surface. The ratio of heat gain to loss reaches a maximum for a sun angle between 25 and 30 degrees.

A transient thermal model of the MEED was set up as shown in Figure 4.3.8-2. The back and sides of the model are insulated (isothermal). The heat inputs  $Q_1$  through  $Q_6$  and  $Q_8$  through  $Q_{10}$  were determined using a simple model of the filter pack consisting of the quartz cover and an interference filter. Transmission and surface reflection losses due to a neutral density filter or the cuvette window were not considered as their effects are small by comparison.

The heat input to the quartz cover ( $Q_1$  to  $Q_5$ , equally distributed) is due to the near total absorption, by quartz, of solar energy above about 2.5 microns wavelength. Except for surface reflection losses, quartz has almost 100 percent transmission of energy below 2.5 microns. Thus, the total heat input to the quartz cover was determined to be  $47. \times 10^{-4}$  watts per  $\text{cm}^2$  (14.9 Btu/hr  $\text{ft}^2$ ).

Of the energy incident on the interference filter, a portion will be reflected, and for the most part, transmitted back out through the quartz cover. Another portion of the incident energy will be transmitted through the filter. The remainder will be absorbed. The measured transmittance of a wideband (25 nm) filter is shown in Figure 4.3.5-6. The measured reflectance of this filter is shown in Figure 4.3.8-3. Using these measured data and the distribution of energy in the solar spectrum, absorption in the filter was determined to be



Heat Gain			Heat Loss			
Direct Solar Input	+	Reflected Solar Input	-	Infrared Exchange With Lunar Surface	=	Loss to Space
$\alpha_1 S$		+	$\alpha_1 F_{12} \rho_2 S \sin i$	-	$\epsilon_1 \epsilon_2 \sigma F_{12} (T_1^4 - T_2^4)$	$= \epsilon_1 \sigma F_{10} T_1^4$
where $F_{12} = 1/2(1 + \cos \theta) = 1/2(1 - \sin i)$						

Figure 4.3.8-1. Thermal Balance



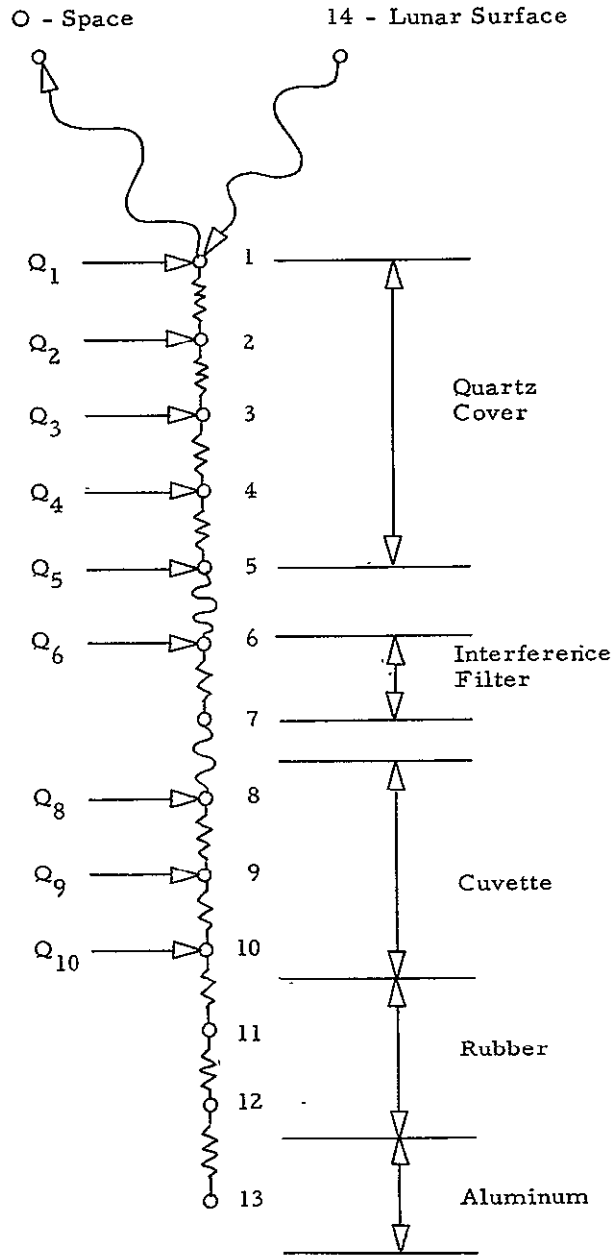


Figure 4.3.8-2. Transient Thermal Model

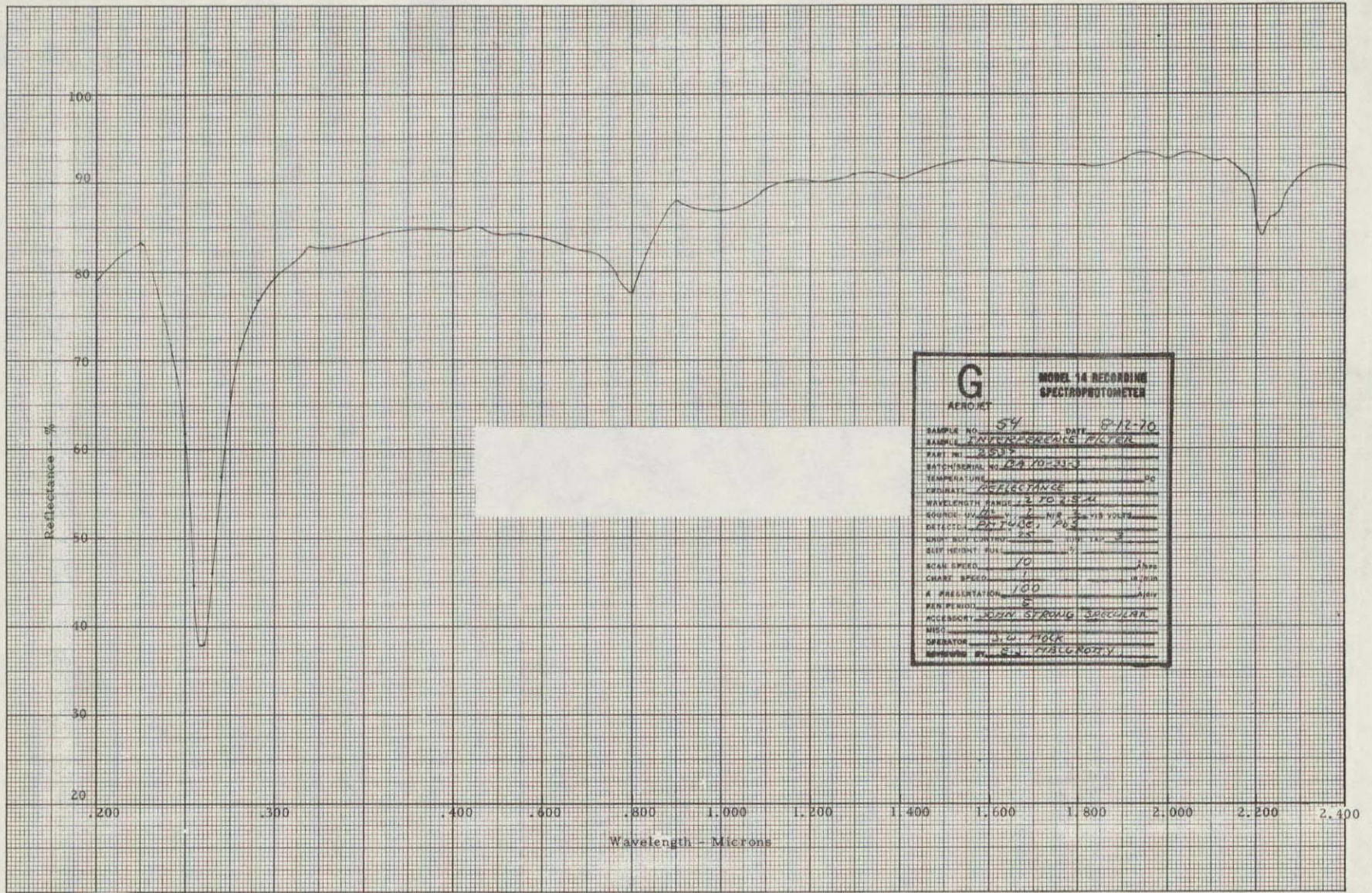


Figure 4.3.8-3. Reflectance of Baird - Atomic Interference Filter  
10-33-3 Normal Incidence

$185. \times 10^{-4}$  watts per  $\text{cm}^2$  ( $58.6$  Btu/hr  $\text{ft}^2$ ) and the transmitted energy was  $0.78 \times 10^{-4}$  watts per  $\text{cm}^2$  ( $.247$  Btu/hr  $\text{ft}^2$ ).

The results of the transient model runs are summarized in Table 4.3.8-1. Typical computer printout is shown in Appendix A. These runs were made using the wideband interference filter and a sun angle of 8 degrees and 23 degrees (approximating the worst case).

As was expected, the results for a 23 degree sun angle show slightly warmer temperatures than the 8 degree cases. The cases with good thermal contact between layers of the filter pack, i. e., no contact resistance at surface interfaces, show less than a  $0.5^{\circ}\text{C}$  cuvette temperature change in 10 minutes and less than  $1^{\circ}\text{C}$  temperature difference between filter pack elements and the cuvettes. This case is idealized since in actual practice there will be a resistance between the various layers. However, the most the resistance could be would correspond to no physical contact at all so that the only mode of heat transfer from layer to layer would be by radiation. These are the conditions which correspond to the poor thermal contact cases shown. Here the quartz cover actually cools off substantially because of its high emissivity. The filter, on the other hand, gets warm because it has poor thermal connections with any other element, and better than 75% of the heat input to the MEED is absorbed in the filter. The cuvettes increase in temperature by less than  $2^{\circ}\text{C}$  to a maximum of  $21.9^{\circ}\text{C}$  for a 23 degree sun angle. Because of the small change in cuvette temperature during the 10 minute exposure, any kind of a heat sink would be relatively ineffective (this is not true during the time that the MEEDs are completely enclosed in the case.) The true situation actually lies between the good contact and poor contact cases.

It is also of interest to gain some understanding of what happens to the cuvette temperature in the event the filter is at a temperature of  $34^{\circ}\text{C}$  when the MEED case is closed. Under these conditions the quartz, the filter and the cuvettes would all reach some equilibrium temperature. If the quartz is neglected and it is assumed

Table 4.3.8-1

## RESULTS OF TRANSIENT MODEL AFTER 10 MINUTE EXPOSURE

INITIAL TEMPERATURE = 20 °C

	Sun Angle	Quartz Cover Temp.	Interference Filter Temp.	Cuvette Temp
Good thermal contact between layers of filter pack	8°	18.2°C (64.8°F)	18.9°C (66.1°F)	19°C (66.2°F)
	23°	19.6°C (67.7°F)	20.4°C (68.7°F)	20.4°C (68.7°F)
Poor thermal contact between cover and filter and filter and cuvette	8°	9.7°C (49.4°F)	33.2°C (91.8°F)	21.8°C (71.3°F)
	23°	13.5°C (56.2°F)	34.1°C (93.4°F)	21.9°C (71.5°F)

that the heat is shared only between the filter and the cuvettes, they will both reach an equilibrium temperature of  $25.3^{\circ}\text{C}$  ( $77.5^{\circ}\text{F}$ ). The entire MEED, however, would reach an equilibrium temperature of  $20.5^{\circ}\text{C}$  ( $69^{\circ}\text{F}$ ). Further analysis is required to show how the entire MEED equilibrates in temperature. This has been deferred until a final design effort is undertaken.

It is concluded from the results of the 10 minute exposure model that there will be no problems in maintaining the cuvettes within acceptable temperatures during the exposure time. It does show, however, that the interference filter should be thermally decoupled from the cuvettes but in good thermal contact with the quartz cover. Bonding of the filter to the quartz cover would be acceptable. The effectiveness of this approach would require close coordination with the filter manufacturer. In order to keep the cuvettes from moving, they should be in contact with or bear against something. For those cuvettes requiring low irradiation levels, a neutral density filter could serve as the bearing surface, or a quartz plate may be used where high irradiation is desired.

Another transient thermal model was set up to evaluate the temperature response of the MEED after the 10 minute exposure period and after the MEED case has been closed. It has been assumed that the MEED is elevated above the lunar surface (e. g. attached to the leg of the LEM), and no attempt has been made to account for the effects of the near proximity of the LEM itself or of shadow areas on the lunar surface. It has further been assumed that exposure would take place when the sun angle was between 8 and 23 degrees and that the MEED would remain outside the LEM for the duration of the lunar mission.

The most desirable operating protocol following UV exposure appears to be to forget about the MEED until such time as the LEM must be prepared for ascent from the lunar surface. It has been mentioned above that the other option available would be to return the MEEDs to the lunar module at the end of the EVA during which the MEED was exposed to UV. This might be acceptable, however, the experiment would be subjected to environmental fluctuations that could be more severe (depending on typical LEM operation) than those external to the LEM. Presently available data suggests that LEM internal temperatures could be between  $13^{\circ}\text{C}$  and  $32^{\circ}\text{C}$  at the end of the EVA. When the LEM is repressurized, the superinsulation of the MEED system becomes several orders of magnitude less effective, and as has already been pointed out in the preliminary calculations, could cause the MEED to exceed  $25^{\circ}\text{C}$ . Assuming there are 3 EVA's, the MEED would be subjected to these temperature fluctuations 3 times. On the other hand, if the MEED experiment remained outside the LEM until the end of the last EVA, it would be exposed to the LEM environment only one time. In the event that the LEM temperature control system can return the internal environment of the module to  $20^{\circ}\text{C} \pm 5$  within a reasonable length of time of about 45 minutes, it is an advantage to return the MEED to the LEM at the end of the 6 hour EVA since this substantially relaxes the requirements on the MEED insulation system. In any case, it is of interest to determine the temperatures of the MEED for a lunar exposure of 72 hours.

For a lunar exposure of at least 72 hours, the following characteristics of the MEED system were determined.

1. The weight of 3 MEEDs was estimated to be 5.66 pounds and an average specific heat of 0.21 Btu/pound  $^{\circ}\text{F}$  was assumed.
2. The weight of the MEED enclosure was estimated to be 2.44 pounds (including hardware and assuming a 0.050" aluminum wall thickness). The average specific heat was assumed to be that of aluminum, 0.22 Btu/lb  $^{\circ}\text{F}$ .
3. The top and sides of the enclosure are painted with gloss white enamel and have a solar absorptance,  $\alpha_s$ , of 0.30 and an infrared emittance,  $\epsilon$ , of 0.81. The bottom of the enclosure is painted with aluminum paint having  $\alpha_s = 0.23$  and  $\epsilon = 0.20$ . These particular surface finishes were selected because they are probably least affected by astronaut handling and they also limit the influence of the lunar surface and provide high emittance to space. Modification of the selected finishes will be necessary during final design efforts when the full effects of the lunar surface and the close proximity of the LEM are included in the analysis.
4. The insulation system selected for the MEED enclosure is a 1/2 inch thick superinsulation blanket of 1/4 mil Mylar aluminized on one side and crinkled (essentially NRC-2 insulation). At a layer density of about 60 layers per inch, the thermal conductivity is about  $1.2 \times 10^{-5}$  Btu/hr ft  $^2$   $^{\circ}\text{F}/\text{ft}$ . To allow for manufacturing tolerances, these insulation k values are typically degraded about one

order of magnitude, to about  $1.2 \times 10^{-4}$ . So that the insulation is not compressed, and in order to support the MEEDs for the required g loads, 32 epoxy standoffs are provided. When the heat conducted through the standoffs is considered, the effective conductance of the insulation increases from  $2.6 \times 10^{-3}$  Btu/hr °F to about  $13.6 \times 10^{-3}$  Btu/hr °F.

Other types of insulation systems for the MEED were investigated. Desirable characteristics of the insulation system are low heat conductance and low mass, able to support MEED loads, low outgassing so that high insulating qualities can be easily maintainable, and easy to fabricate or assemble. The super insulation system selected is not particularly easy to assemble; it requires great care to insure its low vacuum conductance. It is also not well suited for carrying compressive loads - hence the standoffs which in turn degrade the insulation qualities. Rigid foam insulations could support the kinds of loads in the present application. They have a tendency to outgas however, and at the present time it is not known whether this would be permissible considering that it is during the initial exposure to vacuum in this application which is important. Data available in the literature on vacuum conductance of foams is sparse, and up until now does not indicate that the low required conductances can be achieved with foam alone. However, the search continues, particularly for concepts employing aluminized polyester films using rigid open cell foams as separators.



For the selected configuration, the response of the MEED system is shown in Figure 4.3.8-4 during a lunar exposure of at least 72 hours. MEED enclosure temperatures fall within the band indicated. The upper edge of the band being typical of the sunlit side and the lower edge typical of the side opposite. The enclosure is at all times in equilibrium with the environment. If the MEED is exposed when the sun angle is 8 degrees, during the first 25 hours the enclosure temperatures are less than 68°F (20°C), and so the MEED temperature decays until it reaches a minimum at about 27 hours. The heat flow then reverses and the MEED begins to warm up - after 92 hours it reaches the upper limit of 77°F (25°C). The lowest MEED temperature, at 27 hours, is about 2°F or 1°C lower than the lower limit of 59°F (15°C). A slight modification in the effective absorptance to emittance ratio,  $\alpha_s/\epsilon$ , is all that is necessary to raise the lowest temperature to the lower limit of 59°F (15°C) although this has not been done for the present study.

Using the same surface finishes, an additional transient was determined for an exposure beginning when the sun angle is 23 degrees. The enclosure temperatures respond almost immediately to reach equilibrium values identical to the 8 degree exposure conditions. However, because the MEED enclosure and the MEEDs are at about the same initial temperature, as the enclosure temperature rises, so do the MEEDs.

After 51 hours (or when the sun angle reaches 50 degrees) the MEEDs will reach the upper temperature limit of 77°F (25°C). The general trend that is indicated from these results is that for a given enclosure surface finish and orientation, exposures at higher sun angles shorten the time required for the MEED to reach its upper temperature limit. This is a direct result of the drastically different lunar surface temperatures during the lunar mission ( $-29^{\circ}\text{C} \leq T \leq 99^{\circ}\text{C}$ ). Without more definitive information on typical operating conditions for the LEM environmental control system, it is difficult to say whether the greatest margin of safety exists for an exposure of the MEED during the first EVA or during a later EVA.

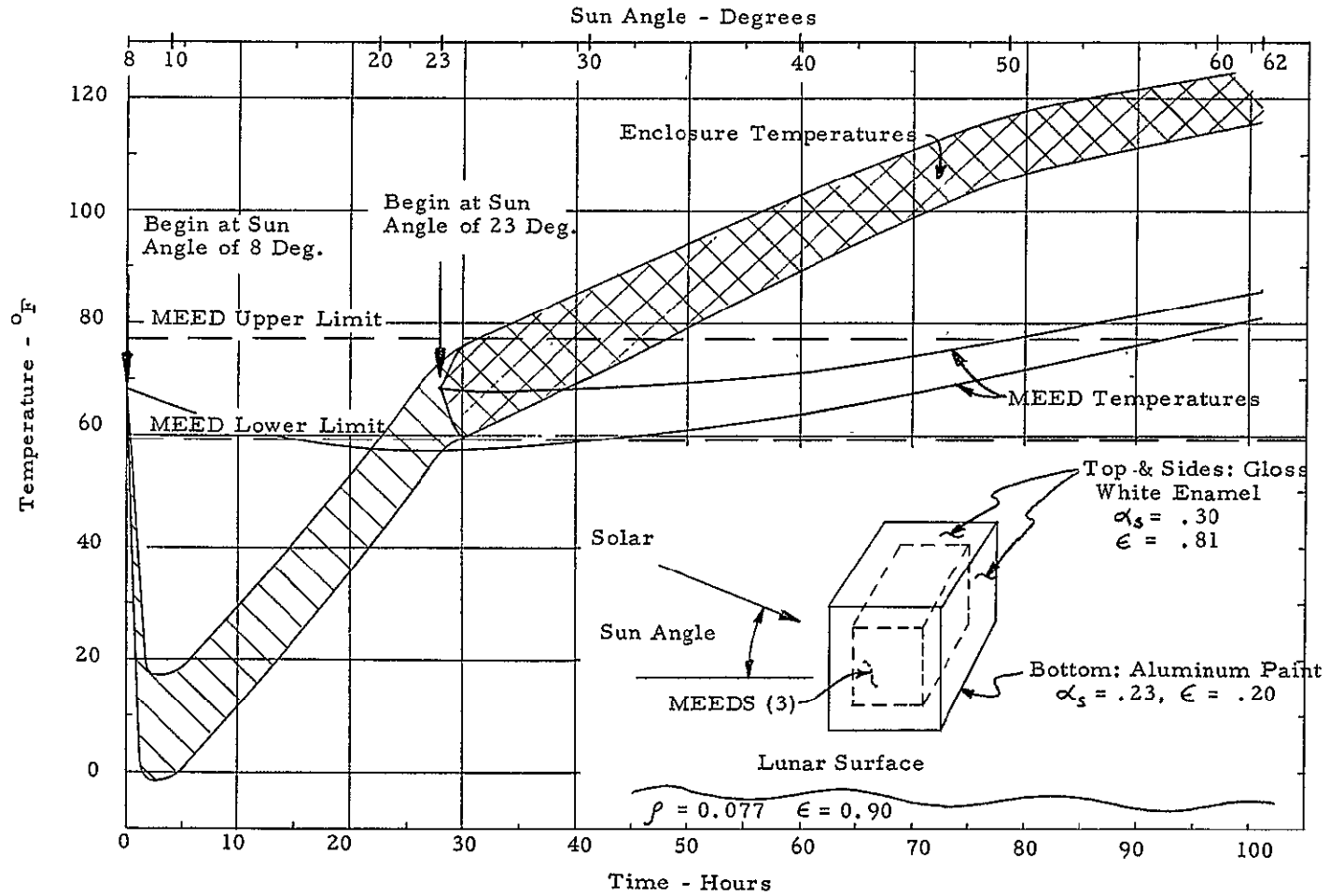


Figure 4.3.8-4. Response of the Enclosed MEEDs for Duration of Lunar Mission Following UV Exposure Period

It does appear that a "universal" set of surface finishes and orientation can be selected such that UV exposure could be made at any time during the lunar mission. Some modification of  $\alpha_s/\epsilon$  will be necessary when the effects of the LEM and local shadow areas on the lunar surface are considered. These effects would also indicate a preferred orientation; for the present analysis the enclosure is assumed to be "broadside" to the solar vector.

#### 4.3.9 WEIGHT ANALYSIS

The weight analysis of Appendix C shows the weight of the MEED flight assembly feasibility design to be 5.1 kg (11.3 lb). At this stage of the design, several components and subassemblies are excessively heavy. A minimal reduction effort would significantly reduce the total weight of the flight assembly, as well as the lunar assembly which must be launched from the lunar surface.

A cursory examination shows that weight savings can readily be accomplished in at least the following two areas:

- MEED Base - The original design included an aluminum base plate that is 0.380 inches (9.7 mm) thick. Rough calculations show that a thickness of 0.100 inches is adequate. This reduces the lunar subassembly weight by 550 gms, the CM subassembly by 275 gms, and the flight assembly by 825 gms.
- Type B MEED - The final design of this type of MEED will substitute an aluminum alloy cover plate for the quartz plate. The reduction in weight will be approximately 80 gms for the lunar subassembly, approximately 80 gms for the CM subassembly, and 160 gms for the flight assembly.

These changes reduce the weight of the flight assembly to 4130 gms (9.5 lb) and the weight of the lunar subassembly to 3190 gms (7.1 lb). The lunar subassembly will also be 250 gms (0.5 lb) lighter weight on earth during the ascent phase because the strut clamp assembly and the "false bottom" will remain on the lunar surface.

General design experience has shown that some weight addition will probably occur during the final hardware design phase, but that a concerted effort to reduce weight can more than compensate for these changes. It is estimated that the weight of the MEED flight assembly and, thus, the lunar subassembly, can be further reduced by approximately 10 percent, or 500 gms (1 lb), during this phase.

#### 4.3.10 PROTOCOL DEVELOPMENT

The following paragraphs comprise a brief discussion of the protocols of Appendix D.

##### 4.3.10.1 PROTOCOL D-1, LUNAR ASSEMBLY DEPLOYMENT

This protocol is based on the modified flight assembly mock-up hardware delivered under this contract. Some simplifications of the hardware are anticipated during the early phases of a flight

hardware program with subsequent changes in the protocol.

#### 4.3.10.2        PROTOCOL D-2

The protocol is based on the assumption that 1) all of the cuvettes in a section tray will contain the same microbial culture, 2) that six levels of intensity of ultraviolet radiation are desired, 3) that all of the radiation impinging on a section tray will be limited to a single wavelength and 4) that 24 cuvettes are available in each section tray. Other alternative arrangements are feasible. Each section tray can have a single wavelength range and a single radiation intensity but small groups of cuvettes of different microbes. The advantage of this latter arrangement is that only one neutral-density filter is required for each section tray. The disadvantage lies in the proximity of the different microbes to each other during the loading process and during the experiment.

#### 4.3.10.3        PROTOCOL D-3, LOADING OF THE LIQUID SAMPLE CUVETTE

This protocol provides for the filling of cuvettes with liquid microbial samples (cultures) and actinometric fluid, and the subsequent sealing with low-melting-point wax.

#### 4.3.10.4        PROTOCOL D-4, LOADING OF CUVETTE-DRY, SEALED

This protocol presumes that the microorganisms have already been deposited on the Millipore filters in accordance with Protocol D-6 and are available for use in sterile containers.

#### 4.3.10.5        PROTOCOL D-5, LOADING OF CUVETTE-DRY, VENTED

This procedure is similar to that of Protocol D-4 in that the cuvettes are not sealed with wax.

#### 4.3.10.6        PROTOCOL D-6, DEPOSITION OF TEST CULTURES ON MILLIPORE FILTERS FOR USE IN THE CUVETTES- DRY, VENTED, AND SEALED

The procedures outlined in this protocol are based on dry-deposition of the microbial samples onto Millipore filters, and is, thus, necessarily complex. Alternate methods employing wet deposition will be simpler and will be given consideration prior to the preparation of the protocol for flight hardware.

#### 4.3.10.7        PROTOCOL D-7, ASSEMBLY AND DISASSEMBLY OF THE MEED

This protocol provides an outline of the steps required to assemble the MEED and is consistent with the cuvette- and

section-tray coding of Protocol D-2.

4.3.10.8      PROTOCOL D-8, RECOVERY-CUVETTE DRY,  
                 SEALED, AND VENTED

The procedure for opening the dry sample (culture) is described in this protocol. An alternative approach is the use of diluent broth in a wet recovery procedure that would result in a simplified procedure.

4.3.10.9      PROTOCOL D-9, RECOVERY OF CUVETTE  
                 LIQUID SAMPLE

The procedures and equipment required to recover both the actinometric fluid and the liquid cultures for analysis after the experiment is performed are described in this protocol. The device for crushing the cuvettes and diluting them with broth (culture) and buffer solution (actinometer) is shown in Figure D.9-1. The tip of the unit that breaks the cuvette is flushed with diluent to prevent the withdrawal of any microbes from the conax centrifuge test tube.

4.3.10.10     PROTOCOL D-10, PROTOCOL FOR THE POTASSIUM  
                 FERRIOXALATE ACTINOMETER

This protocol provides an outline of the steps required to prepare and analyze the actinometer solutions. Sample calculations are also presented.

Section 5

EQUIPMENT LIST

(Purchased Over \$100)

Micro Optics Corp.	GE Type 151 Quartz Windows	15 @ \$12.00	\$ 180.00
Baird-Atomic	10-33-3 Optical Filter	1 @ \$120.00	\$ 120.00
	10-65-8 Optical Filter	1 @ \$120.00	\$ 120.00
Kaylen Mfg. Co.	Cuvette Assembly	12 @ \$16.00	\$ 192.00
West Glass Co.	1 lambda Quartz Cuvette (brazed)	1 @ \$152.60	\$ 152.60
	1 lambda Quartz Cuvette (fused)	1 @ \$152.60	\$ 152.60
	50 lambda Quartz Cuvette (brazed)	1 @ \$152.60	\$ 152.60
	50 lambda Quartz Cuvette	1 @ \$152.60	<u>\$ 152.60</u>
			\$1,222.40

## APPENDIX A

### DESCRIPTION OF STEADY-STATE COMPUTER PROGRAM

This program is written in Fortran for the IBM 360 and evaluates the steady-state temperatures and heat fluxes for a thermal network consisting of isothermal nodes. The Gaussian Reduction solution technique is utilized for the simultaneous equation solution. The program handles heat flow via conduction, radiation, convection, and mass transfer along with external and internal heat generation.

### DESCRIPTION OF TRANSIENT COMPUTER PROGRAM

This program is written in Fortran for the IBM 360 and evaluates the transient temperature history and heat fluxes for a thermal network consisting of lumped capacitance and resistance. Temperature profiles are solved for by a forward finite-difference technique. Heat inputs may be constant or tabular, and temperatures may be either fixed (and tabular) or variable. This program was originally developed for orbital temperature predictions. However, it is equally useful in the present application by specifying a "suitable" orbit period.



THermal TRANSIENT ORBIT PROGRAM

POOR THERMAL COUPLING BETWEEN  
LAYERS OF FILTER PACK

1573FR

MFFD 23 DEG SUN ELFV 2537A FILTER

CONDUCTION COEFFICIENT

NODE I	NODE J	CONDUCTANCE <i>BTU/HR °R</i>	N	TABLE
1	2	1.8000E 02		
2	1	1.8000E 02		
2	3	1.8000E 02		
3	2	1.8000E 02		
3	4	1.8000E 02		
4	3	1.8000E 02		
4	5	1.8000E 02		
5	4	1.8000E 02		
6	7	2.9000E 02		
7	6	2.9000E 02		
8	9	1.4000E 02		
9	8	1.4000E 02		
9	10	1.4000E 02		
10	9	1.4000E 02		
10	11	2.7600E 01		
11	10	2.7600E 01		
11	12	1.5300E 01		
12	11	1.5300E 01		
12	13	3.0600E 01		
13	12	3.0600E 01		

RADIATION COEFFICIENTS

1573FR	NODE I	NODE J	RADIATION COEF.
			<i>BTU/HR. °R<sup>4</sup></i>
	0	1	1.0600E-09
	1	0	1.0600E-09
	1	14	4.3300E-10
	5	6	1.3800E-09
	6	5	1.3800E-09
	7	8	1.3800E-09
	8	7	1.3800E-09
	14	1	4.3300E-10

PROBLFM CONSTANTS

1573FR	1	TIME INTERVAL FOR PRINT	0.0166
	2	TIME CONSTANT (OVERRIDE)	NOT INPUT FOR THIS CASE
	3	MULTIPLYING FACTOR	NOT INPUT FOR THIS CASE
	4	ORBIT PERIOD IS C	0.3330
	5	TIME FOR 1 ORBIT(MIN,)	1.0000
	6	CLOSURE CRITERIA	C.2500
	7	MAX NUMBER OF ORBITS	1
	8	PRINT OPTION 1 OR 0	1
	9	TEMPERATURE XTRAPOLATION	0
	10	EXTRAPOLATION CRITERIA	NOT INPUT FOR THIS CASE
	11	FREQ. OF TIME CON. CALC.	5
	12	CAPACITANCE MULTIPLIER	NOT INPUT FOR THIS CASE
	13	NUMBER OF NODES	14
	14	INITIAL THETA	0.0.

NODAL DESCRIPTION

1573FR

NODE	T-START	Q-CONST.	CAP.	TYPE OF NODE	---SOLAR HEAT---		--MISC. FEAT--		--MISC. HEAT--	
	<i>°F</i>	<i>BTU/HR</i>	<i>BTU/°R</i>		TABLE	MULT.	TABLE	MULT.	TABLE	MULT.
1	68.00	3.000E 00	8.200E-02	VARIABLE	0	0.0	0	0.0	0	0.0
2	68.00	3.000E 00	8.200E-02	VARIABLE	0	0.0	0	0.0	0	0.0
3	68.00	3.000E 00	8.200E-02	VARIABLE	0	0.0	0	0.0	0	0.0
4	68.00	3.000E 00	8.200E-02	VARIABLE	0	0.0	0	0.0	0	0.0
5	68.00	3.000E 00	8.200E-02	VARIABLE	0	0.0	0	0.0	0	0.0
6	68.00	5.860E 01	1.025E-01	VARIABLE	0	0.0	0	0.0	0	0.0
7	68.00	0.0	0.0	VARIABLE	0	0.0	0	0.0	0	0.0
8	68.00	8.200E-02	9.000E-02	VARIABLE	0	0.0	0	0.0	0	0.0
9	68.00	8.200E-02	9.000E-02	VARIABLE	0	0.0	0	0.0	0	0.0
10	68.00	8.200E-02	9.000E-02	VARIABLE	0	0.0	0	0.0	0	0.0
11	68.00	0.0	7.800E-02	VARIABLE	0	0.0	0	0.0	0	0.0
12	68.00	0.0	7.800E-02	VARIABLE	0	0.0	0	0.0	0	0.0
13	68.00	0.0	3.960E-01	VARIABLE	0	0.0	0	0.0	0	0.0
14	110.00	0.0		CONSTANT	0	0.0	0	0.0	0	0.0

TEMPERATURES - °F

TIME	1	2	3	4	5	6	7	8	9	10
HRS.	QUARTZ COVER					INTERFERENCE FILTER		CUVETTE		
1573FR 0.0	68.00	68.00	68.00	68.00	68.00	68.00	68.00	68.00	68.00	68.00
0.0166	65.44	65.74	65.98	66.15	66.25	73.30	73.23	68.12	68.10	68.09
0.0332	63.63	63.94	64.18	64.37	64.49	77.65	77.57	68.38	68.34	68.31
0.0498	62.08	62.38	62.63	62.83	62.97	81.22	81.15	68.72	68.66	68.61
0.0664	60.73	61.04	61.29	61.50	61.65	84.16	84.08	69.10	69.02	68.96
0.0830	59.57	59.88	60.13	60.35	60.51	86.57	86.49	69.50	69.41	69.34
0.0996	58.56	58.86	59.12	59.34	59.52	88.53	88.46	69.91	69.81	69.73
0.1162	57.67	57.98	58.24	58.47	58.65	90.15	90.07	70.32	70.22	70.13
0.1328	56.90	57.20	57.47	57.70	57.89	91.47	91.39	70.74	70.63	70.53
0.1494	56.21	56.52	56.78	57.02	57.22	92.55	92.47	71.16	71.04	70.94
0.1660 - 10 MIN.	55.61	55.91	56.18	56.42	56.62	93.44	93.36	71.58	71.46	71.35
0.1826	55.07	55.37	55.64	55.88	56.09	94.17	94.09	71.99	71.87	71.76
0.1992	54.59	54.89	55.16	55.40	55.62	94.77	94.69	72.41	72.28	72.17
0.2158	54.17	54.46	54.73	54.98	55.19	95.27	95.20	72.82	72.69	72.58
0.2324	53.78	54.08	54.35	54.59	54.81	95.69	95.62	73.22	73.10	72.99
0.2490	53.43	53.73	54.00	54.25	54.47	96.04	95.97	73.63	73.50	73.39
0.2656	53.12	53.41	53.68	53.93	54.15	96.35	96.27	74.02	73.90	73.79
0.2822	52.83	53.13	53.40	53.65	53.87	96.61	96.53	74.42	74.29	74.18
0.2988	52.57	52.87	53.14	53.39	53.62	96.83	96.76	74.81	74.68	74.57
0.3154	52.34	52.63	52.90	53.15	53.38	97.03	96.96	75.19	75.07	74.96
0.3320	52.12	52.42	52.69	52.94	53.17	97.21	97.15	75.57	75.45	75.34
0.3330 - 20 MIN.	52.11	52.40	52.68	52.93	53.16	97.22	97.16	75.60	75.47	75.36

	11	12	13	14
TIME HRS	RUBBER		ALUM BASE	LUNAR SURFACE
1573FF 0.0	68.00	68.00	68.00	110.00
0.0166	68.05	68.01	68.00	110.00
0.0332	68.20	68.02	68.03	110.00
0.0498	68.44	68.20	68.11	110.00
0.0664	68.72	68.38	68.25	110.00
0.0830	69.04	68.61	68.44	110.00
0.0996	69.39	68.88	68.68	110.00
0.1162	69.75	69.18	68.95	110.00
0.1328	70.13	69.51	69.26	110.00
0.1494	70.51	69.86	69.59	110.00
0.1660	70.90	70.22	69.94	110.00
0.1826	71.30	70.59	70.30	110.00
0.1992	71.70	70.98	70.67	110.00
0.2158	72.10	71.36	71.06	110.00
0.2324	72.50	71.76	71.45	110.00
0.2490	72.90	72.15	71.84	110.00
0.2656	73.30	72.55	72.23	110.00
0.2822	73.69	72.94	72.62	110.00
0.2988	74.08	73.33	73.02	110.00
0.3154	74.47	73.72	73.41	110.00
0.3320	74.86	74.11	73.80	110.00
0.3330	74.88	74.14	73.82	110.00

APPENDIX B  
MEED CALCULATION

Pressure on cuvette during shock load

Weight of a single cuvette

$$W = (0.170)^2 \text{ in}^2 \times 0.2 \text{ in (High)} \times 0.036 \frac{\text{lb}}{\text{in}^3} \times 1.5 \text{ (estimated specific gravity)}$$

$$\underline{W = 3.15 \times 10^{-4} \text{ lb (approx)}}$$

Pressure during shock

$$P = \frac{3.15 \times 10^{-4} \text{ lb} \times 78 \text{ (g)}}{0.029 \text{ in}^2 \text{ (top-cuvette)}}$$

$$\underline{P = 0.8 \text{ lb/in}^2}$$

Thus the pressure during the 25 ms shock is less than 1 psi (between cuvette and neutral density filter).

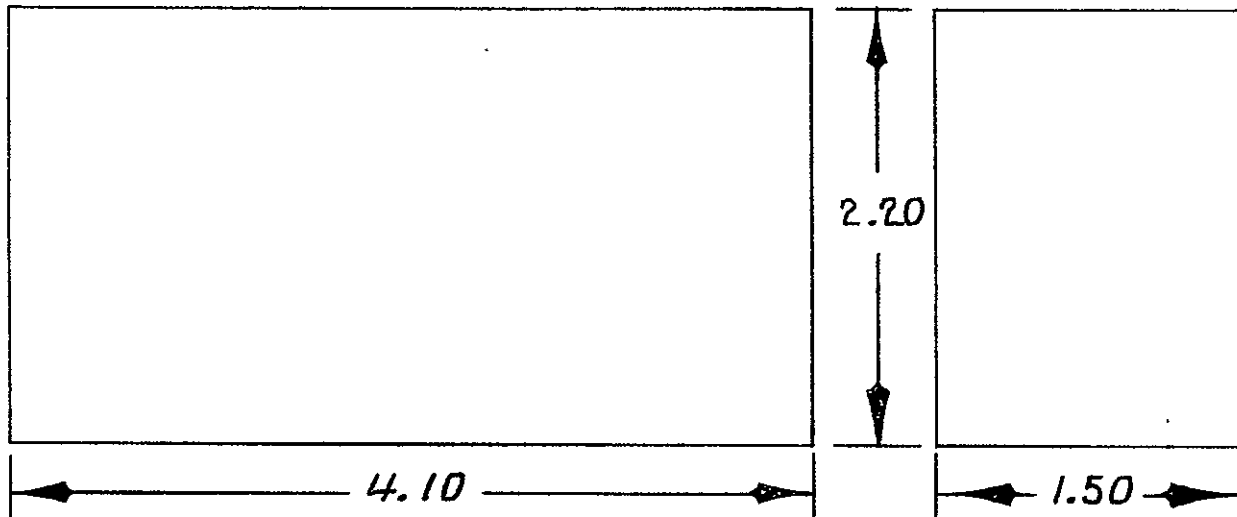
The pressure required to hold the layer of cuvettes in place against the neutral density filter is also less than 1 psi (sponge rubber compression).

APPENDIX B

MEED CALCULATION

Quartz Plate Window Stress

Dimensions:



Maximum stress is at center of plate

Area shown is unsupported area

$$\text{Max } S = B \frac{wb^2}{t^2} \quad \text{where} \quad B = f(\text{length/width})$$

For large plate  $a/b = \frac{4.1}{2.2} = 1.87$ ;  $B = .581$  (Roark, p 225\*)

$$S = 0.581 \times 14.7 \frac{\text{lb}}{\text{in}^2} \times \frac{(2.2)^2}{t^2};$$

$$S = 41.5 / t^2; \quad t = \sqrt{\frac{41.5}{S}}$$

The nominal tensile strength of quartz is 7,000 psi (GE Data). With a design factor of safety of 7:1, the allowable stress becomes 1,000 psi.

The quartz thickness required is:

$$t = \sqrt{\frac{41.5}{1000 \text{ psi}}} = 0.203 \text{ inches}$$

S = Max stress in quartz

t = Quartz thickness

L = Length of Plate

W = Pressure - lb/in<sup>2</sup>

b = Width of plate

B = coefficient = (a/b)

Assume plate simply supported.

$$\underline{\underline{t = 0.203 \text{ in}}}$$



APPENDIX B  
MEED CALCULATION

Quartz Plate Window Stress (con't) - 1

The small window is for the vented section of the MEED, but safety requires that it withstand the full atmospheric pressure. With a thickness of 0.203 in, the stress becomes:

$$a/b = \frac{2.2}{1.5} = \underline{1.47} , \quad B = \underline{0.472}$$

$$S = 0.472 \times 14.7 \text{ lb/in}^2 \times (1.5)^2 / (0.203 \text{ in})^2$$

$$S = \underline{\underline{379 \text{ psi}}}$$

The factor of safety is:

$$\text{F.S.} = \frac{7000 \text{ psi}}{379 \text{ psi}} = \underline{\underline{18.5:1}}$$

For the original design, the plate thickness required is:

$$a/b = \frac{6.25 \text{ in long (one window)}}{2.2 \text{ in wide}} = 2.84$$

$$B = \underline{0.697} \text{ (P 225, Roark)}$$

$$t = \sqrt{\frac{0.697 \times 14.7 \times 2.2^2}{1000 \text{ psi}}} = \sqrt{\frac{49.5}{1000}}$$

$$t = \underline{\underline{0.223 \text{ in}}}$$

A thickness of 0.250 in was selected to permit the use of commercial plate glass in the early stages of testing.

With this thickness, the stress is:

$$S = 49.5/t^2 = 49.5/(\underline{0.25})^2 = \underline{\underline{795 \text{ psi}}}$$

and the factor of safety is:

$$\text{F.S.} = 7000 \text{ psi}/795 \text{ psi} = \underline{\underline{8.8}}$$

APPENDIX B  
MEED CALCULATION

Quartz Plate Window Stress (con't) - 2

A quartz window was burst under pressure of 216 psig in the MEED tray single window design. The factor of safety was:

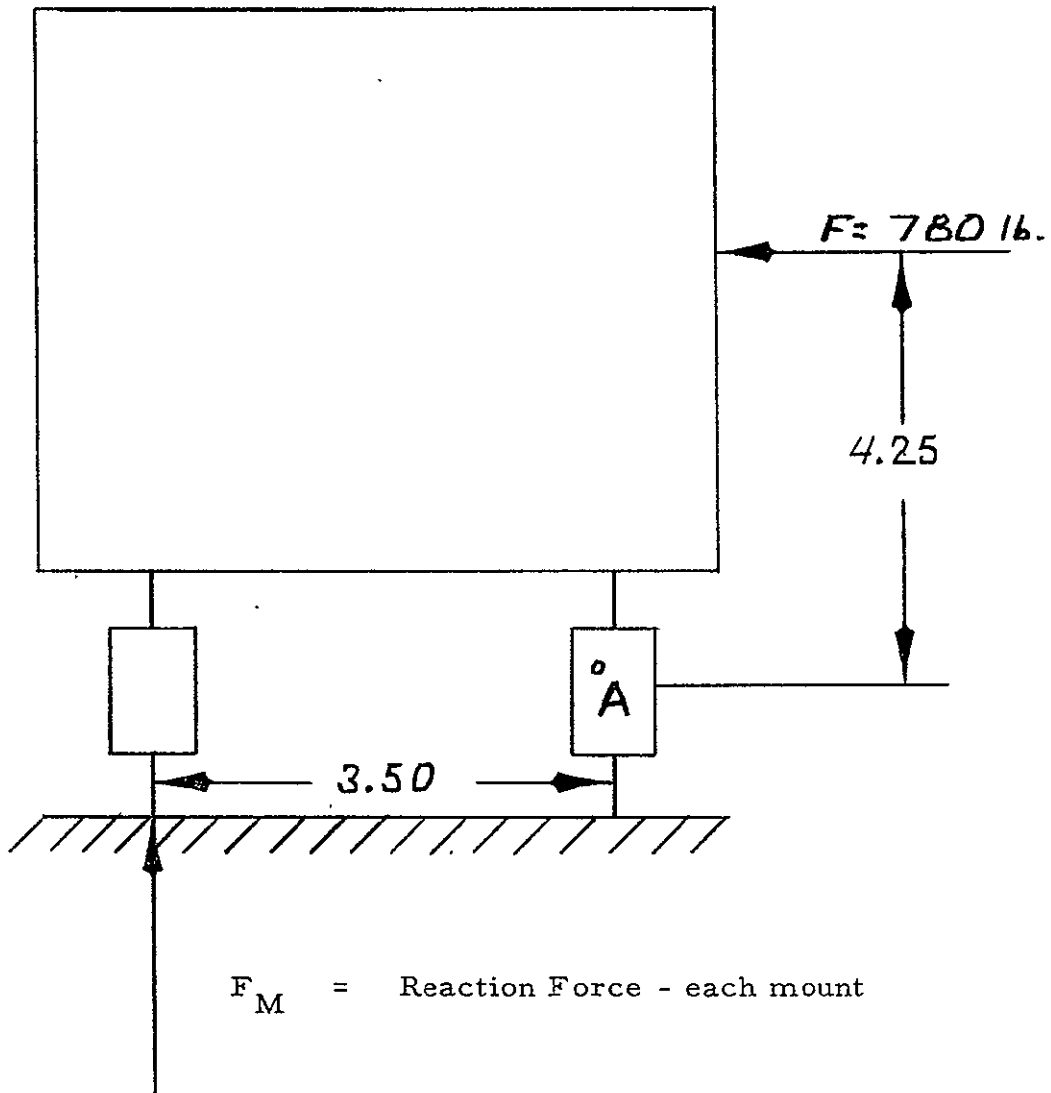
$$\text{F.S.} = 216/14.7 = \underline{\underline{14.7}}$$

The higher factor of safety might be expected as the strong clamping action of the MEED tray cover and base on the window plate provided a support that has characteristics between those of a fully clamped support and a simple support.

Reference: Roark, Raymond, J., Formulas for Stress and Strain, McGraw Hill, 1965.

APPENDIX B  
MEED CALCULATION

Soft Mount Maximum Design Load



$$\Sigma M_A = 780 \text{ lb} \times 4.25 \text{ in} - 2 F_M \times 3.5 \text{ in} = 0$$

$$F_M = \frac{780 \times 4.25 \text{ in lb}}{2 \times 3.5 \text{ in}} = \underline{\underline{473 \text{ lb}}}$$

$F_M$  is an estimate of the maximum force in a single soft mount (vibration isolator).

$$F_s = \text{Maximum Shear Force} = \frac{780}{4} = \underline{\underline{195 \text{ lb}}}$$

APPENDIX C  
MEED WEIGHT ANALYSIS

MEED	Weight Pounds	Weight Grams	Weight Grams	Present Design Weight Grams
Tray Cover	0.31	138.0		
Tray Base	0.79	359.0		
Quartz Window	0.39	176.0		
Cushion Rubber	0.002	0.06		
Gasket Seals (2 req.)	0.015	7.0		
Cuvettes Filled (384 req.)	0.17	74.5		
Screws (28 req.)	0.05	23.0		
MEED Sub-Total	1.72	777.0		
3 MEEDS Sub-Total	5.16	2331.0	2331	
<u>CARRYING CASE LUNAR SUBASSEMBLY</u>				
Outer Case	0.88	400.0		
Inner Box #1	0.36	163.0		
Inner Box #2	0.27	123.0		
False Bottom	0.34	155.0		
Flat Sheet	0.11	50.0		
Retainer	0.03	14.0		
Rubber Gasket	0.34	155.0		
Hinges	0.12	55.0		
Nut Plates	0.04	18.0		
Latches	0.04	20.0		
Stand-off	0.08	36.0		
Screws	0.37	168.0		
Strut Clamp Assembly	0.22	100.0		
Super Insulation	0.08	36.0		
Carrying Case Lunar Subassembly Sub-Total	3.28	1493.0		

	Weight Pounds	Weight Grams	Weight Grams	Present Design Weight Grams
Lunar Subassembly Sub-Total				3849 g (8.45 lb)
<u>Command Module Subassembly</u>				
Outer Case	0.22	100.0		
Inner Case	0.36	163.0		
MEED (1)	1.72	777.0		
Super Insulation	0.01	4.0		
Base Plate	0.36	163.0		
Latches	0.02	8.0		
Cuvettes Filled	0.17	71.5		
Command Module Subassembly Sub-Total	2.84	1289.0		1289 g (2.84 lb)
Total Weight				5113 g (11.3 lb)

PROTOCOL D-1  
LUNAR ASSEMBLY DEPLOYMENT

This protocol is an outline of the procedures required to deploy the MEED hardware on the lunar surface.

1. Install the MEED Flight Assembly in the Command Module soft mount (Figure 4.2-2, 1a).
2. Prior to the lunar landing, detach the Lunar Subassembly and transport to the LM soft mount. The CM Subassembly remains on the CM soft mount. (Figure 4.2-2, 1c, 1d, and 1e.)
3. Install the Lunar Subassembly on the LM soft mount (by clamping) (Figure 4.2-2, 1f).
4. After the lunar landing is complete, unclamp the Lunar Subassembly from the LM soft mount and transport to the mounting point on the LM leg brace that faces the sun. (4.2-2, 1g.)
5. Open the clamp cover on the Lunar Subassembly and swing clamp to deployed position. Cock clamp and handle to open position. (Figure 4.3.1-9).
6. Set the Lunar Subassembly open clamp on the LM brace with the handle facing the astronaut.
7. Snap the lower half of the clamp to the closed position and lock the clamp by closing the handle. (Figure 4.3.1-9).
8. Release the clamps that secure the two halves of the Lunar Subassembly and swing the Assembly to the open position shown in Figure 4.3.1-7.
9. Pull the alignment wand to the fully extended position and align it with the solar rays by re-alignment of the complete Lunar Assembly. (Note: The Assembly clamp will slip and the Assembly will rotate about its vertical axis under predetermined pressure supplied by the astronaut).
10. Pull the MEED cover slides (not shown in Figure 4.3.1-7) and expose the MEEDs for 10 minutes. Push the slides back into position at the end of exposure.
11. Push the wand back into position and clamp the Lunar Subassembly.

12. Pull the clamp hinge pin, leaving the clamp and part of the hinge on the LM leg brace.
13. Replace the Lunar Subassembly on its soft mount in the LM.
14. At the appropriate time after ascent and rendezvous with the Command Module, move the Lunar Subassembly to the Command Module and attach to the CM soft mount.
15. After the landing on Earth is completed, place the Flight Assembly in the special carrying case available on the aircraft carrier for transport to MSC, Houston.



## PROTOCOL D-2

### SECTION TRAY LOADING

1. The four types of cuvettes will be available in assembly trays that are packaged in sterile sealed bags. All parts will be in the fully sterile condition. Each Assembly Tray will contain 144 cuvettes of which 108 are microbial sample cuvettes and 36 are actinometers. The cuvettes from one Assembly Tray are all pre-coded and when filled, will contain one type of microbe and will be exposed to one wavelength of radiation. Equal numbers of the cuvettes will be exposed to each of six radiation intensity levels. The 144 cuvettes and actinometers will be loaded into six section trays in identical patterns.

#### 2. Coding of the Cuvettes

The cuvettes and actinometers are precoded. Each of the four sides of the cuvette has a single digit or a letter stamped on it in ink when received. To read the coding, start with the side with the letter designation for the type of cuvette (A, B, C or I). The "I" stands for intensity of radiation and indicates an actinometer cuvette. Rotate the cuvette  $90^{\circ}$ , clockwise from the top. The single digit is a code for the type of microbial sample. Rotate a second  $90^{\circ}$  increment. The single digit (1-4) is a code for the wavelength of ultraviolet radiation to be received by the cuvette. The last side contains a code digit (1-6) for the radiation intensity to be received by the cuvette.

3. The following steps are to be taken in loading the section trays:

3.1 Take 18 cuvettes of the first intensity level groupings and fill them with the microbial sample, in accordance with Protocol D-3, Loading of the Liquid Cuvette.

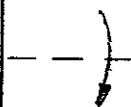
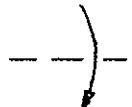
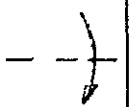
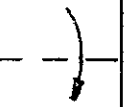
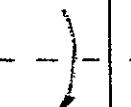

3.2 Replace the cuvettes in the Row 2 compartment for that radiation intensity level (See Figure D-2-1).

3.3 Repeat the filling process for the remaining six intensity levels and place cuvettes in the appropriate Row 2 compartment of the Assembly Tray.

3.4 At this point the Assembly Tray is filled with coded cuvettes and actinometers ready to fill six identical section trays. The six

Figure D-2-1  
ASSEMBLY TRAY SCHEMATIC

Intensity Levels

	1	2	3	4	5	6
Row 1 (Empty Cuvettes)	18	18	18	18	18	18
Row 2 (Filled Cuvettes)						
Row 3 (Actinometers)	6	6	6	6	6	6

section trays will fill one of 16 locations in each of the 5 MEEDs required for a Flight Assembly and Ground Control Unit and provide one spare section tray.

3.5 Take a section tray from the Secondary Assembly Tray, set it in front of the technician with the coding facing the technician.

Fill the section tray with cuvettes and actinometers from the Assembly Tray in the pattern shown in Figure D-2-2.

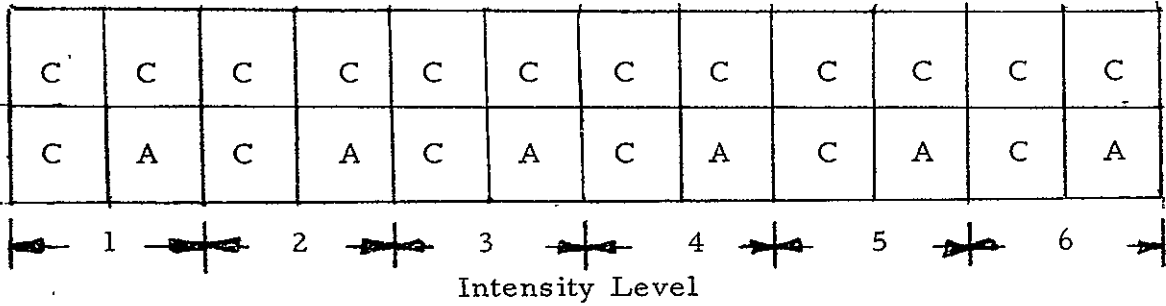
3.6 Replace the section tray in the secondary Assembly Tray. Repeat steps 3.5 and 3.6 for all of the section trays supplied (6).

3.7 At this point, six identical section trays have been filled with cuvettes and actinometers coded for a single microbe, a single radiation wavelength and six levels of radiation intensity. The same procedure will be applied to other types of microbes and other wavelengths, depending upon the requirements of the experiment.

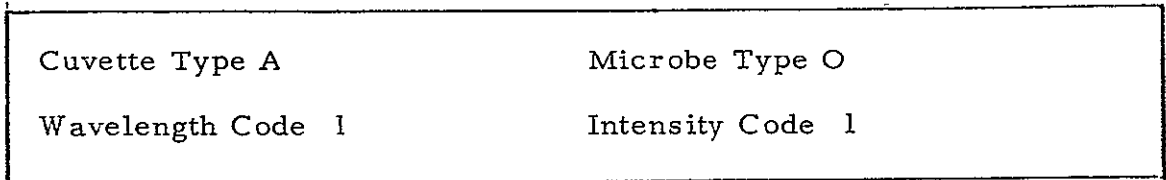
Figure D-2-2

SCHMATIC OF FILLED AND CODED SECTION TRAY

Top View



Side View



Legend:

C - Cuvette

A - Actinometer

Cuvette type A - Liquid Sample

Microbe type O - To be specified

Wavelength Code 1 - 253.7 nm

Intensity Code 1 -  $10 \text{ erg/cm}^2$  10 min

## PROTOCOL D-3

### LOADING OF THE LIQUID SAMPLE CUVETTE

#### Preliminary Steps

1. Fill solution (bacterial or actinometric) should be de-aerated as prescribed before use.
2. Sealing wax should be de-aerated as prescribed before use.
3. Cuvette components should be cleaned and inspected as prescribed before use.

#### Loading of the Cuvette

1. With the fill orifice upright, hold the cuvette at a 45° angle either by hand or in a test jig.
2. Using a syringe filled with the de-aerated fill solution, carefully fill the cuvette up to the base of the fill orifice.
3. Place the filled cuvettes with the fill hole upright on a vibrator platform vibrating at 60 cycles per second for 5 minutes in order to remove any bubbles formed inside of the cuvette.
4. Remove the cuvettes from the vibrator platform and place on a level surface with the fill hole upright.

#### Sealing of the Cuvette

1. Place some de-aerated wax lumps on a clean bunsen flame.
2. Place some de-aerated wax in a clean beaker and place on a constant temperature hot plate set for the wax melt temperature.
3. After the wax has melted, place a pasteur pipette tip with bulb into the molten wax and leave it there to pre-treat.
4. Using the pre-heated pasteur pipette, remove some wax from the heated beaker and deposit it into the cuvette fill orifice, making sure to completely fill the orifice.
5. After sealing the cuvette, allow them to cool for one-half hour.
6. After cooling, shave off the excess waxy flush to the cuvette with a sharp razor blade or xacto knife.
7. The cuvettes are now ready for loading into the MEED tray.

PROTOCOL D-4  
LOADING OF CUVETTE, DRY, SEALED

Preliminary Steps

1. Clean all cuvette components as prescribed.
2. Deposit the prescribed microorganisms on the microporous tape, vis. Millipore GSWP, 0.22 u under sterile conditions as prescribed; place the test filters in an appropriate container and seal it prior to removal from the sterile area.
3. Place the sealed test filter container in the transfer chamber to be used for loading the cuvettes.
4. Place all of the cuvette components, de-aerated sealing wax and accessory equipment into the same test chamber.
5. Seal the transfer chamber.
6. Sterilize the transfer chamber by pressurizing it with ETO for the prescribed time.
7. Following ETO sterilization, put the transfer chamber on positive filtered air for the prescribed time to remove the ETO; leave the transfer chamber on positive filtered air.
8. Unpack the sealed container containing the microorganism test filters.
9. Place a small beaker of the sealing wax on a hot plate in the transfer chamber that is set for the melting point of the wax and turn on the heat control.

Loading of the Cuvette

1. Place the test filter with the deposition surface up on the end of a teflon sponge piston.
2. Holding the cuvette with the opening down, insert the filter-piston assembly into the cuvette, pushing it in until it stops against the cuvette window.
3. Turn the cuvette over and insert the sealing ring in, the unlippped end first.
4. Push the sealing ring down into the cuvette until the lip of the sealing ring snaps into the appropriate groove.

### Sealing of the Cuvette

1. Place the loaded cuvette with the opening up on a level surface.
2. Using a pasteur pipette, fill the seal ring orifice up with wax up to the edge of the cuvette.
3. Do not disturb the cuvette and allow the wax to cool for at least one-half hour.
4. Following cooling of the sealing wax, shave off the excess wax down to the cuvette base using a razor blade or xacto knife.

### Employment of the Cuvette

1. Following the loading and sealing of the cuvettes:
  - a. Place all of them in a sterile container and seal it for shipment.
  - b. Or load them directly into a MEED tray as prescribed.

## PROTOCOL D-5

### LOADING OF CUVETTE, DRY, VENTED

#### Preliminary Steps

1. Refer to Protocol "Loading of Cuvette, Dry, Sealed".

#### Loading of the Cuvette

1. Refer to Protocol "Loading of Cuvette, Dry, Sealed".

#### Sealing of the Cuvette

1. The cuvette, dry, vented is not wax sealed at all; following the insertion of the sealing ring, the sealing is completed.

#### Employment of the Cuvette

1. Refer to Protocol, "Loading of Cuvette, Dry, Sealed" - Employment.



## PROTOCOL D-6

### DEPOSITION OF TEST AGENTS ON MILLIPORE FILTERS FOR USE IN THE CUVETTES, DRY, VENTED AND SEALED

#### A. Preliminary Procedures

1. Clean all apparatus to surgical standards.
2. Foil-wrap and autoclave all apparatus.
3. Autoclave the Millipore filters in an envelope.

#### B. Set-Up Procedure - Refer to Figure D-6-1.

1. Set up the apparatus as prescribed in a filterer-air, laminar-flow transfer hood.
2. Set up a filtered air source (absolute filter) for the deposition stack.
3. Ultraviolet-irradiate the transfer area prior to test.

#### C. Preparation of Agent

1. Weigh-out the prescribed amount of dry bacterial agent.
2. Place the weighed agent in a flat foil packet and crimp-seal it. (Diaphragm packet).

#### D. Loading of Agent

1. Place the diaphragm packet in the nebulizer gun.
2. Place the Millipore filter (0.22 u GSWG) on the frit head, grid side up, and replace the funnel-stack assembly.
3. Turn on the vacuum to the frit vacuum flask.

#### E. Deposition of Agent on the Millipore Filter

1. Attach the gun nozzle to the funnel-stack assembly.
2. Attach pressure tubing to the inlet of the nebulizer gun.
3. Using nitrogen, trigger the nitrogen pressure-release, rupturing the packet and expelling the contents into the funnel-stack assembly; turn off nitrogen pressure.
4. Leave the flask vacuum on for 10 minutes following nebulization to insure hard agent impaction.

#### F. Preparation of Agent Filters for Cuvette Loading

1. Using a No. 1 cork borer or a multiple-punch apparatus, punch out the cuvette filters from the agent-impacted Millipore filter.
2. Using forceps, place the cuvette filter in each cuvette as prescribed under the appropriate protocol.

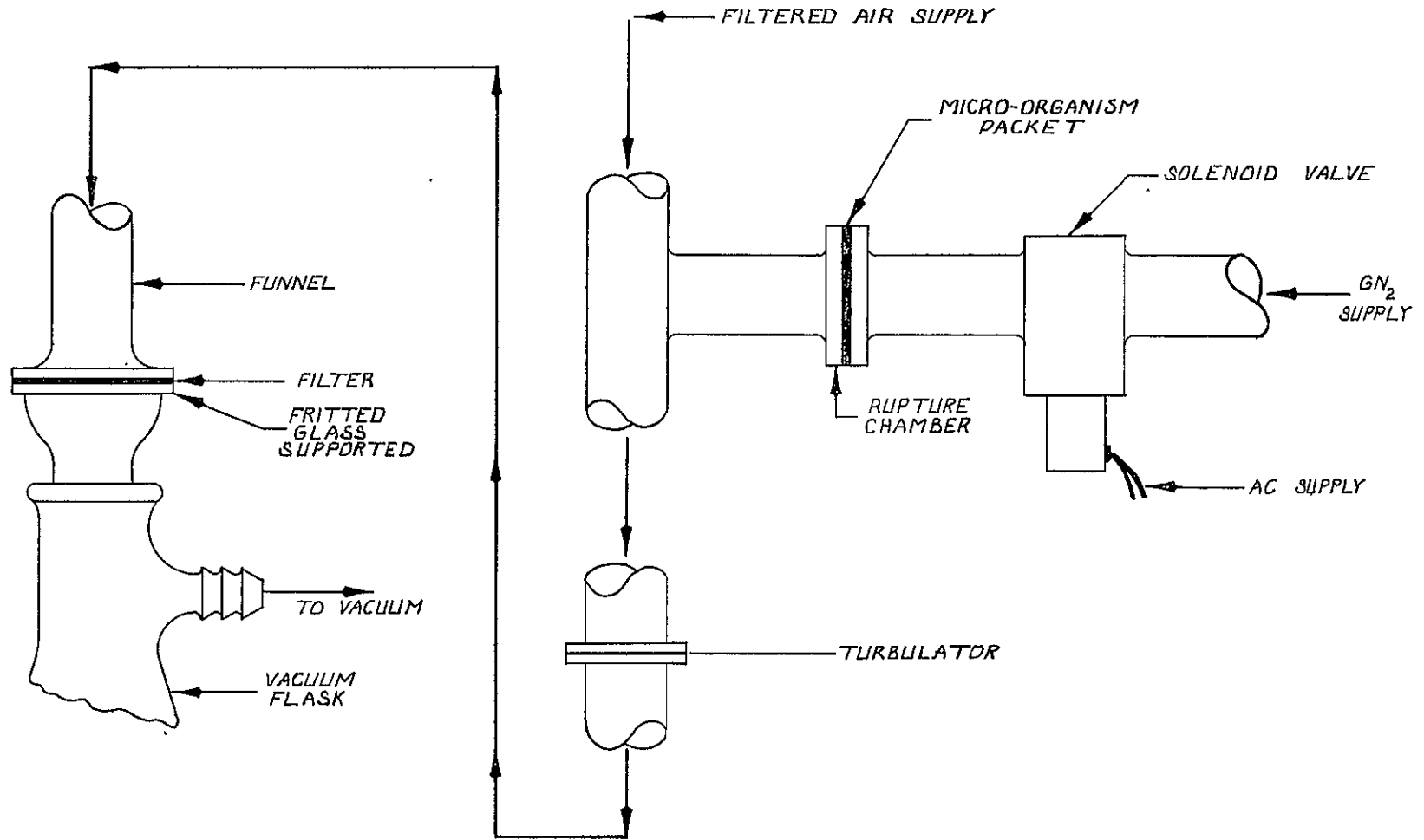


Figure D-6-1. Micro-Organism Deposition Apparatus

G. Assay of the Agent Cuvette Filter

1. Place an impacted agent cuvette filter on a microscope slide, grid surface up.

2. Clarify the filter with immersion oil,  $n = 1.504$  and cover with a cover glass.

3. Observe on a microscope at 1000-1250X and using standard clinical procedures, determine the bacterial count for the entire cuvette filter.

PROTOCOL D-7  
ASSEMBLY AND DISASSEMBLY OF  
THE MEED

1. All required components are in place at the assembly station of the transfer cabinet. Vented and sealed section trays loaded with microbial samples are also available. The following steps refer to Figures D-7-1 through D-7-3.
2. Set tray base in front of operator with vented section (small compartment) on operator's right. Place lubricated "O" ring secondary seal around base (not shown).
3. Place foam rubber pads supplied in the vented and sealed compartments.
4. Remove one Section Tray loaded with cuvettes from each compartment of the Secondary Assembly Tray and place in the appropriate position in the MEED on the foam rubber pads. Section Trays are coded for row and column position in the sealed portion of the tray and for column position (1-4) in the vented portion of the tray as shown in Figure D-7-1. Section Tray coding is facing the operator when in position in the sealed portion of the tray and facing to the operator's right when in position in the vented portion of the tray.
5. Take coded Neutral and Density Filters (6 for each Section Tray) from the Filter Tray and place in position on section trays on top of cuvettes. Neutral Density Filters, numbers 1 through 6, go from the operator's left to right in the sealed section of the MEED tray and from bottom to top in the vented portion of the MEED tray.
6. Take the Interference Filters coded for wavelength and place in position on top of the Neutral Density Filters in the row/column positions indicated by the Filter Location List that is supplied.
7. Place three lubricated small "O" rings in cavities provided on tray base.
8. Place the large (Sealed Section) and small (Vented Section) quartz plate windows in position on top of the Interference Filters. (Note: dimensional control and molded elastomeric seals control loading between cuvettes filters and the quartz plate.).

9. Place the MEED Tray Cover over the assembled base.
10. Put 28 Bolts in holes around periphery of tray. Use torque supplied after setting to 10 02-in position.
11. Place lubricated small "O" rings (not shown) on 3 bolts that are located between the quartz plates and tighten all bolts to 10 02-in in order shown in Figure D-7-2.
12. Tighten all bolts to 30 04-in as shown in proper order (Figure D-7-3).
13. Retighten all bolts to 48 02-in in order shown. Repeat tightening in proper order.
14. MEED is ready for installation in the Flight Assembly.
15. Repeat steps 1-13 for all MEEDES to be assembled.

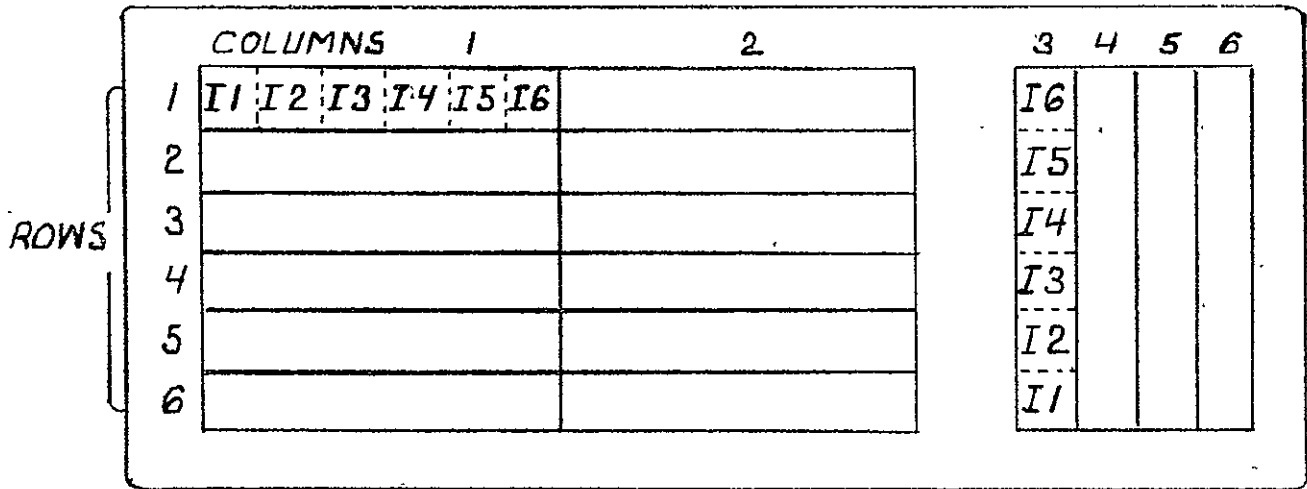


FIGURE D-7-1  
SCHEMATIC PLAN VIEW OF  
LOADED MEED

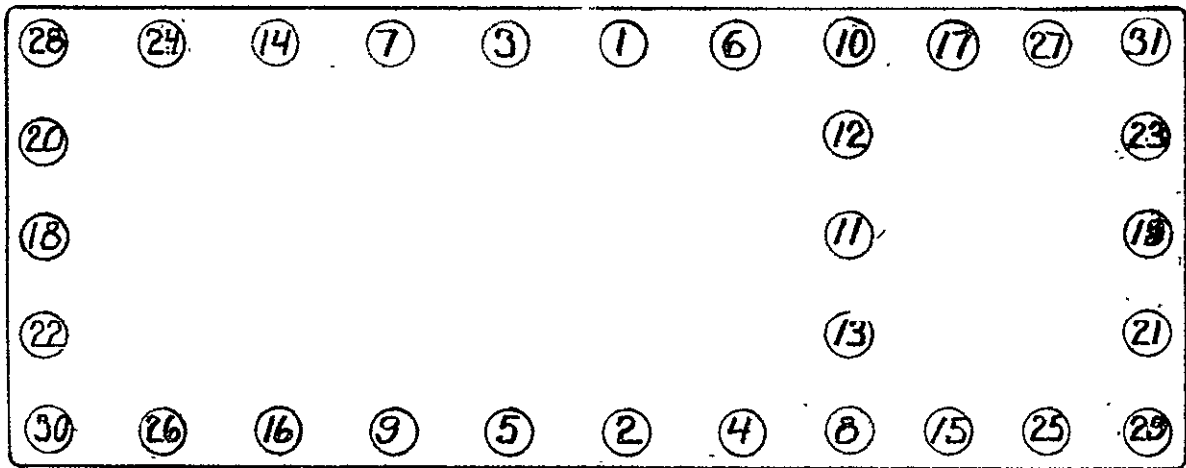


FIGURE D-7-2  
MEED BOLT TIGHTENING  
ORDER

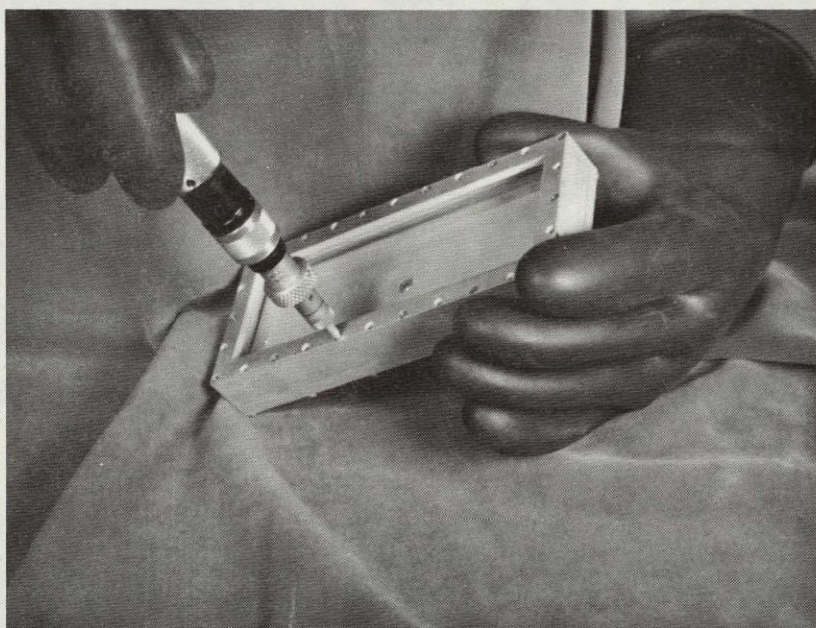


Figure D-7-3. Simulated Transfer Cabinet Assembly of MEED Tray

## PROTOCOL D-8

### RECOVERY - CUVETTE, DRY, SEALED & VENTED (Red Light Only)

#### Preliminary Steps

1. Refer to Protocol "Cuvette, Wet, Sealed", Preliminary Steps.
2. Place the recovered MEED Trays into the test chamber.
3. Seal the vent holes of all of the MEED Trays.
4. ETO sterilize the transfer chamber as prescribed.
5. Remove the ETO and make the transfer chamber positive with filtered air as prescribed.

#### Recovery

1. Place the Corex centrifuge tubes in numerical or code order as prescribed.
2. Remove a cuvette from the MEED Tray and lay it on its side.
3. Heat an xacto knife in a bunsen flame, withdraw it and cheese-cut the cuvette in half between the sponge piston and the sealing ring.
4. Hold the cuvette with the cut end upright and withdraw the piston and test filter from it using a vacuum nozzle for the withdrawal.
5. Place the cuvette window shell and test filter into a Corex centrifuge.
6. Break up the cuvette - filter combination as prescribed under Protocol D-9.
7. Fill the Cornwall apparatus with broth solution.
8. Broth-wash the cuvette-filter fragments and withdraw the Cornwall apparatus.
9. Cotton-plug the tube, shake and incubate as prescribed.



PROTOCOL D-9  
RECOVERY CUVETTE - LIQUID SAMPLE

Cuvette Recovery Apparatus

Parts List

1. "Corex" 15 ml centrifuge tubes - conical with regular nm.
2. Cornwall Dispensing Apparatus.
3. Syringe need with spray nozzle.
4. Vortex mixer.
5. Transfer Cabinet.
6. Solutions
  - a. Actinometer reaction solutions
  - b. Growth media (broth)

Preliminary Steps

1. All apparatus should be sterilized.
  - a. Sterilized with ETO
    - 1) MEED Tray
    - 2) Cuvettes (sealed)
  - b. Sterilized with autoclave
    - 1) Broth media
    - 2) Cornwall apparatus with nozzle tip
    - 3) Corex tubes
    - 4) Cotton plugs
2. Both biological and actinometric recovery shall be performed under red light only in order to prevent any spectral effects on the cuvette contents.
  - a. Biological Recovery

All apparatus and cuvettes are to be placed in a transfer cabinet that has filtered laminar air flow and ultraviolet radiation. Diluent is broth solution.
  - b. Actinometry Recovery

All apparatus and cuvettes are to be placed in a photographic darkroom with the spectrophotometer. An OB (red) safelight may be employed. A calibration curve for the particular spectrophotometer

must be available. Diluent is actinometer solution.

Cuvette Recovery - Refer to Figure D-9-1

1. All apparatus and cuvettes (in sealed plastic bag after ETO sterilization) are to be placed in the transfer cabinet. Ultraviolet irradiation is turned off prior to opening the cabinet.
2. In the prescribed numerical or code order, place each cuvette in its prescribed labeled Corex centrifuge tube.
3. Insert the nozzle tip of the Cornwall apparatus into the Corex tube.
4. Break up the cuvette by striking it with the nozzle tip.
5. Holding the nozzle tip above the cuvette breakage, fully depress the Cornwall apparatus plunger, thus metering out the prescribed volume of diluent; release the plunger and the Cornwall apparatus will automatically prime and refill from the supply vessel.
6. Withdraw the nozzle tip of the Cornwall apparatus:
  - a. For biological recovery, cotton plug the conex tubes, shake and incubate as prescribed.
  - b. For actinometry recovery, evaluate the sample on the spectrophotometer under red light as prescribed.

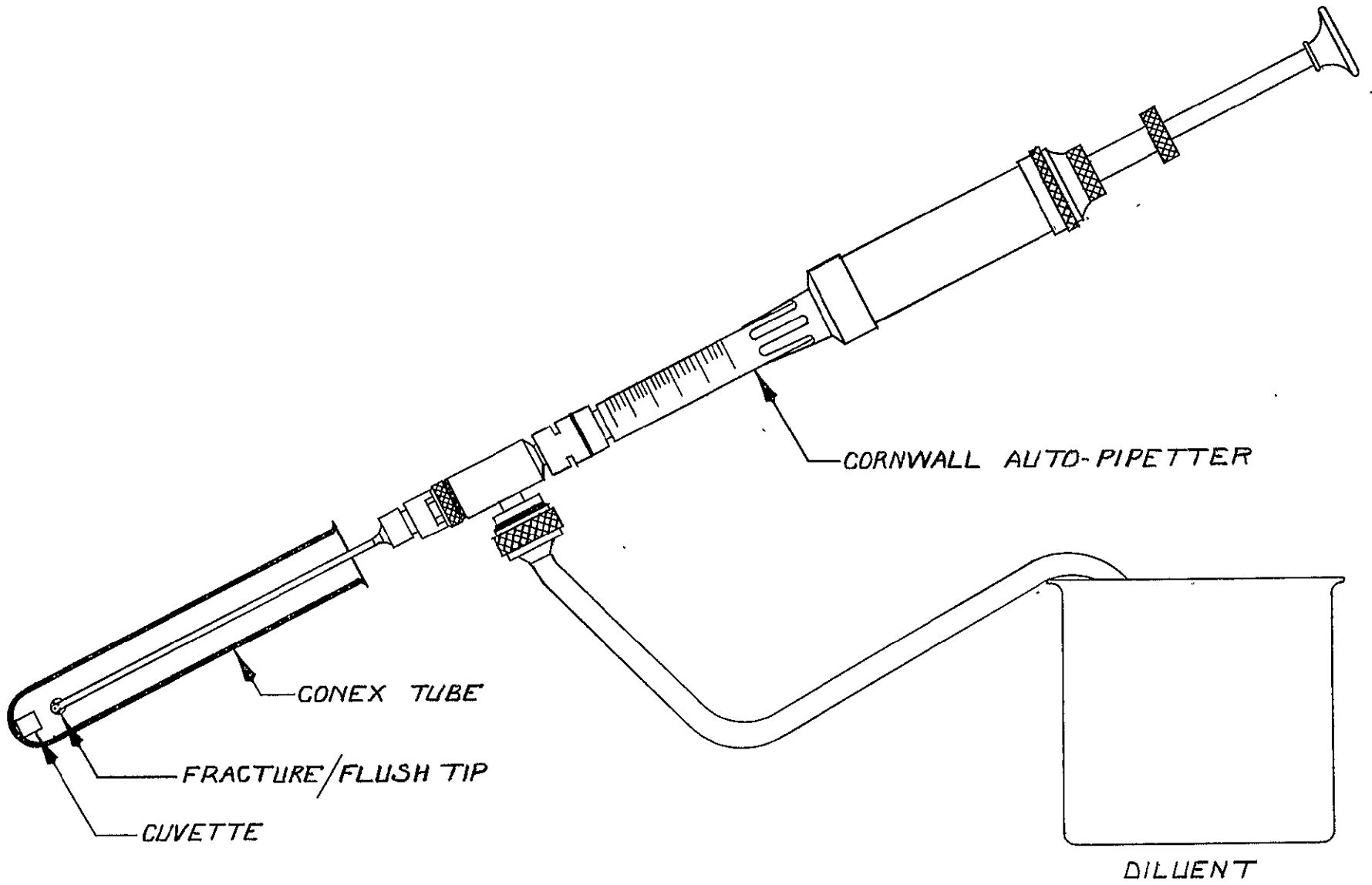


Figure D-9-1. Sample Removal Technique

## PROTOCOL D-10

### PROTOCOL FOR THE POTASSIUM FERRIOXALATE ACTINOMETER

#### A. Preparation of Potassium Ferrioxalate

1. Prepare solutions of 1.5 M ferric chloride and 1.5 M potassium oxalate using analytical grade reagents.

Calculation:  $\text{FeCl}_3$       FW = 270  
 $1.5\text{M} = (1.5) (270) = 405 \text{ gm/litre}$   
or  
40.5 gm/100 ml

$\text{K}_2\text{C}_2\text{O}_4$       FW = 184  
 $1.5\text{M} = (1.5) (184) = 276 \text{ gm/litre}$   
or  
27.6 gm/100 ml

According to Jagger in "Ultraviolet Photobiology", the following Actinometer solution steps should be done in a darkroom illuminated only by a red safe light (Kodak Series 2) while Parker, co-developer of this actinometer technique, Hatchard & Parker 1956 Proc. Roy. Soc., states the preparation should be carried out in a darkroom illuminated only by a yellow safe light (Kodak Series 8). The amb laboratory has found red safe light preferable due to its better spectral quality, lower visible intensity and availability.

2. Under red light, combine the two reagent solutions using a ratio of 3 volumes 1.5 M  $\text{K}_2\text{C}_2\text{O}_4$  to 1 volume 1.5 M  $\text{FeCl}_3$  i.e., 60 ml 1.5 M  $\text{K}_2\text{C}_2\text{O}_4$  to 20 ml 1.5 M  $\text{FeCl}_3$ , and mix thoroughly. Place the mix solution in an amber (lifetime-red, low actinic) 250 ml flask securely stoppered with cotton. White light may now be used.

3. Under white light, place the flask in an oven set for  $\sim 70^\circ\text{C}$  and evaporate the contents to one-quarter of the original volume, i.e.,  $\sim 20$  ml crystals will be observed. Place the flask in a refrigerator for one hour to accelerate crystal precipitation.

4. Under red light, decant and discard the supernatant

and resuspend to the original 80 ml volume with distilled water, dissolving the crystals.

5. Repeat steps 3 and 4 three times, decanting and adding fresh distilled water each time.

6. Under red light, following the last decant, add 100 ml chilled ethyl alcohol to the crystals, shake and decant the alcohol; repeat until the alcohol supernatant is clear.

7. Under red light, remove the crystals from the flask and place on two sheets of #3 filter paper; place the filter paper in a one gallon can and cover with aluminum foil and store in a light-tight box at room temperature until alcohol cannot be detected by smell and the filter paper is dry. A hair dryer is not recommended because it scatters the crystals and visible light is emitted from the brushes of the hair blower motor.

8. Under red light, store the crystals in a capped amber or brown bottle and store in a cool, dark place.

#### B. Preparation of Solutions for Potassium Ferrioxalate Actinometry

1. Actinometer photolyte (solution)  $0.006 \text{ M K}_3\text{Fe}(\text{C}_2\text{O}_4)_3 \cdot 3 \text{ H}_2\text{O}$ .

Dissolve 2.97 g of the crystals in 800 ml of distilled water, add 100 ml of  $1 \text{ N H}_2\text{SO}_4$ , and q. s. to one litre with distilled water. Mix thoroughly and store in separate 50 ml brown or amber bottles. The bottles should be filled to the top, tightly capped and stored in the dark. When a bottle is opened, any contents left over should be discarded.

2. Calibration Solution

Prepare a  $0.1 \text{ M FeSO}_4 \cdot 7 \text{ H}_2\text{O}$  solution as a laboratory standard.

Calculation:  $\text{FeSO}_4 \cdot 7 \text{ H}_2\text{O} \text{ FW} = 278$

$$0.1 \text{ M} = (0.1) (278) = 27.8 \text{ gm/litre}$$

Store in separate 50 ml brown or amber bottles. The bottles should be filled to the top, tightly capped, and stored in the dark. When a bottle is opened, any contents left over should be discarded.

3. Phenanthroline Solution (Redox Indicator)

Dissolve 1 g of 1, 10-phenanthroline monohydrate in

1 litre of water to yield a 0.1% solution. Store in a brown or amber bottle in the dark.

4. Buffer Solution

Mix 600 ml of 1 N sodium acetate and 360 ml of 1 N  $\text{H}_2\text{SO}_4$  and q. s. to one litre with distilled water.

Calculation:  $\text{NaC}_2\text{H}_3\text{O}_2 \cdot 3 \text{H}_2\text{O}$  FW = 136

1 N = (1) (136) = 136 gm/litre

The pH of this solution should be  $4.0 \pm 0.5$

## PREPARATION OF CALIBRATION GRAPH FOR FERROUS IRON

### A. Calibration Test Solution

The calibration test solution should be freshly prepared from the 0.1 M  $\text{FeSO}_4 \cdot 3 \text{H}_2\text{O}$  standardized solution. A solution of  $0.4 \times 10^{-6}$  mole/ml  $\text{Fe}^{++}$  is required.

Calculation: Dilute one part of 0.1 M  $\text{FeSO}_4 \cdot 3 \text{H}_2\text{O}$  to 250 parts of 0.1 N  $\text{H}_2\text{SO}_4$

$0.1 \text{ M } \text{FeSO}_4 \cdot 3 \text{H}_2\text{O} = 0.0004 \text{ moles/litre or}$

dividing by  $10^3 = 0.0000004 \text{ moles/ml}$

or

$= 0.4 \times 10^{-6} \text{ moles/ml in}$   
 $0.1 \text{ N } \text{H}_2\text{SO}_4$

### B. Procedure - to be done with a yellow safe light (Kodak Series 8)

1. Into a series of 20 ml calibrated volumetric flasks, add the following volumes of calibration test solution: 0.0, 0.5, ... 4.5, 5.0 ml.
2. Pipette 0.1 N  $\text{H}_2\text{SO}_4$  to each flask to q. s. to 10 ml final and mix.
3. To each flask pipette 2 ml phenanthroline solution and mix.
4. To each flask q. s. to the 20 ml volume line with the buffer solution and mix.
5. Let stand for at least one-half hour to permit complete reaction of the ferrous sulphate - phenanthroline complex.
6. Measure the optical density of each dilution at 510 m $\mu$  in a 1 cm cuvette with an absorption spectrophotometer, using the flask

without calibration solution ( $\text{Fe}^{++}$ ) as a process control. Figure D-10-1 shows increasing iron concentration from left to right.

7. Construct a graph from the data obtained plotting optical density vs. amount of  $\text{Fe}^{++}$  added ( $0.4 \times 10^{-6} \text{ M Fe}^{++}/\text{ml}$ ).

Calculation: For flask having 2.5 ml calibration solution, the  $\text{Fe}^{++}$  added is  $(2.5) (0.4 \times 10^{-6} \text{ M Fe}^{++}/\text{ml}) = 1 \times 10^{-6}$  moles  $\text{Fe}^{++}$  added.

Since the graph is linear, calculate a spectrophotometric conversion factor for amount of  $\text{Fe}^{++}$  added or present.

Calculation:  $0.6 \text{ OD} = 1 \times 10^{-6} \text{ moles Fe}^{++}$   
 $X (0.6) = 1 \times 10^{-6} \text{ moles Fe}^{++}$   
 $X = 1.66 \times 10^{-6}$

Calculate the conversion factor for three different optical densities and use the average as the final instrument conversion factor. To convert OD to moles of Fe added or present, multiply the optical density by  $1.66 \times 10^{-6}$ .

8. A unique calibration graph and conversion factor must be made for each particular spectrophotometer used in order to compensate for instrument variation.

#### GENERAL PROCEDURE FOR ACTINOMETRY IN THE LABORATORY (Calibration of laboratory standard ultraviolet light source)

##### A. Apparatus Required for Test

1. Ultraviolet light source with a visible light filter.
2. Cuvettes of high ultraviolet transmissivity.
3. Metric tape measure.
4. Accurate timer.
5. Red safe light (Series 2)

##### B. Proceed to Test under Red Light

1. Fill the cuvettes to the top ( $4 \text{ cm}^3$ ) with  $.006 \text{ M K}_3\text{Fe}(\text{C}_2\text{O}_4)$  actinometer solution.
2. Place the cuvettes 1 meter distance from the ultraviolet light source.
3. Place a light-tight box over the cuvettes and put on the ultraviolet safety goggles.

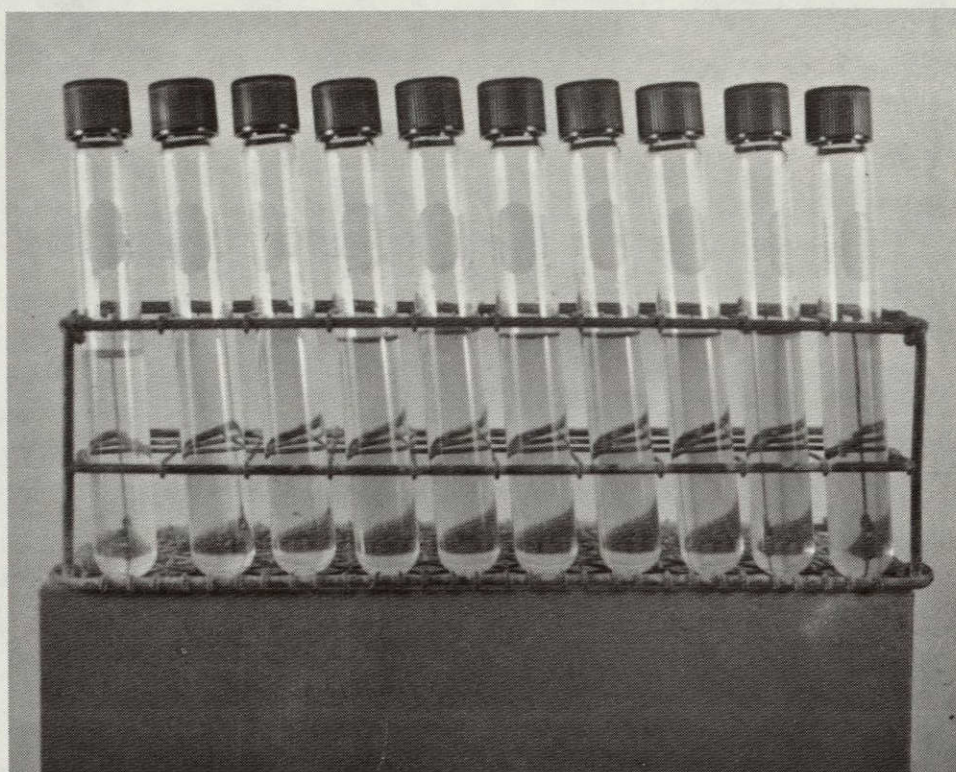


Figure D-10-1.  $\text{FeSO}_4$  Calibration Solutions



4. Turn on the ultraviolet light source and permit it to warm up for five minutes.
5. Set the timer and remove the light-tight box for the prescribed time; then, replace the light-tight box and turn off the ultraviolet light source.
6. Pool the cuvettes into one sample and mix.
7. Into a series of 20 ml flasks with stoppers, place 0, 0.5, ... 0.45, 5.0 ml of photolyte solution with pipette accuracy.
8. To each flask pipette 0.1 N  $\text{H}_2\text{SO}_4$  to q. s. to 10 ml final and mix.
9. To each flask pipette 2 ml phenanthroline solution and mix.
10. To each flask, add buffer solution and q. s. to the 70 ml volume line and mix.
11. Let stand for at least one-half hour to permit complete reaction of the ferrous oxalate-phenanthroline complex.
12. Measure the optical density of each dilution at 510 m  $\mu$  in a 1 cm cuvette with an absorption spectrophotometer, using the flask without the actinometer solution as a process control.

#### CALCULATIONS DERIVED FROM THE ACTINOMETRIC DATA

(Example - calibration data of a UV light source; peak at 350 m  $\mu$ ).

##### A. Calculation of Moles of Ferrous Iron Formed by Ultraviolet Radiation in a 4 ml Cuvette

1. Multiply each optical density reading by the conversion factor to obtain the number of moles of ferrous iron.

Calculation:  $\text{OD} = 0.42$        $\text{CF} = 1.66 \times 10^{-6}$  moles  $\text{Fe}^{++}$

$$\begin{aligned} \text{Moles } \text{Fe}^{++} \text{ formed} &= (\text{O.D.}) (\text{C.F.}) \\ &= (0.42) (1.66 \times 10^{-6} \text{ moles } \text{Fe}^{++}) \\ &= 0.699 \times 10^{-6} \text{ moles } \text{Fe}^{++} / \text{sample volume} \end{aligned}$$

2. Dilution Correction

- a. Convert the quantity of ferrous iron formed in the test volume to the amount formed in the total volume of the irradiated actinometer solution.

- 1) Each cuvette holds 4 ml of actinometer solution.

Calculation: 2) If one ml of irradiated actinometer solution yields  $0.699 \times 10^{-6}$  moles  $\text{Fe}^{++}$  when reacted, then 4 ml yields:

$$4 \text{ ml volume} = 4 (0.699 \text{ moles } \text{Fe}^{++}/\text{ml}) \\ = 2.8 \times 10^{-6} \text{ moles } \text{Fe}^{++} / \\ 4 \text{ ml/cuvette}$$

3) Correct each dilution reading (0.5, 1.0 ... 3.5, 4.0 ml) to 4 ml for a full cuvette; take the average of the corrected readings and accept it as the number of moles of  $\text{Fe}^{++}$  formed in a 4 ml cuvette.

Calculation: 4)  $0.5 \text{ ml} = 0.349 \times 10^{-6}$  moles  $\text{Fe}^{++}$

$$\text{Fe}^{++} \text{ formed}/4 \text{ ml cuvetted} \\ = 8 (0.349 \times 10^{-6} \text{ moles } \text{Fe}) \\ = 2.697 \times 10^{-6} \text{ moles } \text{Fe}^{++}$$

5)  $2.0 \text{ ml} = 1.39 \times 10^{-6}$  moles  $\text{Fe}^{++}$

$$\text{Fe}^{++} \text{ formed}/4 \text{ ml cuvette} \\ = 2 (1.39 \times 10^{-6} \text{ moles } \text{Fe}^{++}) \\ = 2.78 \times 10^{-6} \text{ moles } \text{Fe}^{++}$$

6) Measure  $\text{Fe}^{++}$  formed/4 ml cuvette

$$\bar{X}_{\text{Fe}^{++}} = 1/2 (2.697 \times 10^{-6} \text{ moles } \text{Fe}^{++} \\ + 2.78 \times 10^{-6} \text{ moles } \text{Fe}^{++}) \\ = 2.73 \times 10^{-6} \text{ moles } \text{Fe}^{++} / \\ 4 \text{ ml cuvette average}$$

B. Calculation of the Total Amount of Radiation Intercepted by a 4 ml Cuvette

1. Source Output (einsteins) =  $\frac{\text{moles } \text{Fe}^{++} \text{ formed}/4 \text{ ml cuvette}}{\text{quantum yield of reaction}}$   
@ 350 m $\mu$

Calculation:

$$2. \text{ einsteins} = \frac{2.8 \times 10^{-6} \text{ moles } \text{Fe}^{++}/4 \text{ ml}}{1.23 \text{ moles/einstein}} \\ = 2.26 \times 10^{-6} \text{ einstein}/4 \text{ ml cuvette}$$

\*Regarding the value for the quantum yield of this reaction @ 350 m $\mu$

Hatchard & Parker (1956)	1.22	
Parker (1960)	1.22	$\bar{X} = 1.23$
Jagger (1968)	1.26	

Due to differences in opinion of the quantum yield, an average value was used.

C. Calculation of the Total Amount of Radiation Striking the Window of the 4 ml Cuvette

1. Total radiation = radiation intercepted (einsteins/volume)  
(ergs/einstein @ 350 nm)
2. =  $(2.26 \times 10^{-6} \text{ einstein}) (3.27 \times 10^{12} \text{ ergs/einstein})$   
=  $7.5 \times 10^6 \text{ ergs/4 ml cuvette}$

D. Calculation of Dose of 4 mm Cuvette

1. Dose =  $\frac{\text{radiation striking 4 mm cuvette window}}{\text{area of 4 ml cuvette window}}$
2. Since window is 10 mm x 40 mm, the area is  $400 \text{ mm}^2$  so:  
Dose =  $\frac{7.5 \times 10^6 \text{ ergs}}{400 \text{ mm}^2}$   
=  $1.62 \times 10^4 \text{ ergs/mm}^2$

E. Calculation of Dose Rates:

$$\begin{aligned} \text{Dose rate} &= \frac{\text{dose}}{\text{irradiation time (sec)}} \\ &= \frac{1.62 \times 10^4 \text{ ergs/mm}^2}{60 \text{ sec}} \\ &= 2.7 \times 10^2 \text{ ergs/mm}^2/\text{sec} \end{aligned}$$